P-09-09

Site investigation SFR

Difference flow logging in borehole KFR105

Juha Väisäsvaara, PRG-Tec Oy

September 2009

Svensk Kärnbränslehantering AB
Swedish Nuclear Fuel
and Waste Management Co

Box 250, SE-101 24 Stockholm
Phone +46 8 459 84 00

ISSN 1651-4416
SKB P-09-09

Site investigation SFR

Difference flow logging in borehole KFR105

Juha Väisäsvaara, PRG-Tec Oy

September 2009

Keywords: P-report SKBDoc id 1224517, Review statement SKBDoc Id 1224518, Forsmark, Hydrogeology, Hydraulic tests, Difference flow measurements, KFR105, AP SFR-09-005, Project SFR extension.

Abstract

The Posiva Flow Log, Difference Flow Method (PFL DIFF) uses a flowmeter that incorporates a flow guide and can be used for relatively quick determinations of hydraulic conductivity and hydraulic head in fractures/fractured zones in cored boreholes. This report presents the main principles of the methods as well as the results of measurements carried out in underground borehole KFR105 within the SFR facility at Forsmark, Sweden, in June and July 2009.

The first flow logging measurements were done with a 5 m test section by moving the measurement tool in 0.5 m steps. This method was used to flow log the entire measurable part of the borehole. The flow measurements were repeated using a 1 m long test section, which was moved in 0.1 m steps.

Length calibration was made based on length marks milled into the borehole wall at accurately determined positions along the borehole. The length marks were detected by caliper measurements and by single-point resistance (SPR) measurements using the SPR sensor of the PFL DIFF probe.

The electrical conductivity (EC) and temperature of borehole water were also measured. The EC measurements were used to study the occurrence of saline water in the borehole. The EC of fracture-specific water was measured (1 m test section) for a selection of fractures.

The outflow from the borehole was measured during the time the borehole was open for measurements. The recovery transient of the borehole pressure was measured after the other measurements were finished and the borehole was closed.

Sammanfattning

Posiva Flow Log, Differensflödesloggning (PFL DIFF) är en snabb metod för bestämning av transmissiviteten och hydraulisk tryckhöjd i borrhålssektioner och sprickor/sprickzoner i kärnborrhål. Denna rapport presenterar huvudprinciperna för metoden och resultat av mätningar utförda i borrhål KFR105 inom SFR i Forsmark, Sverige, i juni och juli 2009.

Flödet till eller från en 5 m lång testsektion (som förflyttades successivt med 0,5 m) mättes i borrhålet. Flödesmätningarna upprepades med en 1 m lång testsektion som förflyttades successivt i steg om 0,1 m.

Längdkalibrering gjordes med hjälp av de längdmärken som finns infrästa vid noggrant bestämda positioner längs borrhålet. Längdmärkena detekterades med caliper och punktresistansmätningar (SPR) med hjälp av sensorer anslutna på PFL DIFF sonden.

Elektrisk konduktivitet (EC) och temperatur på borrhålsvattnet mättes också. EC-mätningarna användes för att studera förekomsten av saltvatten i borrhålet. EC mättes även i ett antal utvalda sprickor i borrhålet (1 m lång testsektion).

Utflödet från borrhålet mättes under tiden detta var öppet för mätningarna. Återhämtningstransienten mättes när alla andra mätningar var avslutade och borrhålet stängts.

Contents

1 Introduction

The core drilled borehole KFR105 at Forsmark, Sweden was measured using the Posiva Flow Log, Difference Flow Method (PFL DIFF) which provides a swift, multifaceted characterization of a borehole. The measurements were conducted between June 23 and July 1, 2009. The borehole is located in the so-called lower construction tunnel in the final repository for short-lived radioactive waste (SFR).

KFR105 is 306.81 m long and its inclination at its reference point at –106.82 m.a.s.l. is –10.4° from the horizontal plane. The borehole interval 0 m–2.64 m is cased and its inner diameter is 80 mm. The interval between c 2.64 m and 306.81 m is core drilled with a diameter of c 76 mm.

The location of KFR105 at Forsmark is illustrated in Figure 1-1.

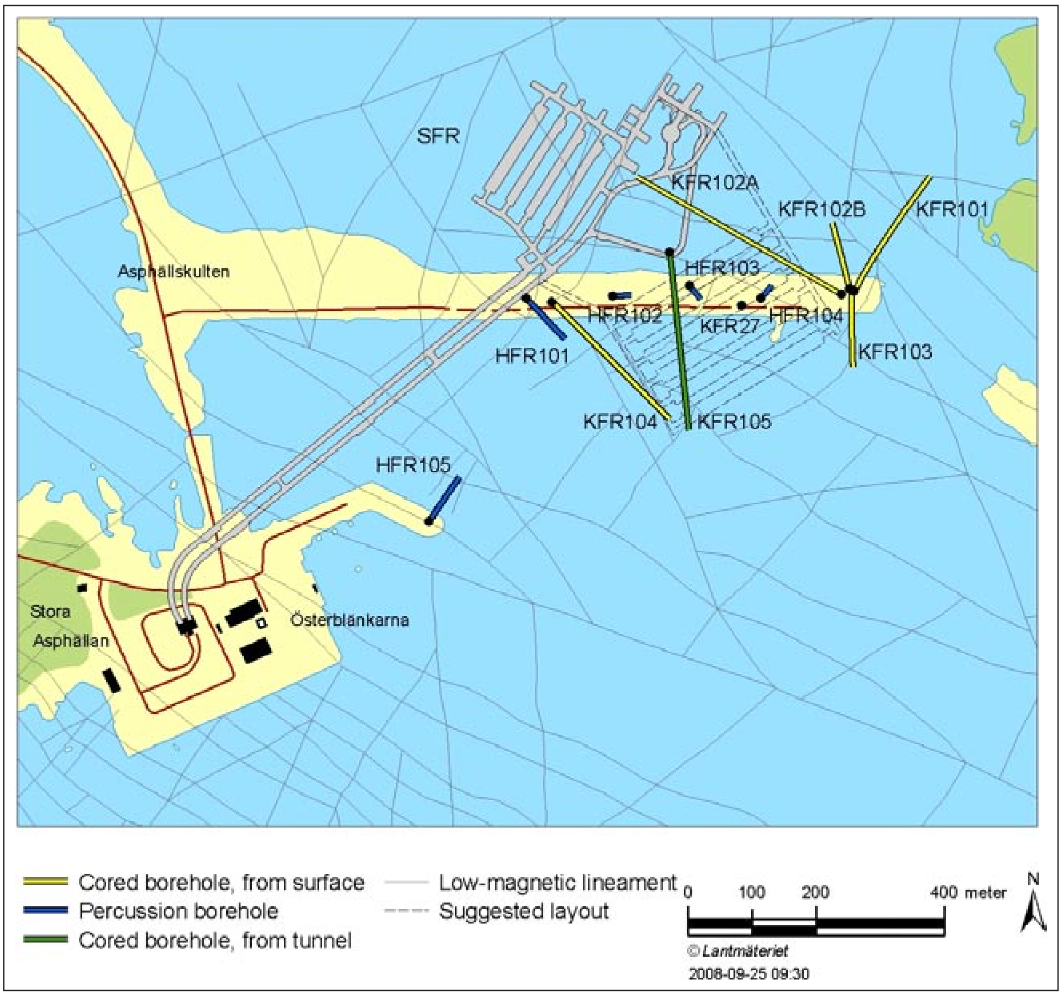

Figure 1-1. Location Map over the SFR facility and the location of the boreholes, including KFR105.

The field work and the subsequent data interpretation were conducted by PRG-Tec Oy as Posiva Oy's subcontractor. PFL DIFF has previously been employed in Posiva's site characterisation programme in Finland as well as at the Äspö Hard Rock Laboratory at Simpevarp, Sweden. The commissions at the latter site included measurements in the 1,700 m long cored borehole KLX02 at Laxemar together with a methodology study /Ludvigson et al. 2002/. PFL DIFF has also been employed in SKB's site characterisation programme at Laxemar and Forsmark.

This document reports the results acquired by PFL DIFF in borehole KFR105. The measurements were carried out as a part of a project named "Projekt SFR-utbyggnad" and in accordance to SKB's internal controlling document AP SFR-09-005. The controlling documents for performing according to this Activity Plan are listed in Table 1-1. The list of the controlling documents excludes the assignment-specific quality plans. Both the Activity Plan and the Method Descriptions are SKB's internal controlling documents. The measurement data and the results were delivered to the SKB site characterization database SICADA and are traceable by the Activity Plan number.

Table 1-1. SKB's internal controlling documents for the activities concerning this report.

Activity Plan	Number	Version
Difference flow logging in borehole KFR105	AP SFR-09-005	1.0
Method Descriptions	**Number**	**Version**
Method Description for Difference flow logging	SKB MD 322.010e	2.0
Instruktion för rengöring av borrhålsutrustning och viss markbaserad utrustning	SKB MD 600.004	1.0
Instruction for length calibration in investigation of core boreholes	SKB MD 620.010e	2.0
Instruktion för analys av injektions- och enhålspumptester	SKB MD 320.004	2.0

2 Objective and scope

The main objective of the PFL DIFF measurements in KFR105 was to identify water-conductive sections/fractures suitable for subsequent hydro-geochemical characterisation. Secondly, the measurements aimed at a hydrogeological characterisation, which includes the estimates of the transmissivity of tested sections and detected fractures. Based on the results of these investigations, a more detailed characterisation of flow anomalies along the borehole, e.g. an estimate of the conductive fracture frequency (CFF), may be obtained.

Besides difference flow logging, the measurement programme also included supporting measurements, performed in order to gain a better understanding of the overall hydrogeochemical conditions. These measurements included the electrical conductivity (EC) and the temperature of the borehole fluid as well as the single-point resistance of the borehole wall. The electrical conductivity of a number of selected high-transmissive fractures (the electrical conductivity of the water in the fractures) in the borehole was also measured. Furthermore, the flow rate out from the open borehole was recorded and the groundwater pressure was recorded during the recovery phase after the borehole was closed.

Single-point resistance measurements were also combined with caliper (borehole diameter) measurements to detect depth marks milled into the borehole wall at accurately determined positions. This procedure allowed for the length calibration of all other measurements.

3 Principles of measurement and interpretation

3.1 Measurements

Unlike conventional borehole flowmeters which measure the total cumulative flow rate along a borehole, PFL DIFF probe measures the flow rate into or out of defined borehole sections. The advantage that follows from measuring the flow rate in isolated sections is improved detection of incremental changes of flow along the borehole. As these are generally very small, they can easily be missed when using conventional flowmeters.

Rubber sealing disks located at the top and bottom of the probe are used to isolate the flow of water in the test section from the flow in the rest of the borehole, see Figure 3-1. Flow inside the test section is directed through the flow sensor. Flow along the borehole is directed around the test section by means of a bypass pipe and is discharged at either the upper or lower end of the probe. The entire structure is called the flow guide.

Generally two separate measurements with two different section lengths (e.g. 5 m and 1 m) are used. The 5 m setup is usually used first to obtain a general picture of the flow anomalies. It is also good for measuring larger (less than 5 m in length) fractured zones. The 1 m section setup can separate anomalies which are close to each other. There are also many other advantages to using different section lengths.

Flow rates into or out of the test section are monitored using thermistors, which track both the dilution (cooling) of a thermal pulse and its transfer by the moving water /Öhberg and Rouhiainen 2000, 11–13/. The thermal dilution method is used in measuring flow rates because it is faster than the thermal pulse method, and the latter is used only to determine flow direction within a given time frame. Both methods are used simultaneously at each measurement location.

In addition to incremental changes in flow, the PFL DIFF probe can also be used to measure:

- The electrical conductivity (EC) of both borehole water and fracture-specific water. The electrode used in EC measurements is located at the top of the flow sensor, see Figure 3-1.
- The single point resistance (SPR) of the borehole wall (grounding resistance). The electrode used for SPR measurements is located between the uppermost rubber sealing disks, see Figure 3-1, and is used for the high-resolution depth determination of fractures and geological structures.
- The prevailing water pressure profile in the borehole. Located inside the watertight electronics assembly, the pressure sensor transducer is connected to the borehole water through a tube, see Figure 3-2. Water pressure measurement is not important in nearly horizontal boreholes as in KFR105.
- The temperature of the water in the borehole. The temperature sensor is part of the flow sensor, see Figure 3-1.

The principles behind PFL DIFF flow measurements are shown in Figure 3-3. The flow sensor consists of three thermistors (Figure 3-3 a). The central thermistor, A, is used both as a heating element and to register temperature changes (Figures 3-3 b and c). The side thermistors, B1 and B2, serve as detectors of the moving thermal pulse caused by the heating of A.

Flow rate is measured by monitoring heat transients after constant power heating in thermistor A. The measurement begins by constant power (P_1) heating. After the power is cut off the flow rate is measured by monitoring transient thermal dilution (Figure 3-3 c). If the measured flow rate exceeds a certain limit, another constant power heating (P_2) period is started after which the flow rate is re-measured from the following heat transient.

Flows are measured when the probe is at rest. After transferring the probe to a new position, a waiting period (which can be adjusted according to the prevailing circumstances) is allowed to elapse before the heat pulse (Figure 3-3 b) is applied. The measurement period after the constant-power thermal pulse (normally 100 s each time the probe has moved a distance equal to the test section length and 10 s in every other location) can also be adjusted. The longer (100 s) measurement time is used to allow the direction of even the smallest measurable flows to be visible.

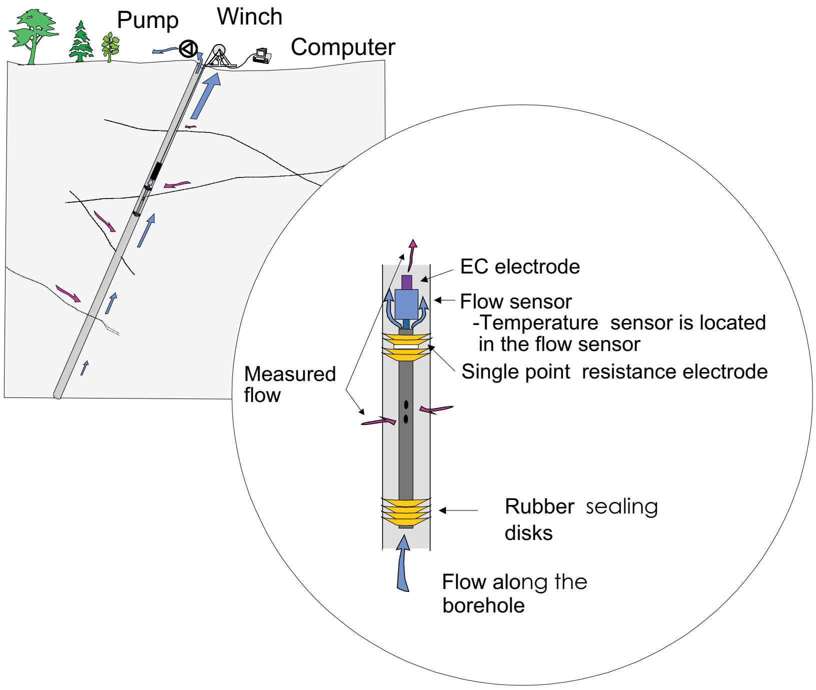

Figure 3-1. *Schematic of the probe used in the PFL DIFF.*

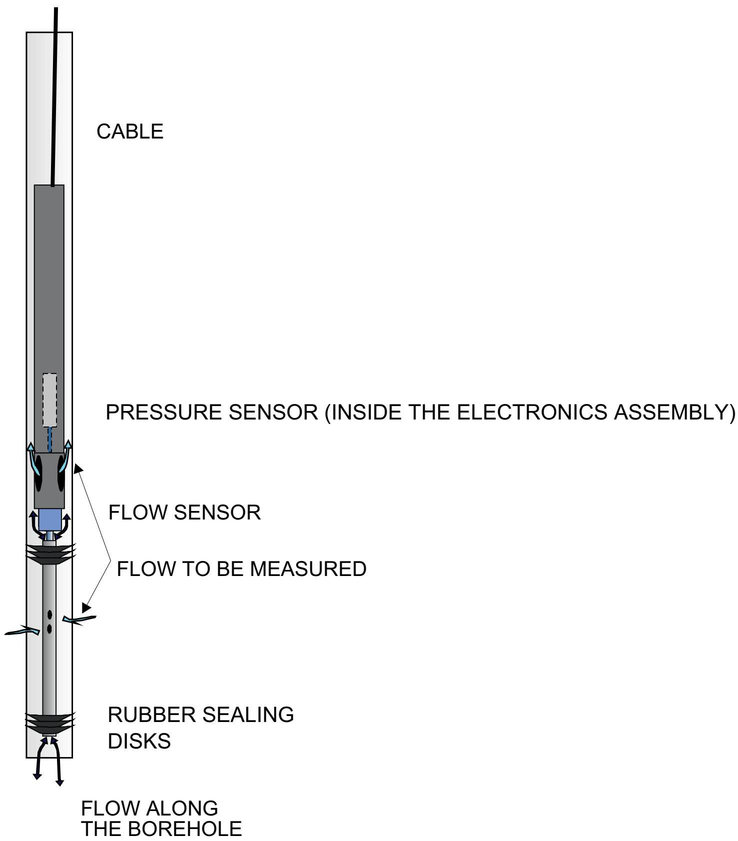

Figure 3-2. *The absolute pressure sensor is located inside the electronics assembly and connected to the borehole water through a tube.*

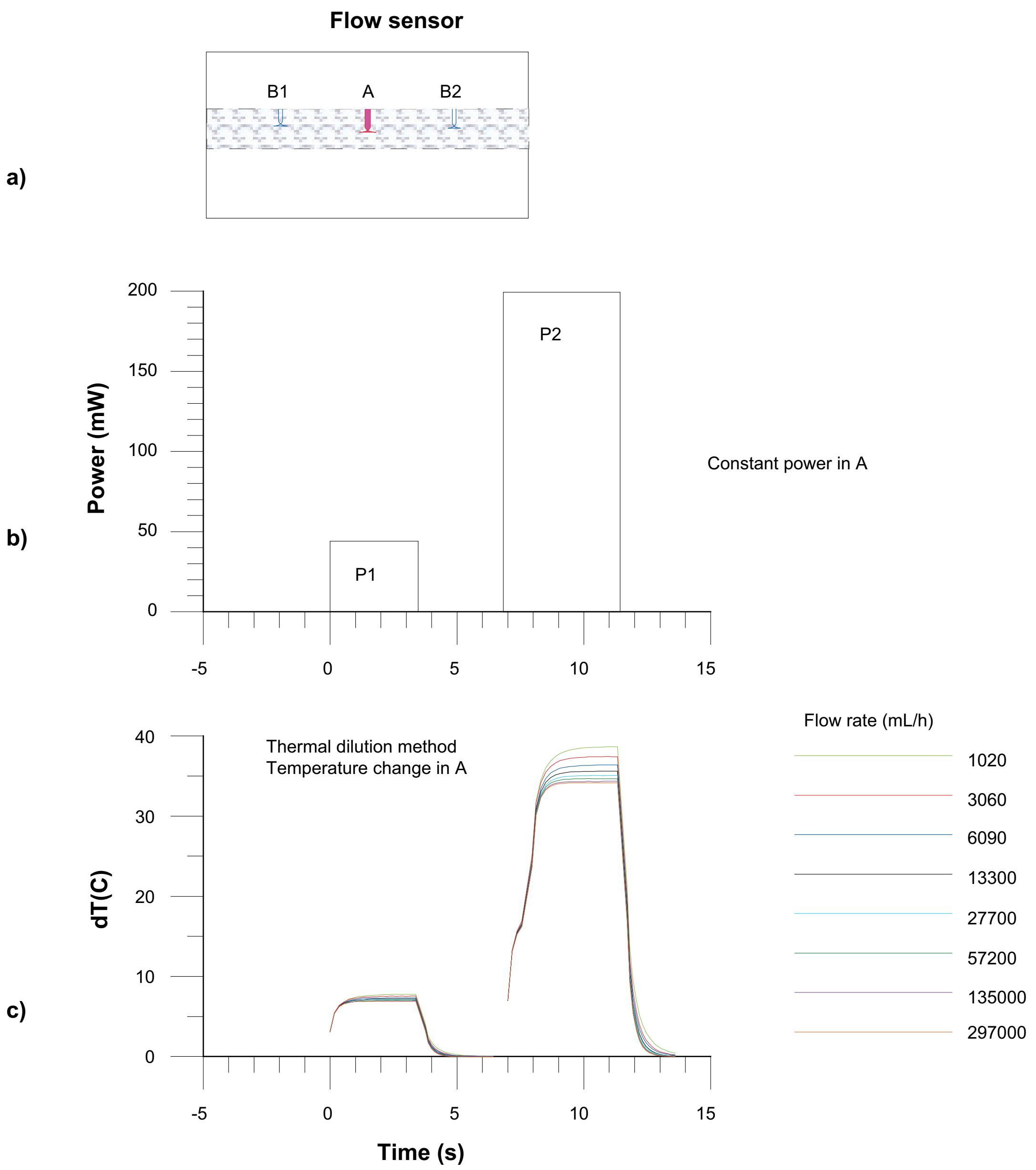

Figure 3-3. *Flow rate measurement.*

The flow rate measurement range is 30–300,000 mL/h. The lower limit of measurement for the thermal dilution method is the theoretical lowest measurable value. Depending on conditions in the borehole, these flow limits may not always prevail. Examples of possible disturbances are drilling debris entrained in the borehole water, bubbles of gas in the water and high flow rates (some 30 L/min, i.e. 1,800,000 mL/h or more) along the borehole. If the disturbances encountered are significant, limits on practical measurements are calculated for each set of data.

The device depth reference point in the PFL DIFF is situated at the upper end of the test section.

3.2 Interpretation

The interpretation of data is based on Thiem's or Dupuit's formula, which describes a steady state and two-dimensional radial flow into the borehole /Marsily 1986/:

$h_s - h = Q/(T \cdot a)$ (Eq. 3-1)

where h is the hydraulic head in the vicinity of the borehole and $h = h_s$ at the radius of influence (R),

Q is the flow rate into the borehole,

T is the transmissivity of the test section,

a is a constant depending on the assumed flow geometry. For cylindrical flow, the constant a is:

$a = 2 \cdot \pi / \ln(R/r_0)$ (Eq. 3-2)

where

r_0 is the radius of the well and

R is the radius of influence, i.e. the zone inside which the effect of pumping is felt.

If measurements of flow rate are carried out using two levels of hydraulic head in the borehole, i.e. natural and pump-induced heads, then the undisturbed (natural) hydraulic head and the transmissivity of the borehole sections tested can be calculated. Equation 3-1 can be reformulated in the following two ways:

$Q_{s0} = T_s \cdot a \cdot (h_s - h_0)$ (Eq. 3-3)

$Q_{s1} = T_s \cdot a \cdot (h_s - h_1)$ (Eq. 3-4)

where

h_0 and h_1 are the hydraulic heads in the borehole at the test levels,

Q_{s0} and Q_{s1} are the measured flow rates in the test section,

T_s is the transmissivity of the test section and

h_s is the undisturbed hydraulic head of the tested zone far from the borehole.

In general, since very little is known about the flow geometry, cylindrical flow without skin zones is assumed. Cylindrical flow geometry is also justified because the borehole is at a constant head, and no strong pressure gradients along the borehole exist except at its ends.

The radial distance R to the undisturbed hydraulic head h_s is not known and must be assumed. Here a value of 500 is selected for the quotient R/r_0.

The hydraulic head and the test section transmissivity can be deduced from the two measurements:

$h_s = (h_0 - b \cdot h_1)/(1 - b)$ (Eq. 3-5)

$T_s = (1/a)\ (Q_{s0} - Q_{s1})/(h_1 - h_0)$ (Eq. 3-6)

where

$b = Q_{s0}/Q_{s1}$

The transmissivity (T_f) and hydraulic head (h_f) of individual fractures can be calculated provided that the flow rates at the individual fractures are known. Similar assumptions to those employed above must be used (a steady-state cylindrical flow regime without skin zones).

$h_f = (h_0 – b \cdot h_1)/(1–b)$ (Eq. 3-7)

$T_f = (1/a)\ (Q_{f0} – Q_{f1})/(h_1 – h_0)$ (Eq. 3-8)

where

Q_{f0} and Q_{f1} are the flow rates at a fracture and h_f and T_f are the hydraulic head (far away from borehole) and transmissivity of a fracture, respectively.

Since the actual flow geometry and any skin effects are unknown, transmissivity values should only be considered as an indication of the prevailing orders of magnitude. As the calculated hydraulic heads do not depend on geometrical properties but only on the ratio of the flows measured at different heads in the borehole, they should be less sensitive to unknown fracture geometry. A discussion of potential uncertainties in the calculation of transmissivity and hydraulic head can be found in /Ludvigson et al. 2002/.

The transmissivity of the entire borehole can be evaluated in several ways using the data from the flow period and recovery period. The assumptions above (cylindrical and steady-state flow) lead to Dupuits formula /Marsily 1986/:

$$T = \frac{Q}{s2\pi} \ln\left(\frac{R}{r_0}\right)$$ (Eq. 3-9)

where

s is drawdown (m) and

Q is the pumping rate at the end of the flow period (m^3/s)

In Moye's formula /Moye 1967/ it is assumed the steady-state flow is cylindrical near the borehole (to a distance r = L/2, where L is the length of the test section) and spherical further away from the borehole:

$$T = \frac{Q}{s2\pi}\left[1 + \ln\left(\frac{L}{2r_0}\right)\right]$$ (Eq. 3-10)

where L is length of the test section (m), in this case the water filled uncased part of the borehole and r0 is the diameter of the borehole (m).

The transient recovery period is evaluated according to SKB MD 320.004 (SKB internal controlling document).

4 Equipment specification

In the PFL DIFF method, the flow of groundwater into or out of a borehole section is monitored using a flow guide which employs rubber sealing disks to isolate any such flow from the flow of water along the borehole. This flow guide defines the test section being measured without altering the hydraulic head. Groundwater flowing into or out of the test section is guided to the flow sensor, and flow is measured using the thermal pulse and thermal dilution methods. Measured values are transferred to a computer in digital form.

Type of instrument:	PFL DIFF probe.
Borehole diameters:	56 mm, 66 mm and 76 mm (or larger).
Length of test section:	The flow guide length can be varied.
Method of flow measurement:	Thermal pulse and thermal dilution.
Range and accuracy of measurement:	See Table 4-1.
Additional measurements:	Temperature, Single point resistance, Electrical conductivity of water, Water pressure.
Winch:	Mount Sopris Wna 10, 0.55 kW, conductors, Gerhard-Owen cable head.
Depth determination:	Based on a digital distance counter.
Logging computer:	PC (Windows XP).
Software:	Based on MS Visual Basic.
Total power consumption:	1.5–2.5 kW depending on the type of pump employed.
Calibration of flow probe:	October 2008 (Probe FL14).

The range and accuracy of the sensors used is shown in Table 4-1.

Table 4-1. Range and accuracy of sensors.

Sensor	Range	Accuracy
Flow	30–300 000 mL/h	± 10% curr.value
Temperature (central thermistor)	0–50°C	0.1°C
Temperature difference (between outer thermistors)	–2 – +2°C	0.0001°C
Electrical conductivity of water (EC)	0.02–11 S/m	± 5% curr.value
Single point resistance (SPR)	5–500 000 Ω	± 10% curr.value
Groundwater level sensor	0–0.1 MPa	± 1% full-scale
Air pressure sensor	800–1060 hPa	± 5 hPa
Absolute pressure sensor	0–20 MPa	± 0.01% full-scale

5 Execution of measurements

5.1 General

The work commission was performed according to Activity Plan AP SFR-09-005 following the SKB Method Description 322.010e, Version 2.0 (Method Description for Difference flow logging), see Table 1-1. The Activity Plan and the Method Description are both SKB's internal controlling documents. Prior to the measurements, the downhole tools and the measurement cable were disinfected. Time was synchronized to local Swedish time, UTC +2 (Central European Summer Time). The activity schedule of the borehole measurements is presented in Table 5-1. The items and activities in Table 5-1 are the same as in the Activity Plan.

Logging cables, wires, and pipe strings are exposed to stretching when lowered into a vertical or sub-vertical borehole. This will introduce a certain error in defining the position of a test tool connected to the end of a logging cable. Immediately after completion of the drilling operations, length marks were milled into the borehole wall at certain intervals to be used for length calibration of various logging tools. By using the known positions of the length marks, logging cables etc. can be calibrated in order to obtain an accurate length correction of the testing tool. Each length mark consists of two 20 mm wide tracks in the borehole wall. The distance between the tracks is 100 mm. The upper track defines a reference level.

The groundwater pressure in the borehole was measured before the borehole was opened and after it was closed (Items 10 and 19). The outflow from the borehole was measured during the entire time the borehole was open.

The dummy logging (Item 8) of the borehole is done in order to assure that the measurement tools do not get stuck in the borehole. The dummy also collects solid material from the borehole wall. The solid material in the dummy is used for evaluation whether it is safe to continue with other logging tools.

Caliper measurements were used in combination with single-point resistance measurements for detection of length marks (Item 9). These methods also reveal parts of the borehole widened for some reason (fracture zones, breakouts etc.). The length calibration was performed before any other measurements were started.

The electrical conductivity (EC) and temperature of borehole water (Item 12) were measured before flow logging.

The combined overlapping/sequential flow logging (Item 13) was carried out in the borehole with a 5 m section length and in 0.5 m length increments (step length).

Flow logging was continued by re-measuring the borehole with a 1 m section length and a 0.1 m step length (Item 14).

The fracture specific EC of water from some selected fractures (Item 15) was performed in conjunction with Item 14.

The EC of borehole water (Item 16) was logged after the flow loggings. After this, the borehole was closed (Item 17) and the recovery of the groundwater pressure was monitored (Item 19).

Table 5-1. Flow logging and testing in KFR105. Activity schedule.

Item	Activity	Explanation	Date
2	Mobilisation at site	Unpacking the trailer.	2009-06-23
10	Pressure measurement	Measurement of the groundwater pressure in the borehole prior to opening the borehole.	2009-06-23
11	Opening of the borehole	–	2009-06-23
8	Dummy logging	Borehole stability/risk evaluation.	2009-06-23–2009-06-24
9	Calibration	SKB Caliper and SPR. Logging without the lower rubber sealing disks.	2009-06-24
12	EC- and temp-logging of the borehole fluid	Logging without the lower rubber sealing disks.	2009-06-24–2009-06-25
13	Combined overlapping/ sequential flow logging	Section length L_w=5 m. Step length dL=0.5 m.	2009-06-25–2009-06-26
14 / 15	Overlapping flow logging and fracture-specific EC-measurements in pre-selected fractures	Section length L_w=1 m. Step length dL=0.1 m, pumping. Fracture-specific EC in pre-selected fractures.	2009-06-26–2009-06-30
15	EC- and temp-logging of the borehole fluid	Logging without the lower rubber sealing disks.	2009-06-30–2009-07-01
17	Closing of the borehole	–	2009-07-01
19	Recovery transient	Measurement of absolute pressure in the borehole after the borehole was closed. Measured manually by PRG-Tec Oy. Additional automatic measurement by Geosigma AB on 2009-07-02.	2009-07-01
21	Demobilisation	Packing the trailer.	2009-07-01

5.2 Nonconformities

Measurements of total water volume outflow from the borehole during this campaign was cancelled by SKB, because the working platform required for these measurements was not available.

It was not physically possible to measure approximately 0.95 m of the bottom of the borehole. There was a centralizer in the measurement device, which reduces the measured distance by c 0.85 m. The rubber sealing disks in the device must also be flipped before the measurement begins. This reduces the measured distance for approximately 10 cm.

6 Results

6.1 Length calibration

6.1.1 Caliper and SPR measurement

An accurate length scale for the measurements is difficult to achieve in long boreholes. The main cause of inaccuracy is the stretching of the logging cable. The stretching depends on the tension on the cable, the magnitude of which in turn depends, among other things, on the inclination of the borehole and the roughness (friction properties) of the borehole wall. The cable tension is larger when the borehole is measured upwards. The cables, especially new cables, may also stretch out permanently.

Length marks on the borehole wall can be used to minimize the length errors. The length marks are initially detected with the SKB caliper tool. The length scale is first corrected according to the length marks. Single-point resistance is recorded simultaneously with the caliper logging. All flow measurement sequences can then be length corrected by synchronising the SPR results (SPR is recorded during all the measurements except borehole EC measurements) with the original caliper/SPR-measurement.

The procedure of the length correction was as follows:

– The caliper/SPR-measurements (Item 9) were initially length corrected in relation to the known length marks, Appendix KFR105.1.14, black curve. Corrections between the length marks were obtained by linear interpolation.

– The SPR curve of Item 9 was then compared with the SPR curves of Items 13 and 14/15 to obtain relative length errors of these measurement sequences.

– All SPR curves could then be synchronized, as can be seen in Appendices KFR105.1.2–KFR105.1.13.

The results of the caliper and single-point resistance measurements from all measurements in the entire borehole are presented in Appendix KFR105.1.1. Three SPR-curves are plotted together with the caliper-data. These measurements correspond to Items 9, 13 and 14/15.

Zoomed results of the caliper and SPR data are presented in Appendices KFR105.1.2–KFR105.1.13. The detectability of the length marks is listed in Table 6-1. All the length marks were detected by the caliper tool.

All the length marks were also adequately detected in the single-point resistance measurements. The SPR-anomaly is complicated due to the four rubber sealing disks used at the upper end of the section, two at each side of the resistance electrode, but it is often possible to successfully detect the length marks even if the caliper tool has not found the marks.

The aim of the plots in Appendices KFR105.1.2–KFR105.1.13 is to verify the accuracy of the length correction. The curves in these plots represent length corrected results. These appendices also illustrate a few locations where SPR anomalies that could be used to help in determining the location of the measurement tool in the borehole were found.

The magnitude of length correction along the borehole is presented in Appendix KFR105.1.14. The negative values of the error represent the situation where the logging cable has been extended, i.e. the cable is longer than the nominal length marked on it.

Table 6-1. Detected length marks.

Length marks given by SKB (m)	Length marks detected by caliper	Length marks detected by SPR
50	both	yes
99	both	yes
153	both	yes
203	both	yes
262	both	yes

6.1.2 Estimated error in location of detected fractures

In spite of the length correction in described above, there can still be length errors due to the following reasons:

1. The point interval in the overlapping mode flow measurements is 0.1 m. This could cause an error of ± 0.05 m.
2. The length of the test section is not exact. The specified section length denotes the distance between the nearest upper and lower rubber sealing disks. Effectively, the section length can be larger. At the upper end of the test section there are four rubber sealing disks. The distance between them is 5 cm. This will cause rounded flow anomalies: a flow may be detected already when a fracture is situated between the upper rubber sealing disks. These phenomena can cause an error of ± 0.05 m when the short step length (0.1 m) is used.
3. Corrections between the length marks can be other than linear. This could cause an error of ± 0.1 m in the caliper/SPR-measurement.
4. SPR curves may be imperfectly synchronized. This could cause an error of ± 0.1 m.

In the worst case, the errors from sources 1, 2, 3 and 4 are summed and the total estimated error between the length marks would be ± 0.3 m.

The situation is slightly better near the length marks. In the worst case, the errors from sources 1, 2 and 4 are summed and the total estimated error would be ± 0.2 m.

Knowing the location accurately is important when different measurements are compared, for instance flow logging and borehole TV. In that case the situation may not be as severe as the worst case above, since some of the length errors are systematic and the error is nearly constant in fractures that are close to each other. However, the error from source 1 is random.

Fractures nearly parallel with the borehole may also be problematic. Fracture location may be difficult to define accurately in such cases.

6.2 Electrical conductivity and temperature

6.2.1 Electrical conductivity and temperature of borehole water

The electrical conductivity of the borehole water (borehole EC) was initially measured before the flow logging measurements. The measurement was performed upwards, see Appendices KFR105.2.1 (linear scale) and KFR105.2.2 (logarithmic scale), light green curve.

The EC measurement was repeated after the flow logging measurements, see Appendices KFR105.2.1 and KFR105.2.2, green curve. Borehole EC was higher during the latter borehole EC measurement, about 0.04 S/m higher at the end of the borehole and about 0.06 S/m higher at the top. Some of the fracture-EC transients were poorly stabilized (Appendices KFR105.11.1–KFR105.11.3) indicating that EC of fracture-specific water could be in changing state.

The temperature of the borehole water was measured simultaneously with the EC measurements. The EC values are temperature corrected to 25°C to make them more comparable with other EC measurements /Heikkonen et al. 2002/. The temperature plots in Appendix KFR105.2.3 have the same length axis as the EC plots in KFR105.2.1 and KFR105.2.2. There is a sharp increase of temperature at the end of the borehole, especially in the first (2009-06-25) measurement. In both cases the measurement began at the end of the borehole. In the first measurement, the tool had stayed a night at the end of the borehole before the measurement could be started. This could explain the difference between the two measurement at the end of the borehole.

There is probably a flow yielding fracture at the bottom of the borehole, see flow and single point curves in Appendix KFR105.3.16. Its length coordinate would be 306.1 m. It is not included in the list of inferred flow anomalies since its flow value could not be determined. A small flow from this fracture could be a reason to the increase of temperature at the end of the borehole.

The small temperature anomalies in the results of measurements on 2009-06-25 are artefacts and related to the thermal inertia of the tool. These anomalies are caused by tool stop at 5 m intervals.

The length calibration of the measurement of borehole EC is not as accurate as in other measurements, because single-point resistance is not registered. The length correction of the SPR/caliper-measurement was applied to the borehole EC measurements, black curve in Appendix KFR105.1.14.

6.2.2 Electrical conductivity of fracture-specific water

If the flow direction in a fracture is from the fracture into the borehole, the determination of electrical conductivity from fracture-specific water is possible. Both electrical conductivity and temperature of flowing water from the fractures were measured.

The fractures detected in the flow measurements can be measured for electrical conductivity later. These fracture-specific measurements begin near the fracture which has been chosen for inspection. The tool is first moved stepwise closer to the fracture until the detected flow is larger than a predetermined limit. At this point the tool is stopped. The measurement is continued at the given position allowing the fracture-specific water to enter the section. The waiting time for the EC measurement can be automatically calculated from the measured flow rate. The aim is to flush the water volume within the test section sufficiently to gain accurate results. The measuring computer is programmed so that the water in the test section will be replaced approximately three times over. After the set of stationary measurements, the tool is once again moved stepwise past the fracture. The electrical conductivity is also measured during the stepwise movement before and after the set of stationary measurements.

The test section in these measurements was 1 m long and the tool was moved in 0.1 m steps. The water volume in a 1 m long test section is 3.6 L. The results are presented in Appendices KFR105.11.1–KFR105.11.3. The blue symbol represents the conductivity value when the tool was moved and the red symbol is used for the set of stationary measurements.

Lengths to the upper and lower ends of the section, fracture locations and the final EC values for borehole are listed in Table 6-2. The uncertain fracture at 173 m was measured along with the fracture at 172.2 m. The obtained EC value represents both of these fractures although the flow of the 172.2 m fracture is significantly larger and therefore should be predominant in the results. The measured locations were chosen based on the 5 m section length measurements in which the resolution for anomaly detection is not as good as in the 1 m section length measurements.

For comparison, the fracture-specific EC and temperature results are also plotted with the EC and temperature results of borehole water, see Appendices KFR105.2.1–KFR105.2.3.

Table 6-2. Fracture-specific EC.

Upper end of section (m)	Lower end of section (m)	Measured fractures(m)	EC (S/m) at 25°C
282.79	283.79	283.5	1.00
266.51	267.51	267.3	1.11
172.06	173.06	172.7,173	1.08
133.10	134.10	133.7	1.07
123.49	124.49	124.1	1.14
107.20	108.20	107.7	1.13
76.64	77.64	77.3	1.21
38.65	39.65	39.4	1.06

6.3 Pressure measurements

No absolute pressure measurements were conducted during this measurement campaign because the borehole is nearly horizontal. Absolute pressure measurement is carried out because the density of the borehole fluid is not exactly constant. In deep vertical boreholes absolute pressure varies not only by depth but also by the density of the water column above the point of measurement. In horizontal boreholes the latter effect is insignificant.

6.4 Flow logging

6.4.1 General comments on results

The measuring programme contained several flow logging sequences. They were gathered on the same diagram with single-point resistance (right hand side) and caliper plots (in the middle), see Appendices KFR105.3.1–KFR105.3.16. SPR has a lower value on a fracture where flow is detected. Many other resistance anomalies result from other fractures and geological features. As the electrode of the SPR tool is located within the upper rubber sealing disks of the probe, the locations of resistance anomalies associated with leaky fractures coincide with the lower end of the flow anomalies.

The caliper tool has been adjusted and specified to change its output from a high voltage value to a low voltage value between borehole diameters 77–78 mm.

The flow logging was first performed with a 5 m section length and with 0.5 m length increments. The method (overlapping flow logging) gives the length and the thickness of conductive zones with a length resolution of 0.5 m.

The direction of small flows (< 100 mL/h) cannot be detected in the normal overlapping mode (thermal dilution method). Therefore the measurement time was longer (so that the thermal pulse method could be used) at every 5 metre interval in the 5 m section measurement. It is common that the flows in open underground boreholes are directed towards the borehole.

The test section length determines the width of a flow anomaly of a single fracture. If the distance between flow yielding fractures is less than the section length, the anomalies will overlap, resulting in a stepwise flow data plot. The overlapping flow logging was repeated using a 1 m long test section and 0.1 m length increments.

The positions (borehole length) of the detected fractures are shown on the caliper scale. They are interpreted on the basis of the flow curves and therefore represent flowing fractures. A long line represents the location of a leaky fracture; a short line denotes that the existence of a leaky fracture is uncertain. The short line is used if the flow rate is less than 30 mL/h or the flow anomalies are overlapping or unclear because of noise.

The coloured triangles show the magnitude and direction of the measured flows. The triangles have the same colour than the corresponding curves.

The explanations to the tables in Appendices KFR105.5 and KFR105.7 are given in Appendix KFR105.4.

6.4.2 Transmissivity of borehole sections

Two sets of flow measurements are needed for calculation of transmissivity as described in Section 3, Equation 3-6. The head in the borehole h_1 corresponds the situation in a pumped borehole. In this case the borehole is freely flowing into the tunnel and h_1 is the water level at the top of the borehole (–106.82 m in RHB 70 scale). The un-pumped condition when the hydraulic head in the borehole would be h_0 could be the case when the borehole is closed. In that case h_0 would be closer to the sea level, i.e. h_0 0. For technical reasons, flow rates at this pressure were not measured.

The assumptions for calculation of transmissivity are $(h_1–h_0)$ h_1 and $(Q_{S0}–Q_{S1})$ $–Q_{S1}$ in Equation 3-6.

The two assumptions made above would mean that the hydraulic head of all fractures crossed by the borehole is nearly zero, i.e. they are hydraulically well connected to the ground surface but not to the tunnel. In such case there would be no internal flows in the closed borehole.

It is clear that the assumptions made above do not hold and the calculated transmissivities are only rough estimates. Typically the assumptions hold better for fractures or sections far away from the tunnel. The transmissivity values are too small for fractures or sections that are well hydraulically connected to the tunnel. There is even a risk that some of such transmissive fractures remained undetected.

The results of the flow logging measurements with a 5 m section length are presented in tables, see Appendices KFR105.5.1–KFR105.5.3. Only the results with 5 m length increments are used. All borehole sections are shown in Appendices KFR105.3.1–KFR105.3.16. Secup and Seclow in Appendices KFR105.5.1–KFR105.5.3 are the distances along the borehole from the reference level (tunnel wall) to the upper end of the test section and to the lower end of the test section, respectively.

In Appendices KFR105.5.1–KFR105.5.3 h_{0FW} was assumed to be zero and h_{1FW} is the hydraulic head of the borehole for the flow measurement with the 5 m section length (–106.82 m in RHB 70 scale).

The flow rates are positive if the flow direction is from the bedrock into the borehole and vice versa. 55 sections were detected as flow yielding in the 5 m section length measurement. All of the flows were positive.

It is also possible to detect the existence of flow anomalies below the measurement limit (30 mL/h = $8.33 \cdot 10^{-9}$ m^3/s), even though the exact numerical values below the limit are uncertain.

The flow data is presented as a plot, see Appendix KFR105.6.1. The left-hand plot in each diagram represents flow from the borehole into the bedrock for the respective test sections, while the right-hand plot represents flow from the bedrock into the borehole. If flow could not be detected (zero flow), no corresponding point will be visible on the logarithmic plots in the appendices.

The lower and upper measurement limits of the flow are also presented in the plot (Appendix KFR105.6.1) and in the tables (Appendix KFR105.5). There are theoretical and practical lower limits of flow, see Section 6.4.4.

Since in this case there was only one measurement, the hydraulic head of sections could not be calculated. The transmissivity results are illustrated in Appendix KFR105.6.2. The upper and lower limits of transmissivity are only qualitative because the assumptions described above (Appendix KFR105.5 and Appendix KFR105.6.2).

The sum of all the detected flows (Q_1) was $1.65 \cdot 10^4$ m^3/s (9.93 L/min). The outflow from the borehole was approximately 12.6 L/min during the measurement. These values should normally be equal if all the flows in the borehole are not disturbed by noise or other external factors, the outflow is constant and the fractures are at steady state pressure. There may be leaks at the interface between the casing and the borehole. Such flows cannot be properly measured because of the wide diameter of the casing tube. The centralizer in the measurement device and drill debris in the borehole prohibit measuring the borehole all the way to the bottom, and it is possible that there are flows in this area.

6.4.3 Transmissivity of fractures

An attempt was made to evaluate the magnitude of fracture-specific flow rates. The results for a 1 m section length and 0.1 m length increments were used for this purpose. The first step in this procedure is to identify the locations of individual flowing fractures and then evaluate their flow rates.

In cases where the fracture distance is less than one metre, it may be difficult to evaluate the flow rate. There are such cases for instance in Appendix KFR105.3.3. In these cases a stepwise increase or decrease in the flow data plot equals the flow rate of a specific fracture (filled triangles in the appendices).

The total amount of detected flowing fractures was 150. These fractures were used for transmissivity estimations. Transmissivity of fractures is presented in Appendices KFR105.7 and KFR105.8.

Some fracture-specific results were classified to be "uncertain." The basis for this classification is either a minor flow rate (< 30 mL/h) or unclear fracture anomalies. Anomalies are considered unclear if the distance between them is less than 1 m or their nature is unclear because of noise.

Fracture-specific transmissivities were compared with transmissivities of sections in Appendix KFR105.9. All fracture-specific transmissivities within each 5 m interval were first summed together to make them comparable with measurements with a 5 m section length. The results are fairly consistent between the two types of measurements. The decrease of outflow as a function of time can be seen in some fractures. The 1 m section measurements were carried out later than the 5 m section measurements and therefore flow rate and transmissivity can be smaller in the 1 m section measurement results.

The sum of the detected flows, $1.59\cdot10^{4}$ m^3/s (9.56 L/min), was again smaller than the average pumping rate which was approximately 12.4 L/min and it further supports the possibility that there is one or more flows near the bottom or at the casing borehole interface.

6.4.4 Theoretical and practical measurement limits of flow and transmissivity

The theoretical minimum for measurable flow rate is some 30 mL/h. The upper limit of flow measurement is 300,000 mL/h. As these upper and lower limits are determined by flow calibration, it is assumed that flows can be reliably detected between the upper and lower theoretical limits in favorable borehole conditions.

In practice, the minimum measurable flow rate may be much higher. Borehole conditions may have an influence on the flow base level (i.e. noise level). Noise levels can be evaluated in intervals along the borehole where there are no flowing fractures or other complicating structures, and may vary along a borehole.

There are several known reasons for increased noise in the flow:

1) Roughness of the borehole wall.
2) Solid particles such as clay or drilling debris in the water.
3) Gas bubbles entrained in the water.
4) High flow rate along the borehole.

Roughness in the borehole wall always results in high levels of noise, not only in the flow results, but also in the SPR results. The flow curve and SPR curves are typically spiky when the borehole wall is rough.

Drilling debris usually increases noise levels. This kind of noise is typical for both natural (un-pumped) and pumped conditions.

Pumping results in lower pressure in the borehole water and in the water in fractures located near the borehole. This may lead to the release of dissolved gas and increase the quantity of gas bubbles entrained in the water. Some fractures may produce more gas than others. Sometimes, when the borehole is being measured upwards, increased noise levels are observed just above certain fractures. The reason for this is assumed to be gas bubbles.

The effect of a high flow rate along the borehole can often be seen above fractures with a high flow. Any minor leakage in the seal provided by the lower rubber sealing disks will appear in the measurement as increased levels of noise.

A high level of noise in a flow will mask the “real” flow if this is smaller than the noise. Real flows are registered correctly if they are about ten times larger than the noise but are totally invisible if they are some ten times smaller than the noise. Experience indicates that real flows between one-tenth of the noise level and 10 times the noise level are summed with the noise. Noise levels could therefore be subtracted from measured flows to get real flows. This correction has not yet been carried out because the cases to which it is applicable are unclear.

The practical minimum for measurable flow rate is presented in Appendices KFR105.3.1–KFR105.3.16 using a grey dashed line (Lower limit of flow rate). The practical minimum level of the measurable flow was evaluated using the flow data obtained in the 1 m section length measurements. The limit is an approximation. It is evaluated to obtain a limit below which there may be fractures or structures that remain undetected.

The noise level varied between 30 mL/h and 150 mL/h. It is possible to detect the existence of flow anomalies below the theoretical limit of the thermal dilution method (30 mL/h). The noise line (grey dashed line) was never drawn below 30 mL/h, because the values of flow rate measured below 30 mL/h are uncertain.

In some boreholes the upper limit of flow measurement (300,000 mL/h) may be exceeded. Such fractures or structures hardly remain undetected (as the fractures below the lower limit). There were no such fractures detected during this campaign.

The practical minimum for measurable flow rate is also presented in Appendix KFR105.5 (Q-lower limit P) and is obtained from the plots in Appendix KFR105.3 (Lower limit of flow rate). The practical minimum of measurable transmissivity can be evaluated using Q-lower limit and the assumed head difference at each measurement location, see Appendix KFR105.5 (T_D-measl$_{LP}$). The theoretical minimum for measurable transmissivity (T_D-measl$_{LT}$) is evaluated using a Q value of 30 mL/h (the minimum theoretical flow rate using the thermal dilution method). The upper measurement limit for transmissivity can be evaluated using the maximum flow rate (300,000 mL/h) and the assumed head difference as above, see Appendix KFR105.5 (T_D-measl$_U$). These transmissivity limits are only qualitative because of the assumptions described in Section 6.4.2.

All three flow limits are plotted with the measured flow rates, see Appendix KFR105.6.1.

The three transmissivity limits are also presented graphically, see Appendix KFR105.6.2.

Similar flow and transmissivity limits are not provided for the fracture-specific results as the limits for these are harder to define. The situation is similar for the upper flow limit. If several high-flowing fractures are positioned closer to one another than a distance of 1 m, the upper flow limit will depend on the sum of these flows, and this must be below 300,000 mL/h.

6.5 Borehole pressure and natural outflow from the borehole

The pressure in the borehole was measured initially before the borehole was opened for measurements. After the measurements were complete the recovery transient of the borehole pressure was measured manually by PRG-Tec Oy. The results are shown in Appendix KFR105.10.1. The build-up of pressure was also measured automatically by Geosigma Oy on July 2 after they had finished their own measurements in the borehole, see Appendix KFR105.10.2.

The outflow from the borehole was measured manually during the flow logging measurements. The results are presented in Appendix KFR105.10.1.

6.5.1 Transmissivity of the entire borehole

(by J-E Ludvigson, Geosigma AB)

In KFR105, a separate pressure build-up test was performed after a flow period. A packer was installed just inside the end of the casing in the core borehole interval. The test is utilized to evaluate the transmissivity of this interval. Firstly, the transmissivity is estimated by two steady-state methods using Moye's equation and Dupuit's formula, respectively from the flow period of the test as described in Chapter 3.2. In addition, transient analysis is performed on the pressure recovery period after the flow period.

Transient analysis on the pressure recovery period is done in accordance with Instruction SKB MD 320.004 for analysis of hydraulic injection and single-hole pumping tests (SKB internal controlling document). Briefly, it specifies that the transient analysis of the pressure recovery should be made versus Agarwal equivalent time in log-log and semi-log plots including the pressure derivative. The storativity S was estimated from an empirical relationship between T and S described in the MD above.

Furthermore, the skin factor, borehole storage coefficient C and the radius of influence r_i of the dominating structure intersecting the borehole were also be estimated. If the transmissivity changes during the test, e.g. due to hydraulic boundaries or other hydraulic structures with deviating transmissivity, the estimated hydraulic properties (and radius of influence) should be based on the early response before any effects of hydraulic boundaries are observed.

KFR105

Steady-state analysis

The final flow rate Q_p was c 14 L/min during the first flow period which had a duration of c 42 min. The maximal pressure change during this period was estimated to s_p= 93.04 m. The initial pressure p_i before the first flow period was assumed as the final pressure during the subsequent pressure recovery period, cf Figure 6-1. The second flow period was not analysed. The steady-state transmissivity calculated with Dupuit's formula (Equation 3-9) and Moye's equation (Equation 3-10), respectively from the first flow period is shown in Table 6-5. In Dupuit's formula, the ratio R/r_0 is assumed to be 500, cf Chapter 3. In Moye's formula, the length of the isolated test section L is c 303 m (c. 1 m packer length) and the borehole diameter $2r_0$ is 0.0758 m. The borehole is 306.81 m long and cased in the interval 0–2.64 m with an inner diameter of 0.080 m.

Transient analysis

Figures 6-2a and b shows log-log and semi-log plots respectively of the transient pressure recovery after the first flow period in the cored interval of KFR105. The pressure recovery seems to be dominated by wellbore storage only during the first few seconds. After a transition period, pseudo-radial flow (PRF) occurs between c 70–200 s, cf Figure 6-2a. After this time slightly pseudo-spherical (leaky) flow is indicated by the pressure derivative.

From the transient response during the recovery period test parameters were estimated for an assumed storativity value (calculated from the empirical relationship between T and S). The best fit simulation with a model based on radial flow transiting to pseudo-spherical (leaky) flow yields a transmissivity $T = 1.8·10^{–6}$ m^2/s, a skin factor of –3.0 and a wellbore storage coefficient of $C=1.8·10^{–9}$ m^3/Pa for the isolated test section. The latter coefficient is calculated from the simulated effective casing radius r_c of the borehole. The estimated transmissivity of borehole KFR105 according to the three methods described above is given in Table 6-3. The transient transmissivity T_T was selected as the most representative for the borehole.

Table 6-3. Estimated transmissivity of borehole KFR105.

Method	Transmissivity (m^2/s)
Dupuit	$2.5·10^{–6}$
Moye	$3.7·10^{–6}$
Transient	$1.8·10^{–6}$

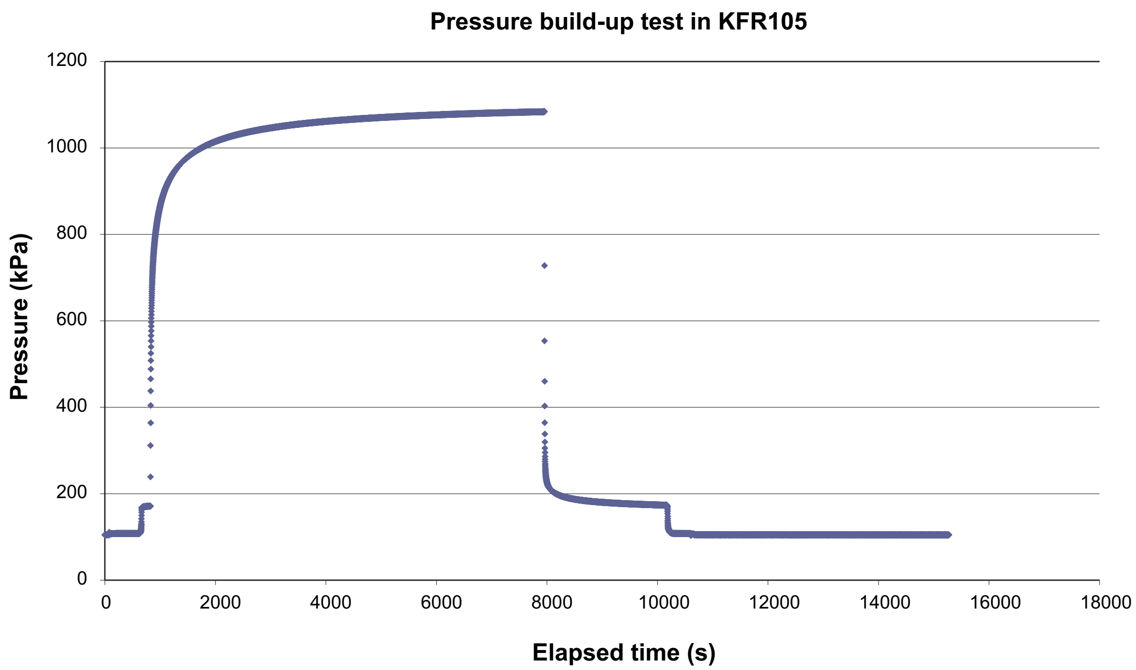

Figure 6-1. *Lin-lin overview plot of the pressure history during the pressure build-up test in KFR105 (isolated core borehole section) showing the observed pressure during the end of the first flow period and the subsequent pressure recovery followed by a second flow period.*

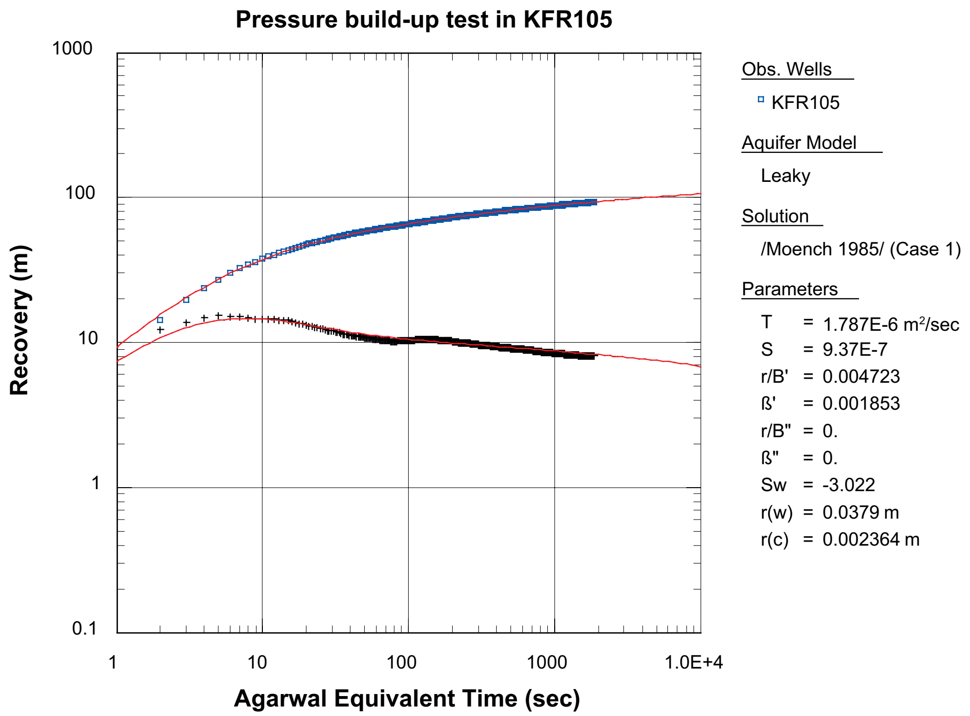

Figure 6-2a. *Log-log plot of the pressure recovery in KFR105 (isolated borehole section) with the observed pressure recovery (□) and associated derivative (+) versus Agarwal equivalent time together with simulated best fit curves of the pressure recovery and its derivative (–).*

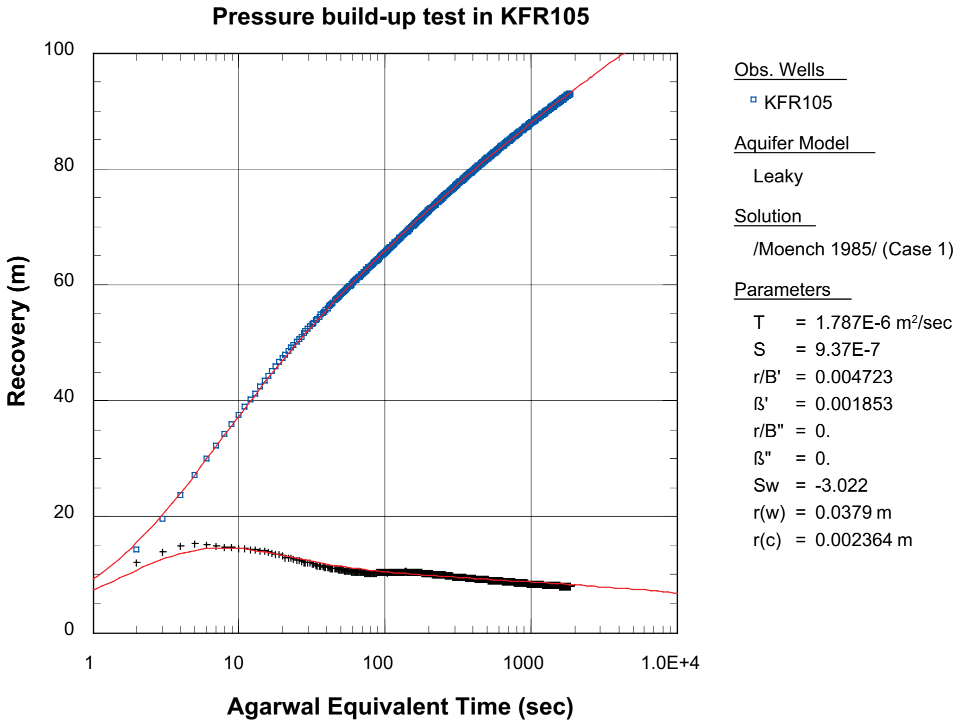

Figure 6-2b. *Lin-log plot of the pressure recovery in KFR105 (isolated borehole section) with the observed pressure recovery (□) and associated derivative (+) versus Agarwal equivalent time together with simulated best fit curves of the pressure recovery and its derivative (–).*

7 Summary

In this study, the Posiva Flow Log, Difference Flow Method has been used to determine the location and flow rate of flowing fractures or structures in borehole KFR105 at Forsmark, Sweden. A 5 m section length with 0.5 m length increments was used initially. The borehole was re-measured with a 1 m section and a 0.1 m measurement interval.

Length calibration was made in using the length marks in the borehole wall. The length marks were detected by caliper and single-point resistance logging. The latter method was also performed simultaneously with the flow measurements, and thus all flow results could be length calibrated by synchronizing the single-point resistance logs.

The distribution of saline water along the borehole was logged by electrical conductivity and temperature measurements of the borehole water. In addition, the electrical conductivity of fracture-specific water was measured in selected flowing fractures.

The water level in the borehole during pumping and its recovery after the pump was turned off were also measured.

The total amount of detected flowing fractures was 150. Transmissivity was calculated for measured borehole sections and fractures. The highest estimated fracture transmissivity ($6.5 \cdot 10^{7}$ m^2/s) was at 133.7 m. The calculated transmissivities are rough estimates because the measurements were carried out in only one pressure condition. The highest section transmissivities were detected at length interval 132.91–137.91 m and 167.95–177.97 m.

References

Heikkonen J, Heikkinen E, Mäntynen M, 2002. Mathematical modelling of temperature adjustment algorithm for groundwater electrical conductivity on basis of synthetic water sample analysis. Helsinki, Posiva Oy. Working report 2002-10 (in Finnish).

Ludvigson J-E, Hansson K, Rouhiainen P, 2002. Methodology study of Posiva difference flow meter in borehole KLX02 at Laxemar. SKB R-01-52, Svensk Kärnbränslehantering AB.

Marsily G, 1986. Quantitative Hydrogeology, Groundwater Hydrology for Engineers. Academic Press, Inc. London.

Moench A F, 1985. Transient flow to a large-diameter well in an aquifer with storative semiconfining layers, Water Resources Research, vol. 21, no. 8, pp 1121–1131.

Moye D G, 1967. Diamond drilling for foundation exploration. Civil Eng. Trans. Inst. Eng. Australia, 95–100.

Öhberg A, Rouhiainen P, 2000. Posiva Groundwater Flow Measuring Techniques. Posiva 2000-12.

Appendices

Appendices	KFR105.1.1–KFR105.1.13	SPR and Caliper results after length correction
Appendix	KFR105.1.14	Length correction
Appendices	KFR105.2.1–KFR105.2.2	Electrical conductivity of borehole water
Appendix	KFR105.2.3	Temperature of borehole water
Appendices	KFR105.3.1–KFR105.3.16	Flow rate, caliper and single point resistance
Appendix	KFR105.4	Explanations for the tables in Appendices 5 and 7
Appendices	KFR105.5.1–KFR105.5.3	Results of sequential flow logging
Appendix	KFR105.6.1	Plotted flow rates of 5 m sections
Appendix	KFR105.6.2	Plotted transmissivity and head of 5 m sections
Appendices	KFR105.7.1–KFR105.7.4	Inferred flow anomalies from overlapping flow logging
Appendix	KFR105.8	Plotted transmissivity of detected fractures
Appendix	KFR105.9	Comparison between section transmissivity and fracture transmissivity
Appendix	KFR105.10.1	Borehole pressure and natural outflow from the borehole
Appendix	KFR105.10.2	Pressure build-up test
Appendices	KFR105.11.1–KFR105.11.3	Fracture-specific EC results by date

Forsmark, borehole KFR105
SPR and Caliper results after length correction

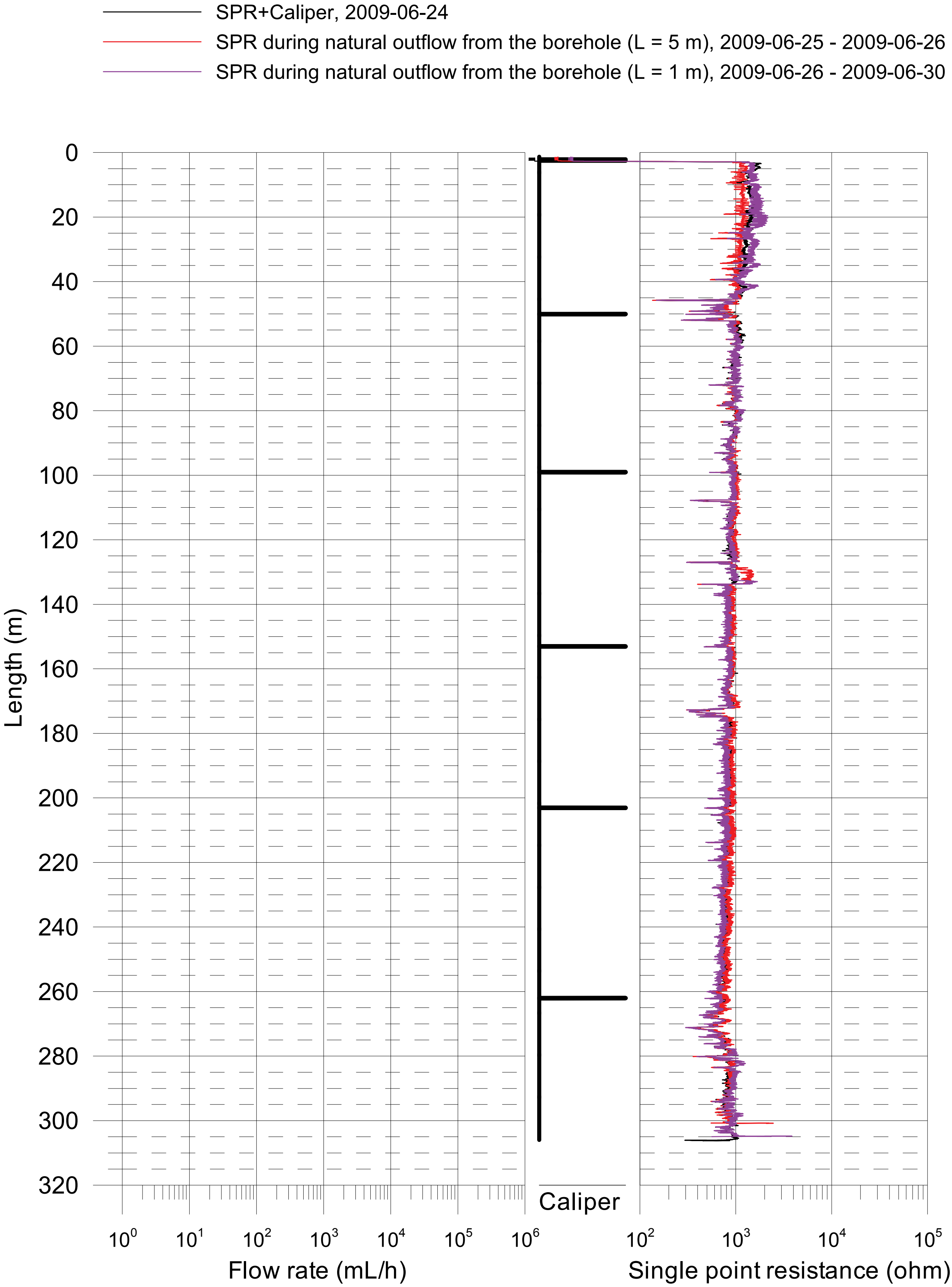

Forsmark, borehole KFR105
SPR and Caliper results after length correction

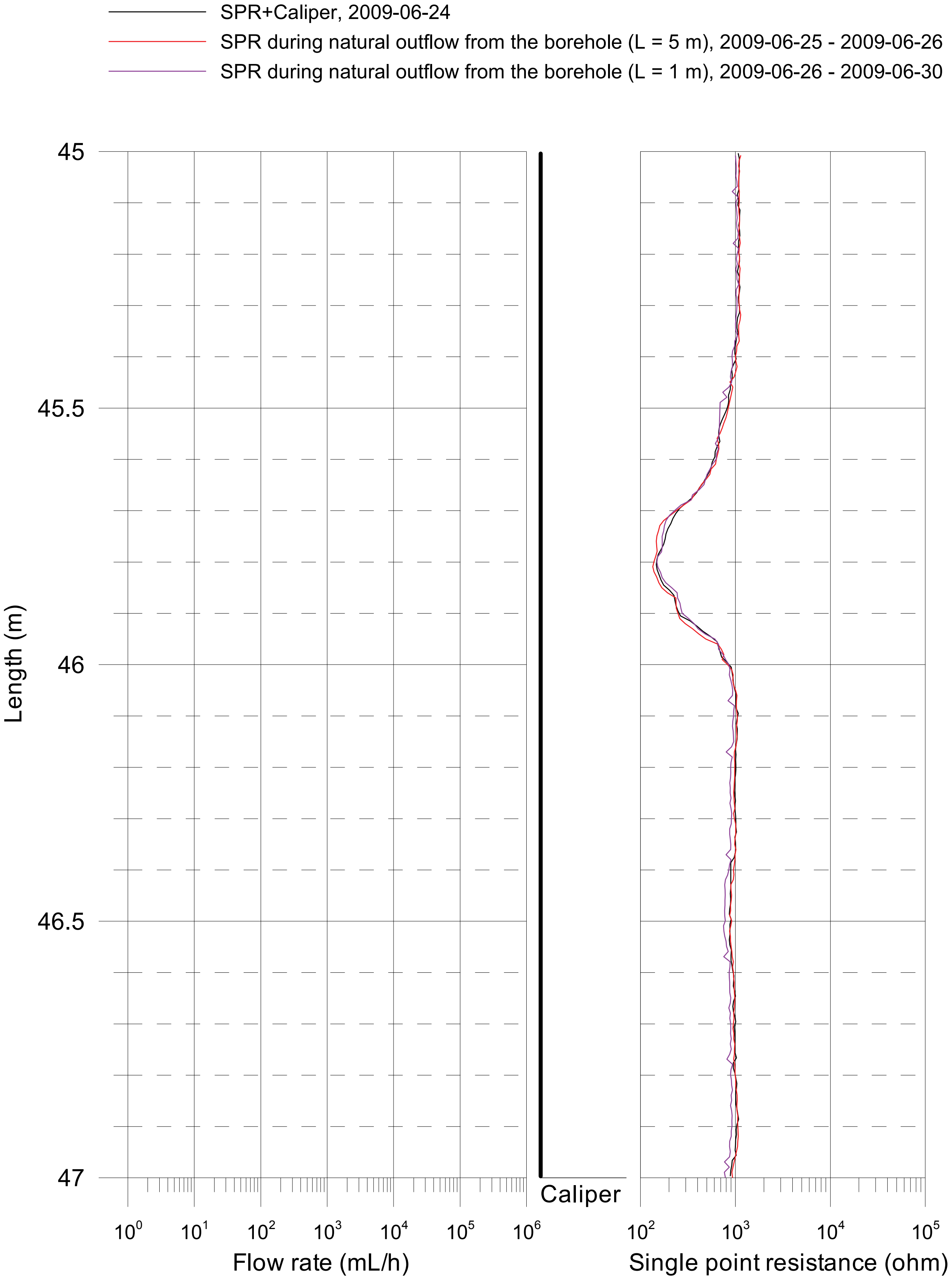

Forsmark, borehole KFR105
SPR and Caliper results after length correction

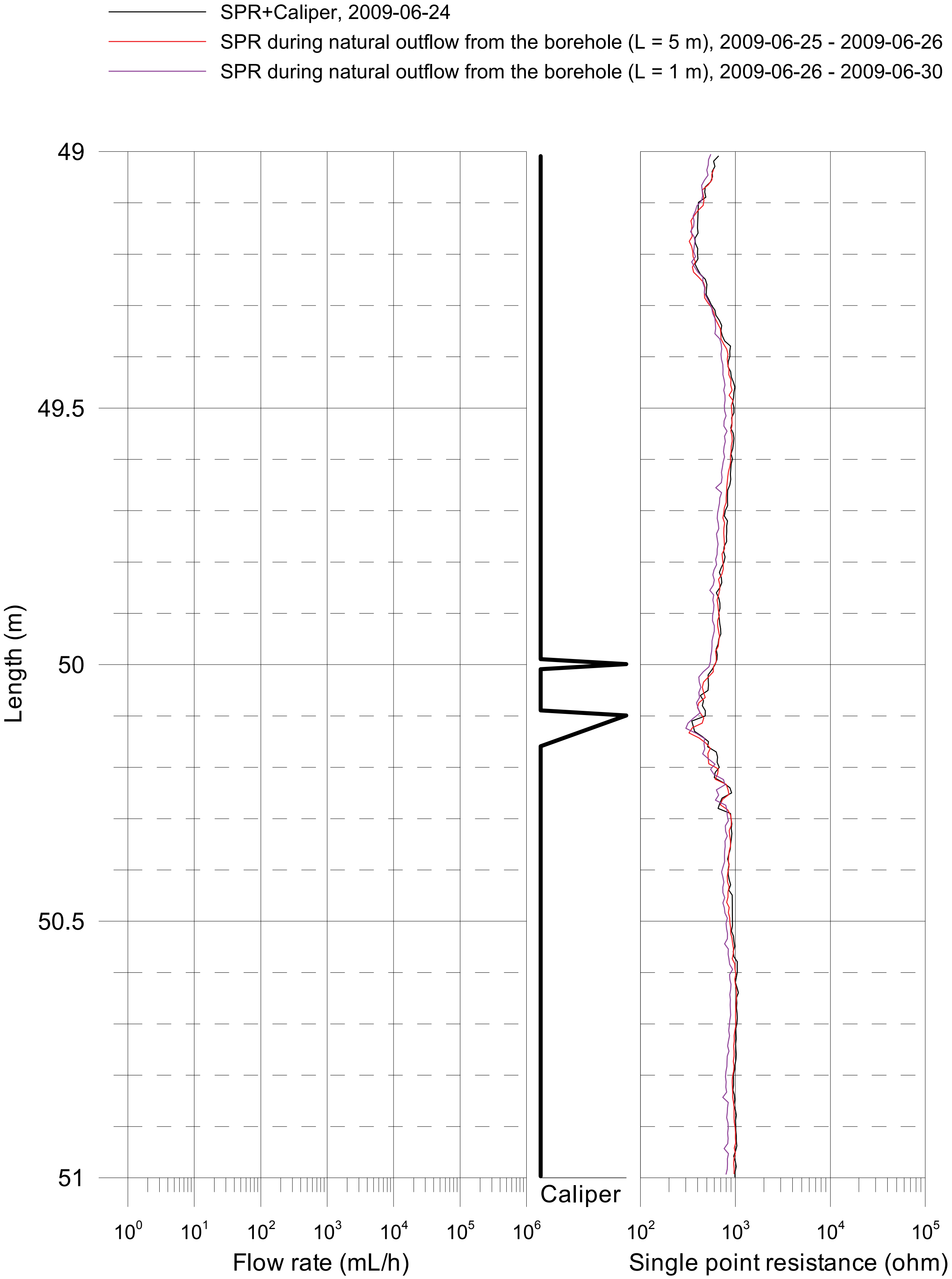

Forsmark, borehole KFR105
SPR and Caliper results after length correction

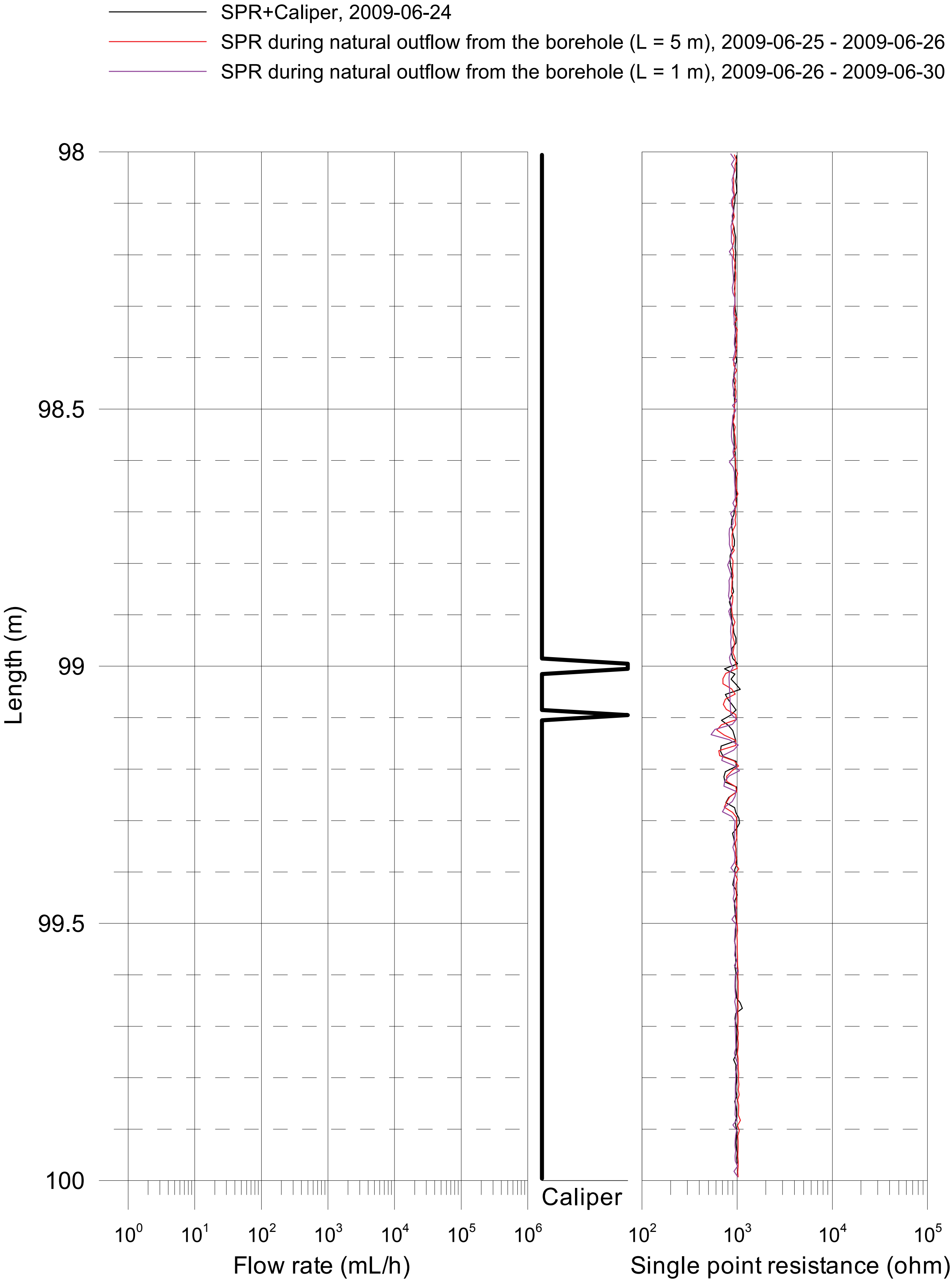

Forsmark, borehole KFR105
SPR and Caliper results after length correction

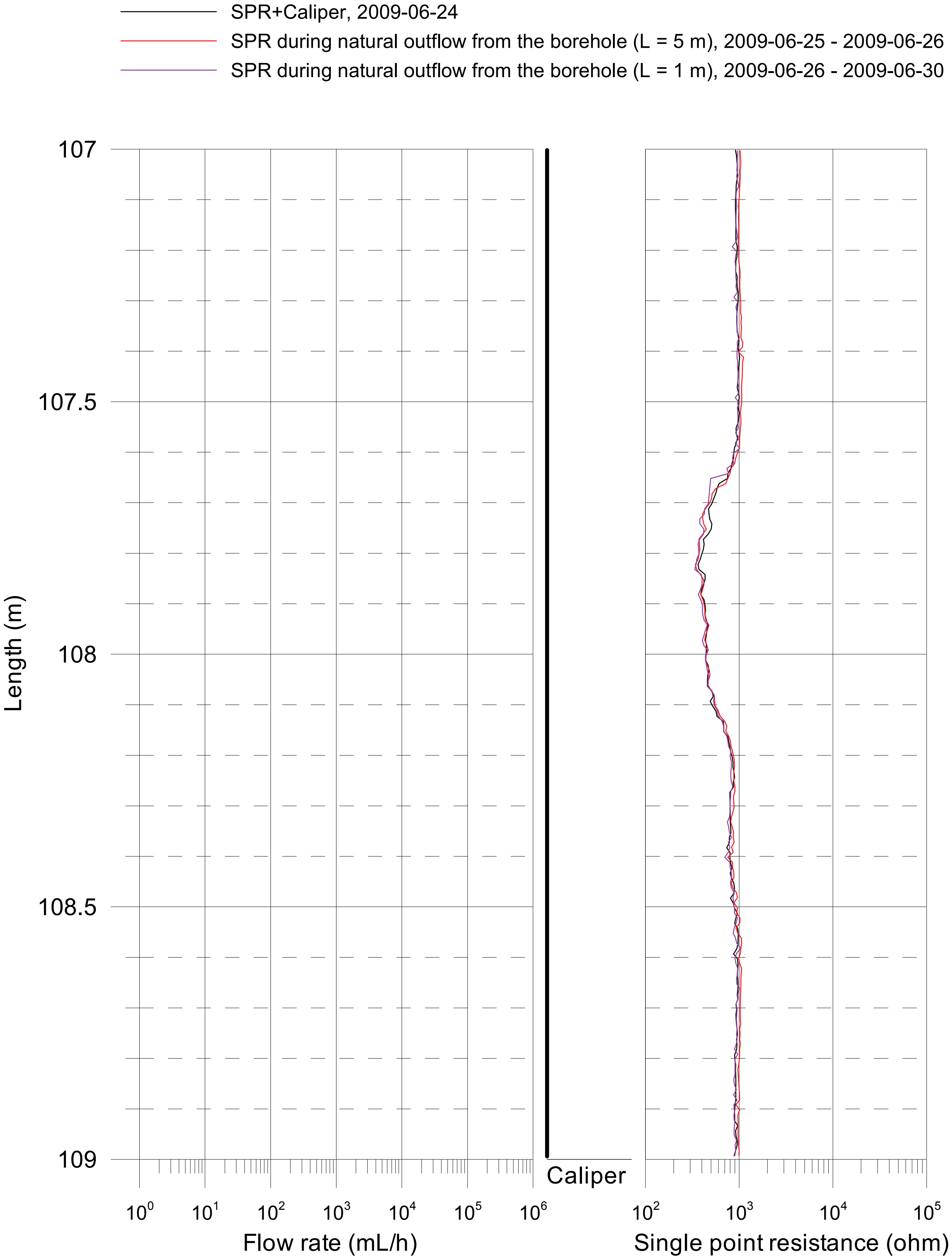

Forsmark, borehole KFR105
SPR and Caliper results after length correction

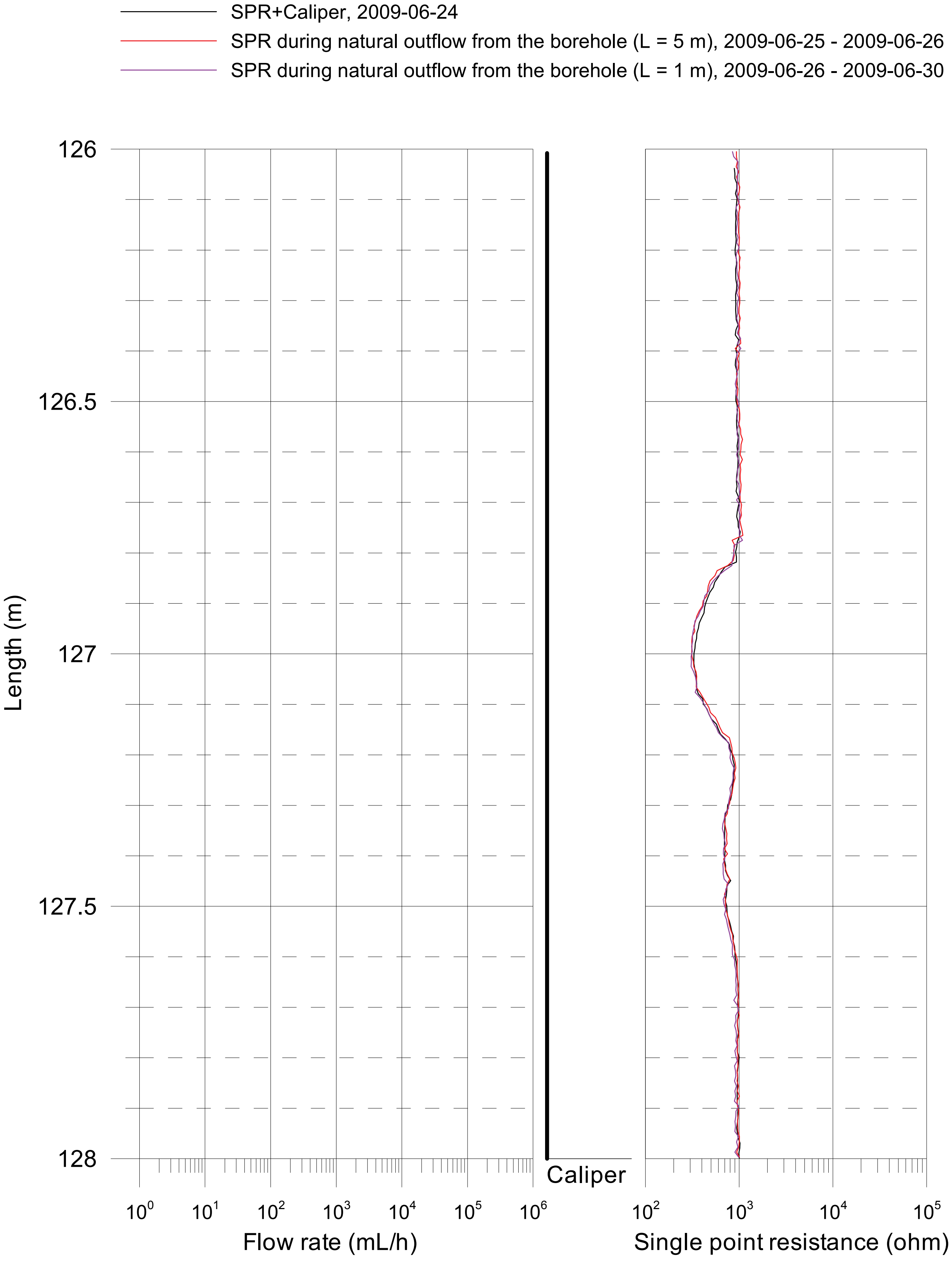

Forsmark, borehole KFR105
SPR and Caliper results after length correction

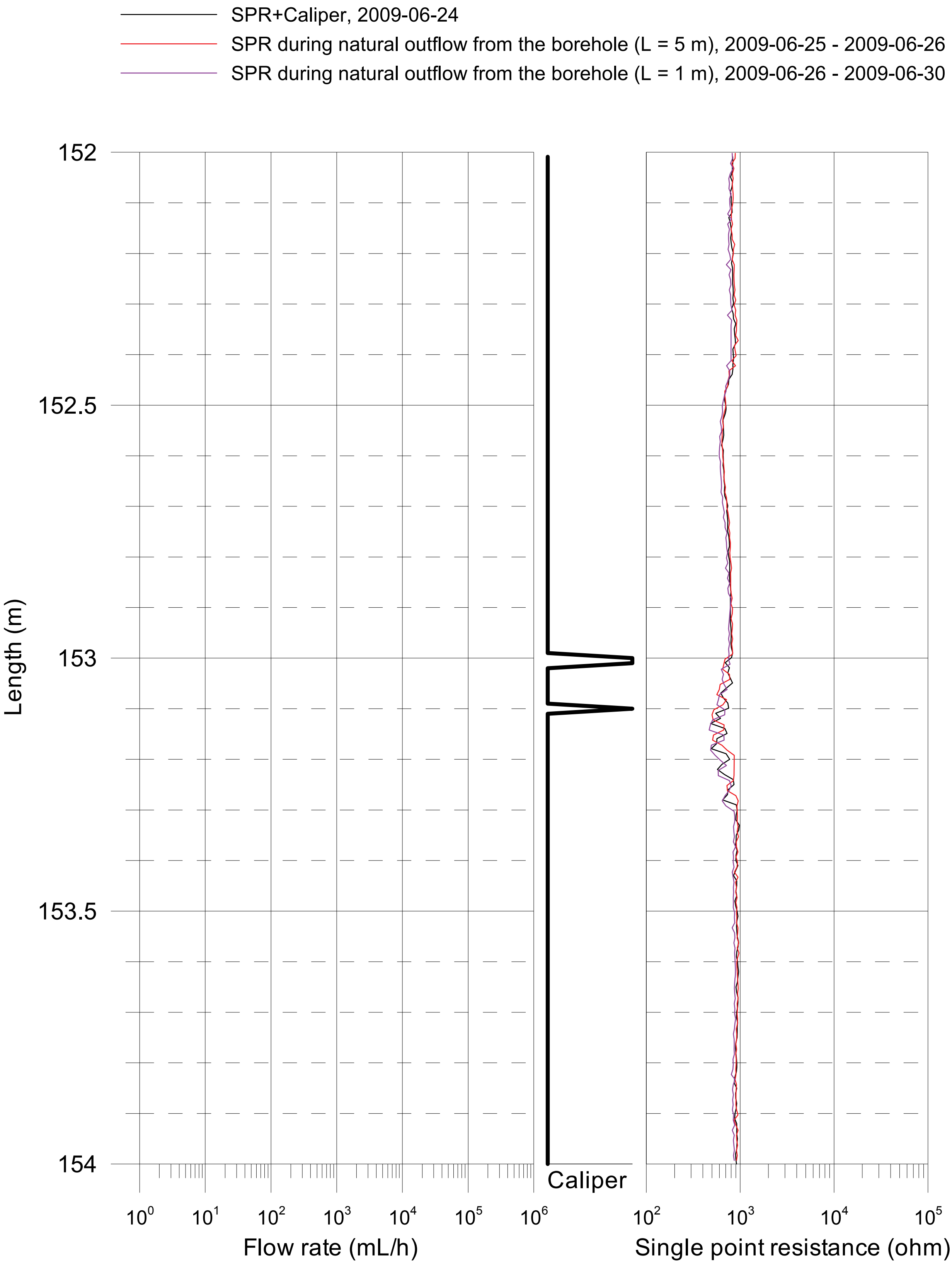

Forsmark, borehole KFR105
SPR and Caliper results after length correction

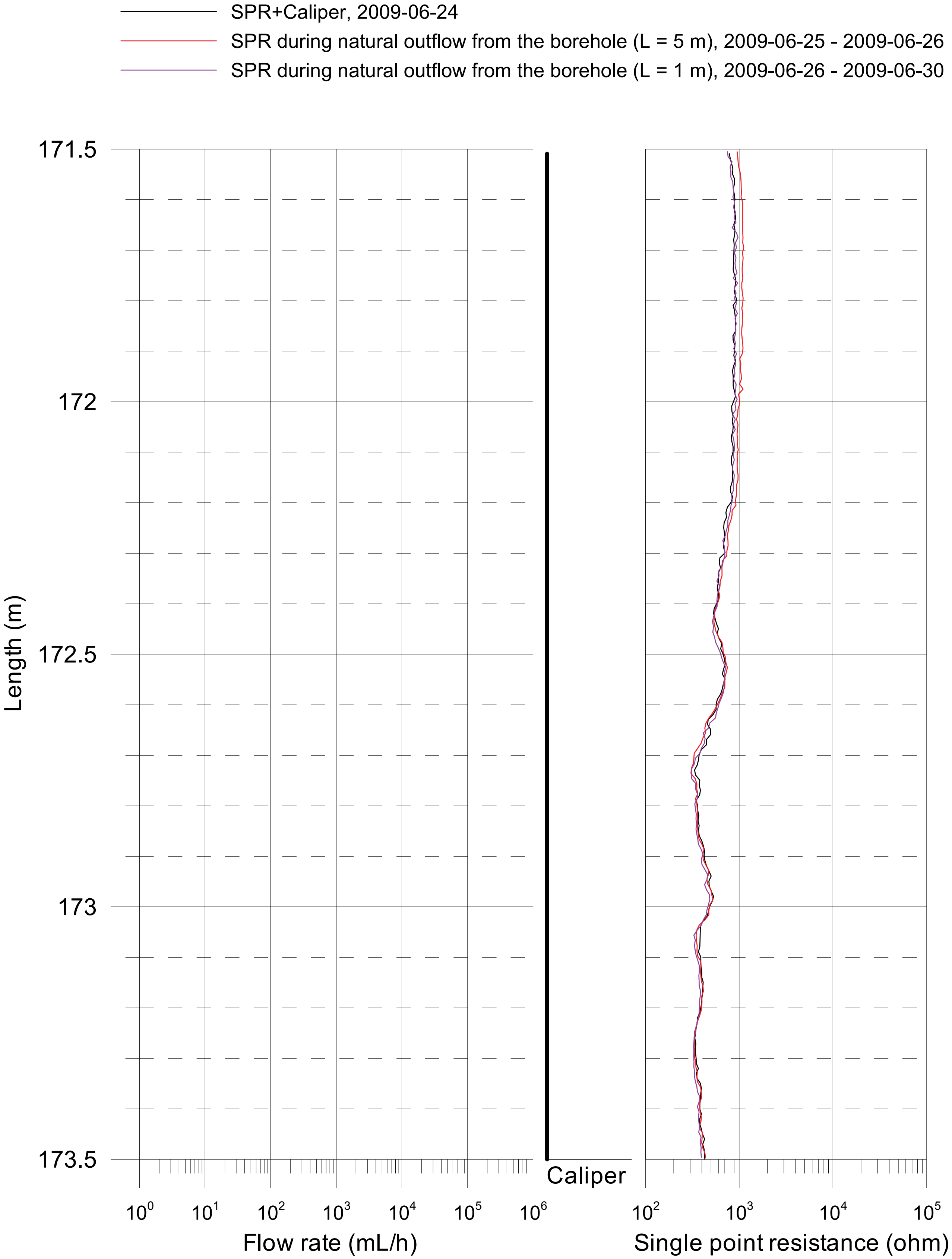

Forsmark, borehole KFR105
SPR and Caliper results after length correction

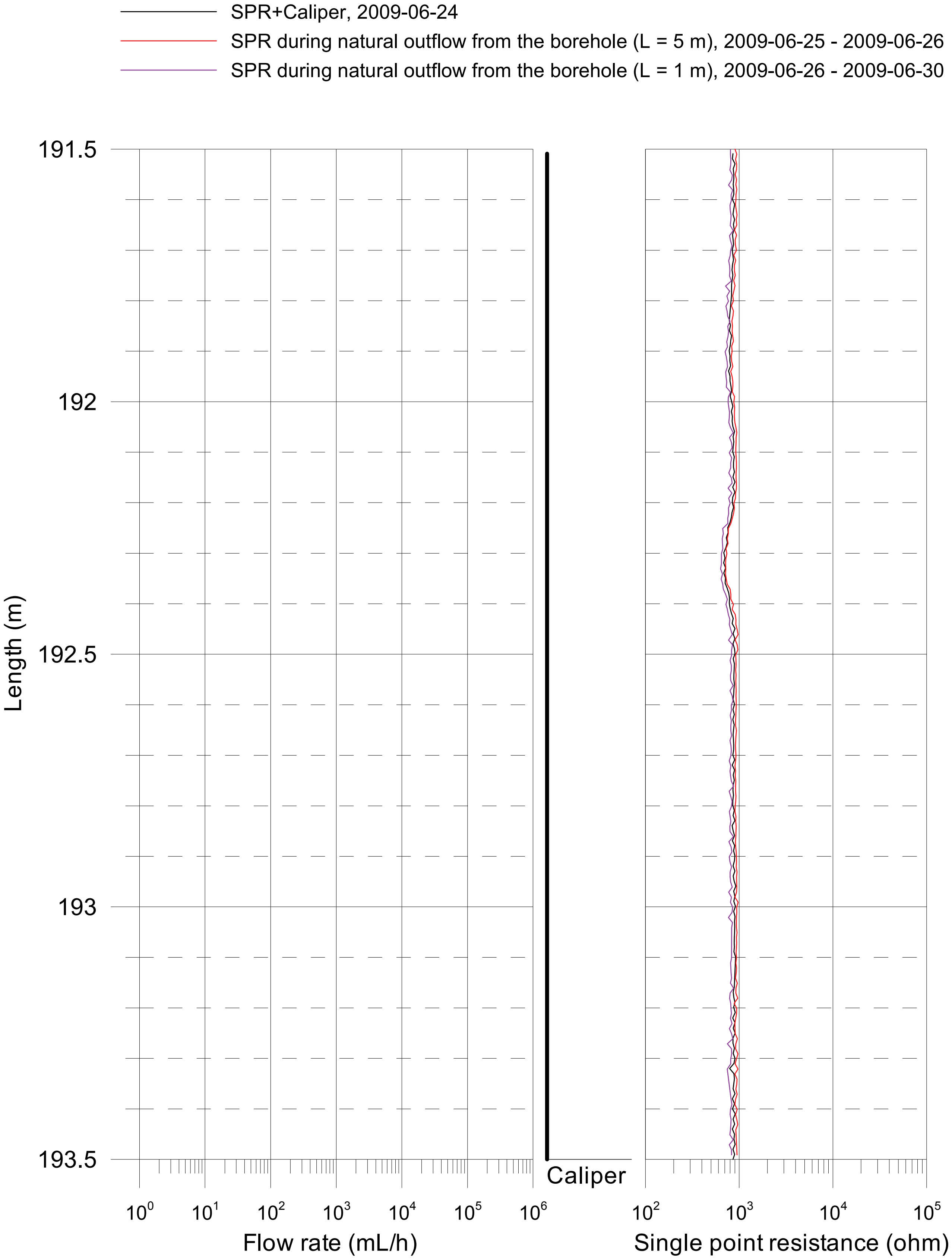

Forsmark, borehole KFR105
SPR and Caliper results after length correction

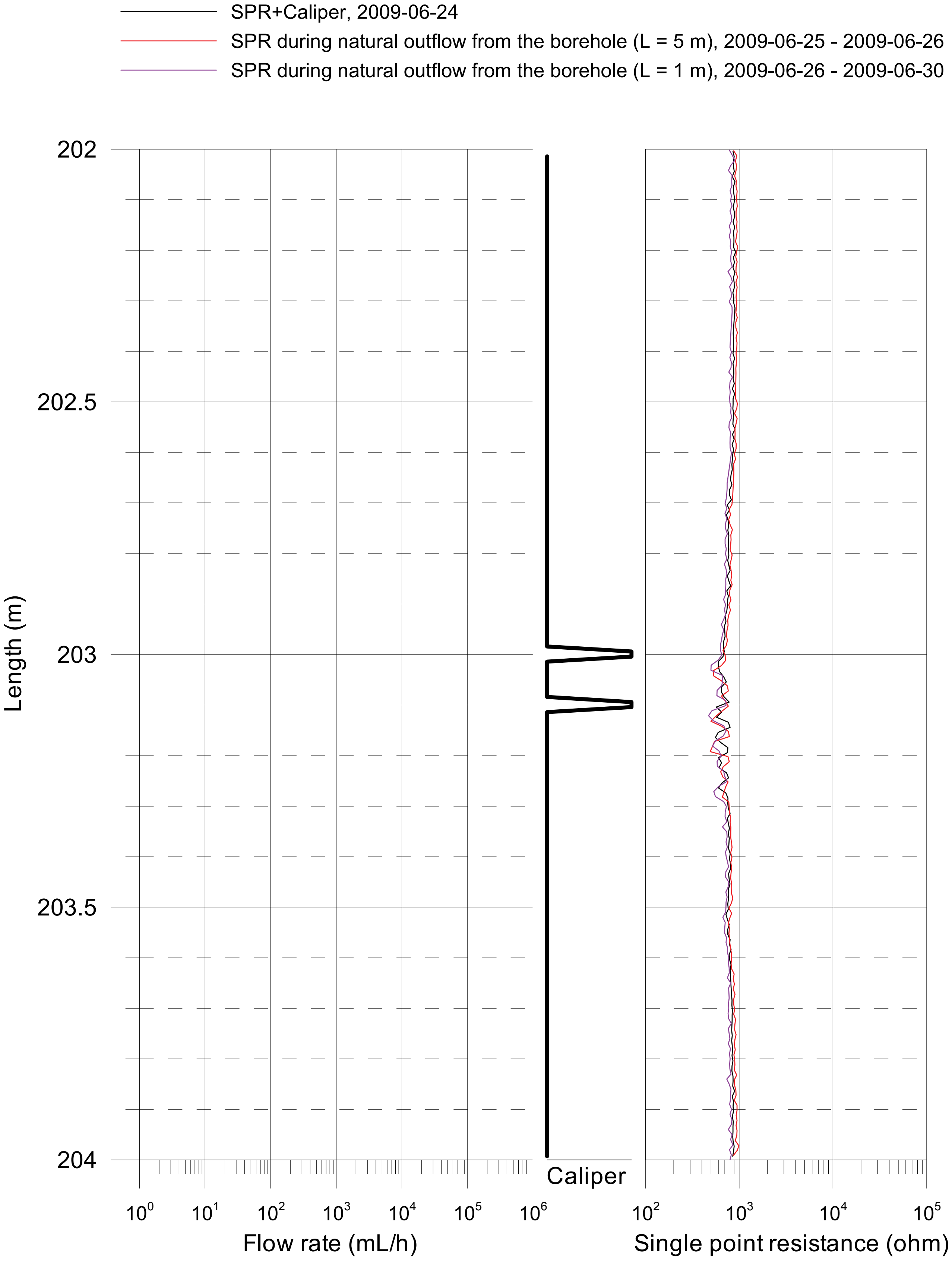

Forsmark, borehole KFR105
SPR and Caliper results after length correction

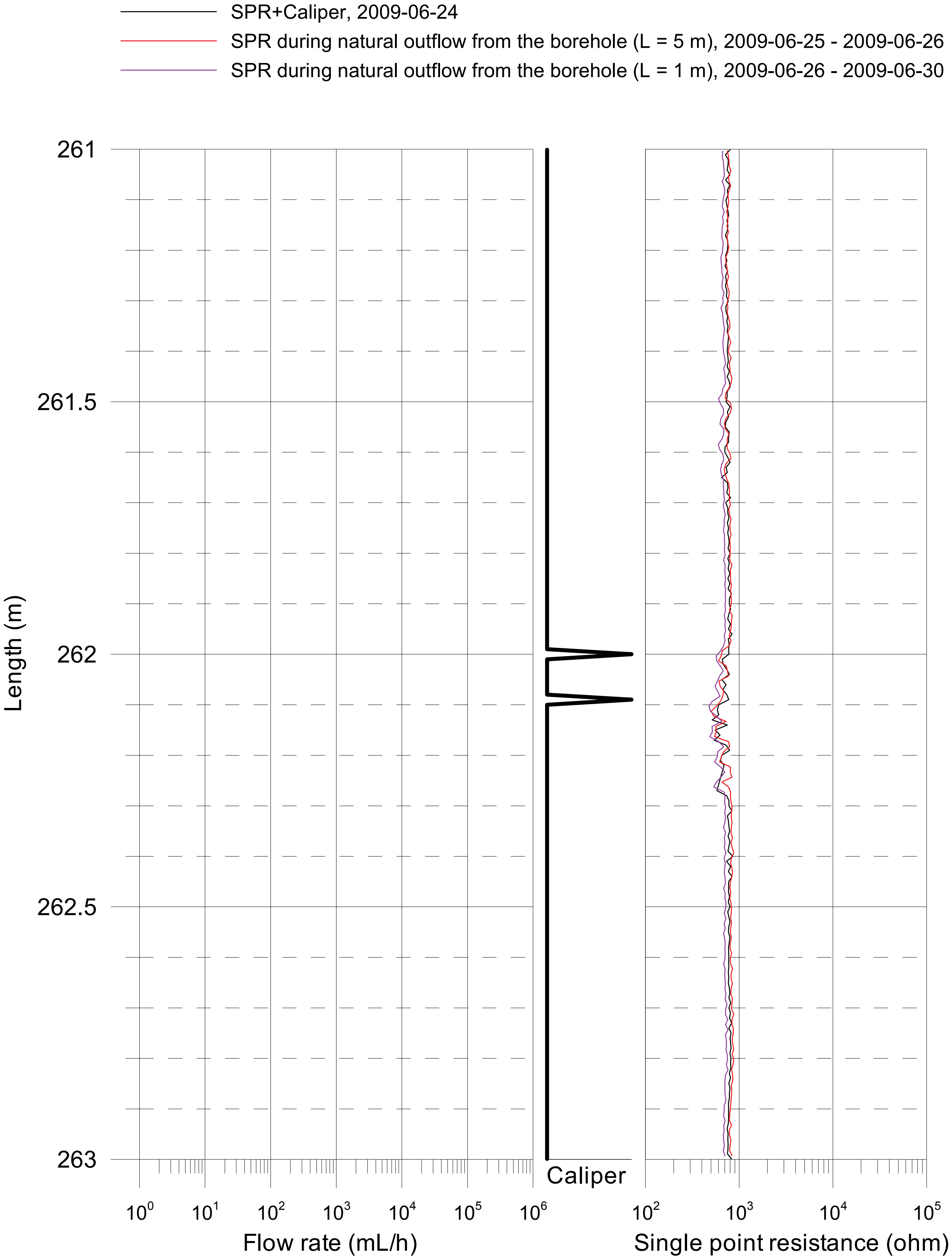

Forsmark, borehole KFR105
SPR and Caliper results after length correction

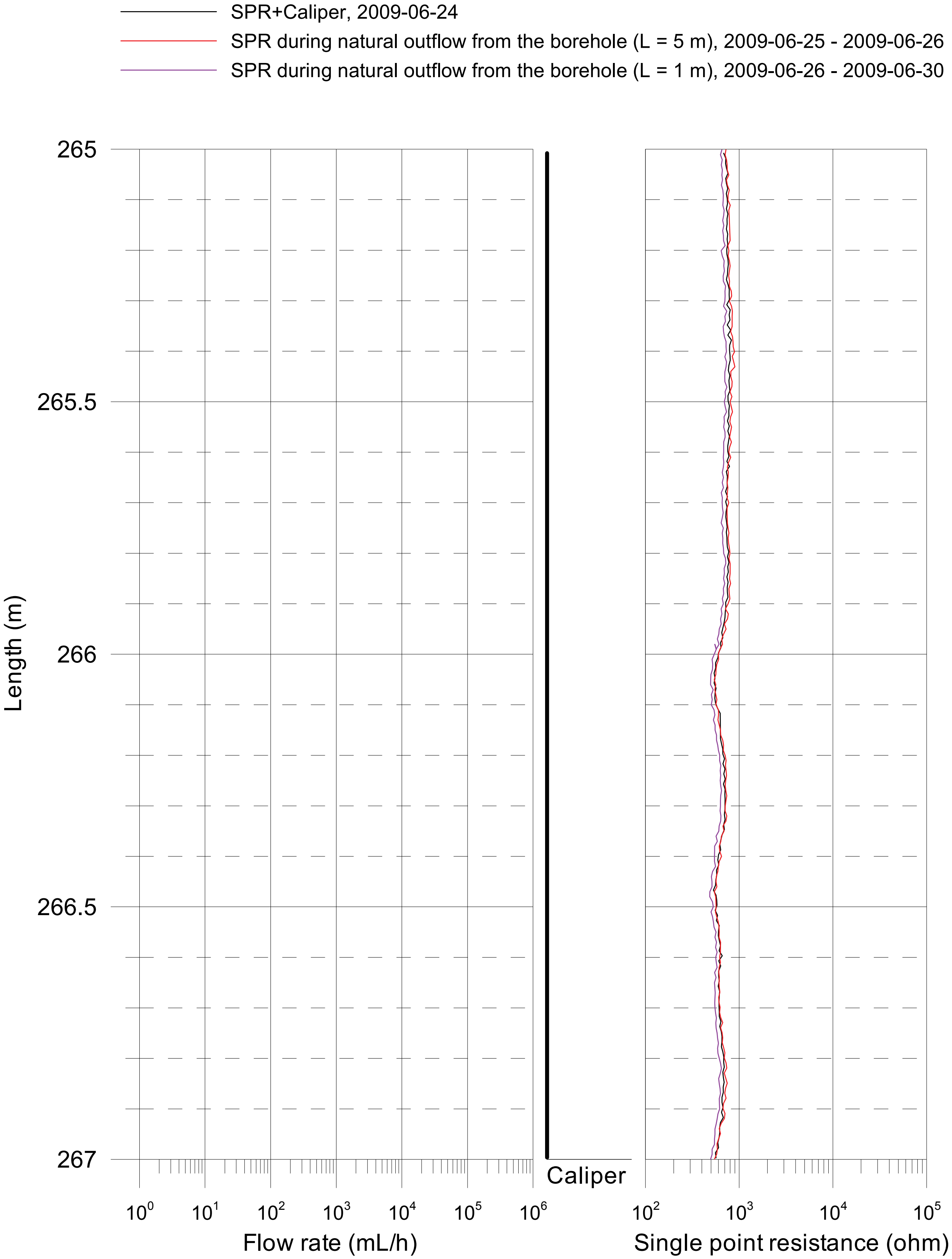

Forsmark, borehole KFR105
SPR and Caliper results after length correction

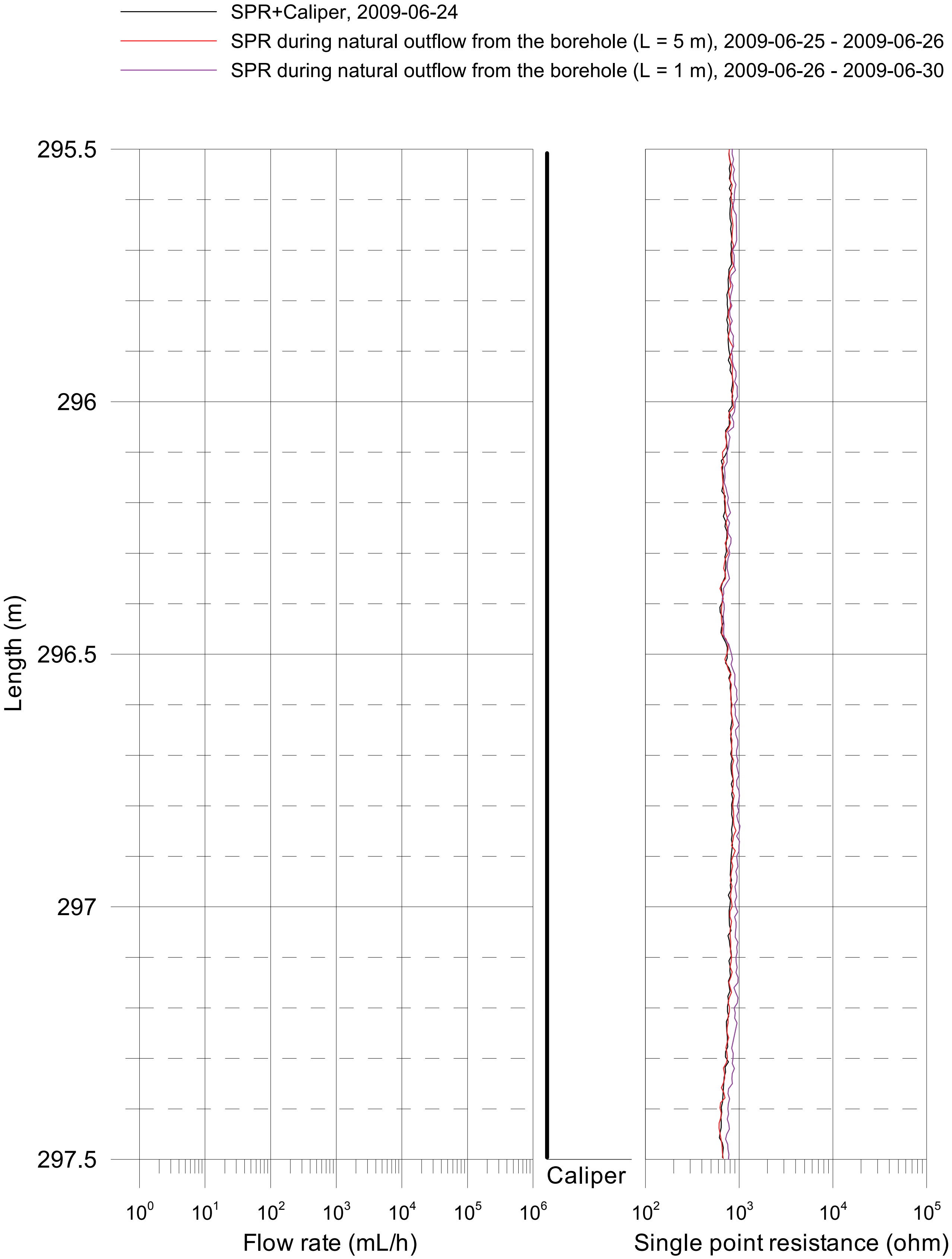

Forsmark, borehole KFR105
Length correction

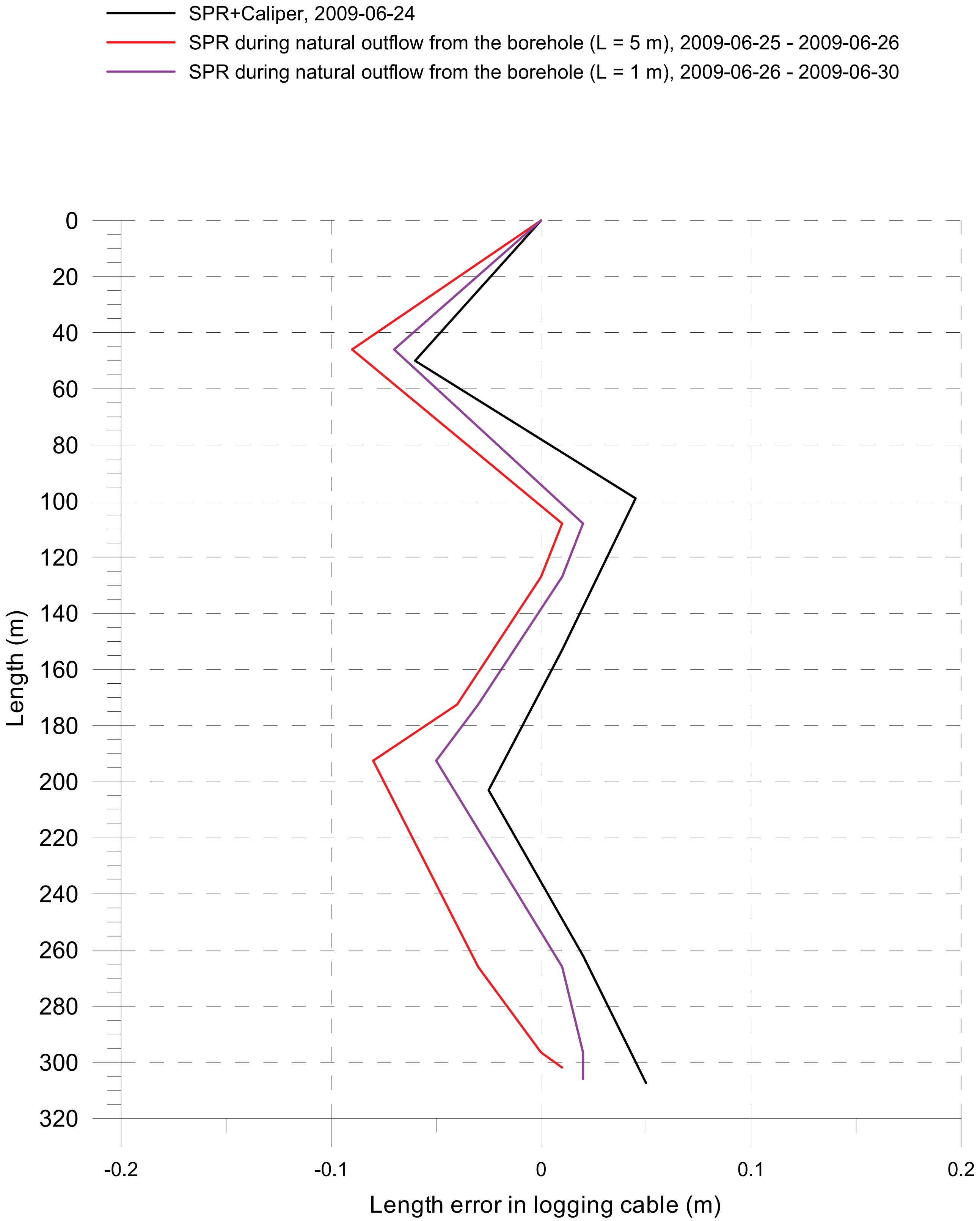

Forsmark, borehole KFR105
Electrical conductivity of borehole water

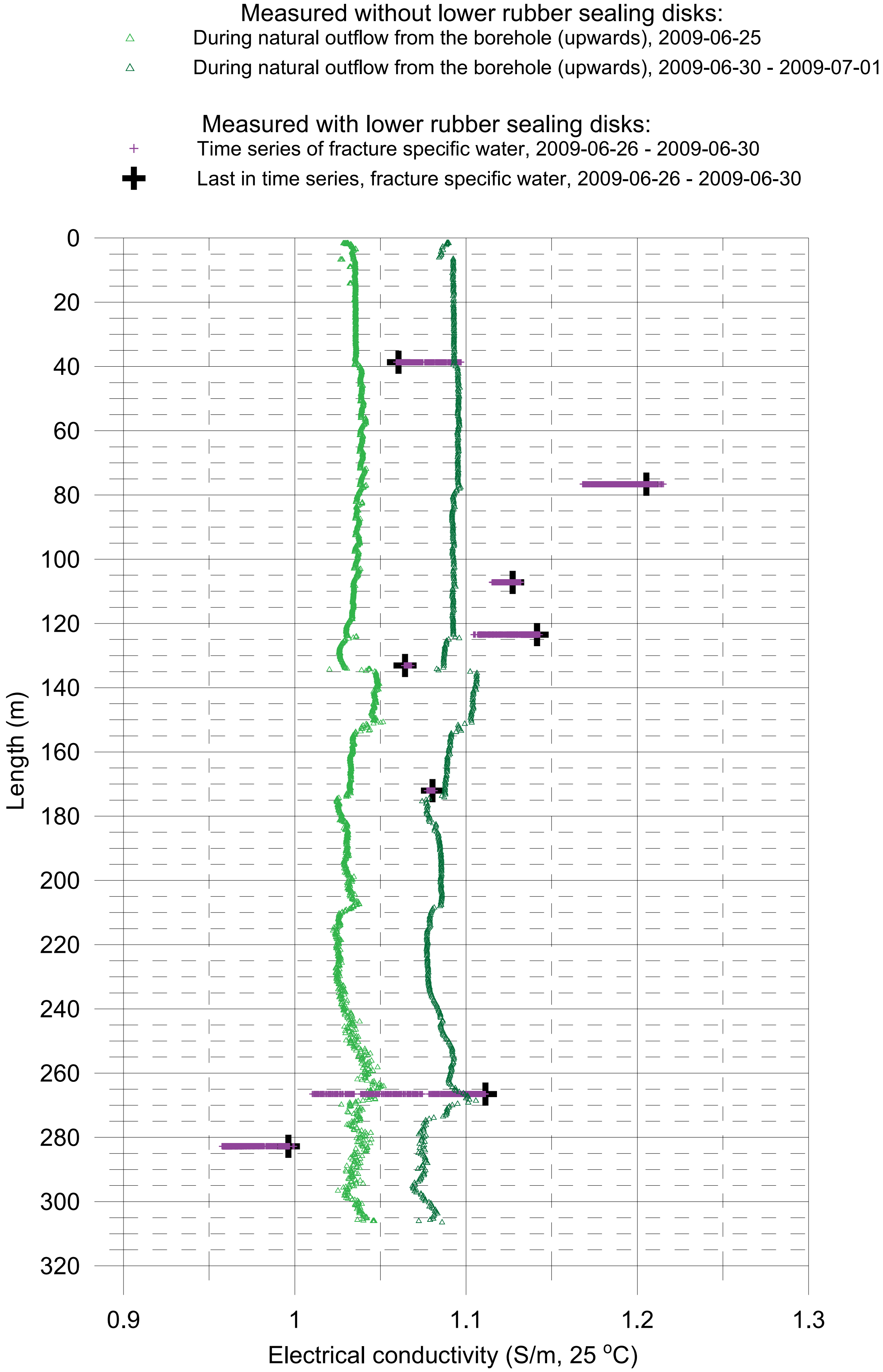

Forsmark, borehole KFR105
Electrical conductivity of borehole water

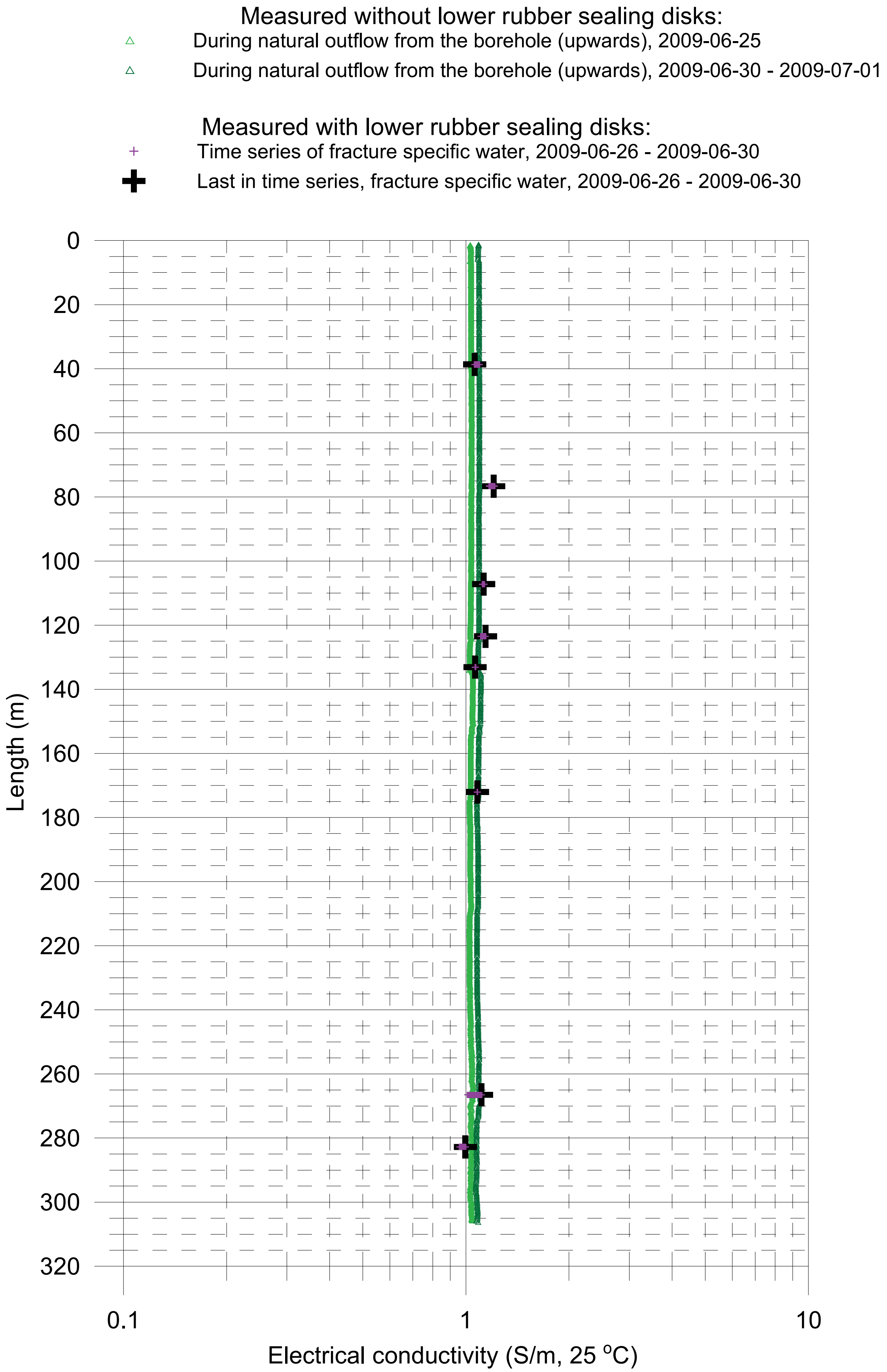

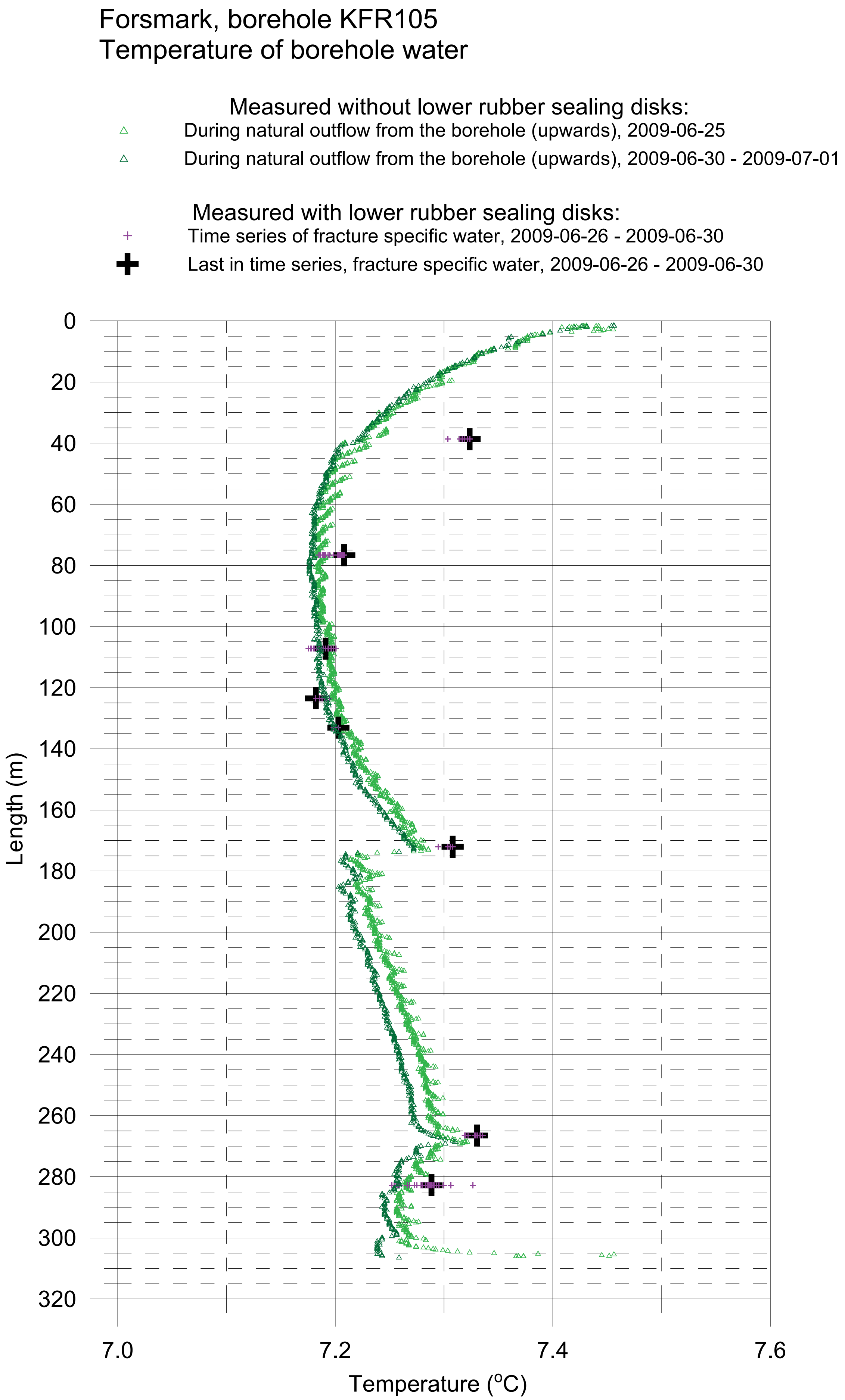
Forsmark, borehole KFR105
Temperature of borehole water
Measured without lower rubber sealing disks:
During natural outflow from the borehole (upwards), 2009-06-25
During natural outflow from the borehole (upwards), 2009-06-30 - 2009-07-01
Measured with lower rubber sealing disks:
Time series of fracture specific water, 2009-06-26 - 2009-06-30
Last in time series, fracture specific water, 2009-06-26 - 2009-06-30
Length (m)
0
20
40
60
80
100
120
140
160
180
200
220
240
260
280
300
320
7.0
7.2
7.4
7.6
Temperature (°C)

Forsmark, borehole KFR105
Flow rate, caliper and single point resistance

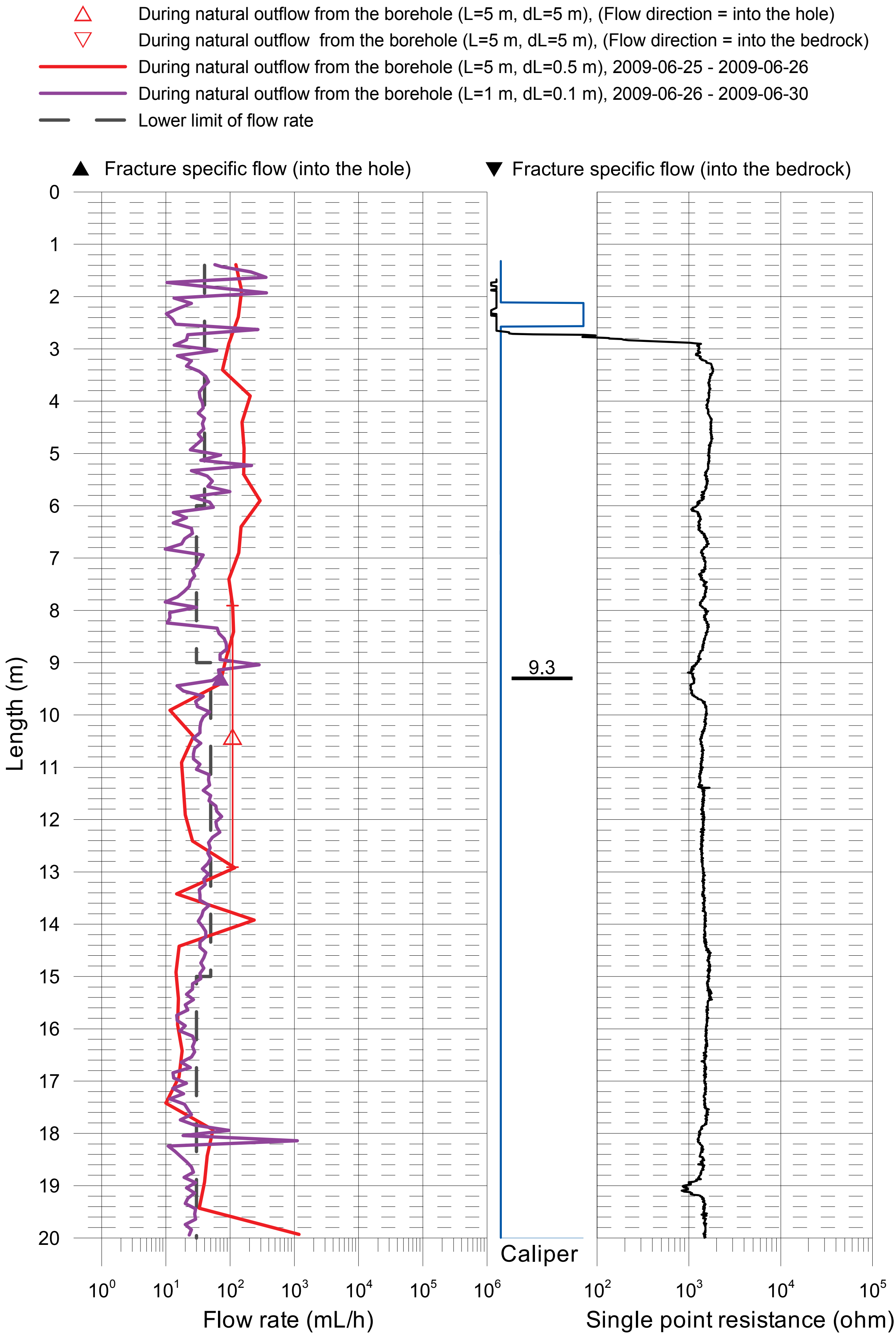

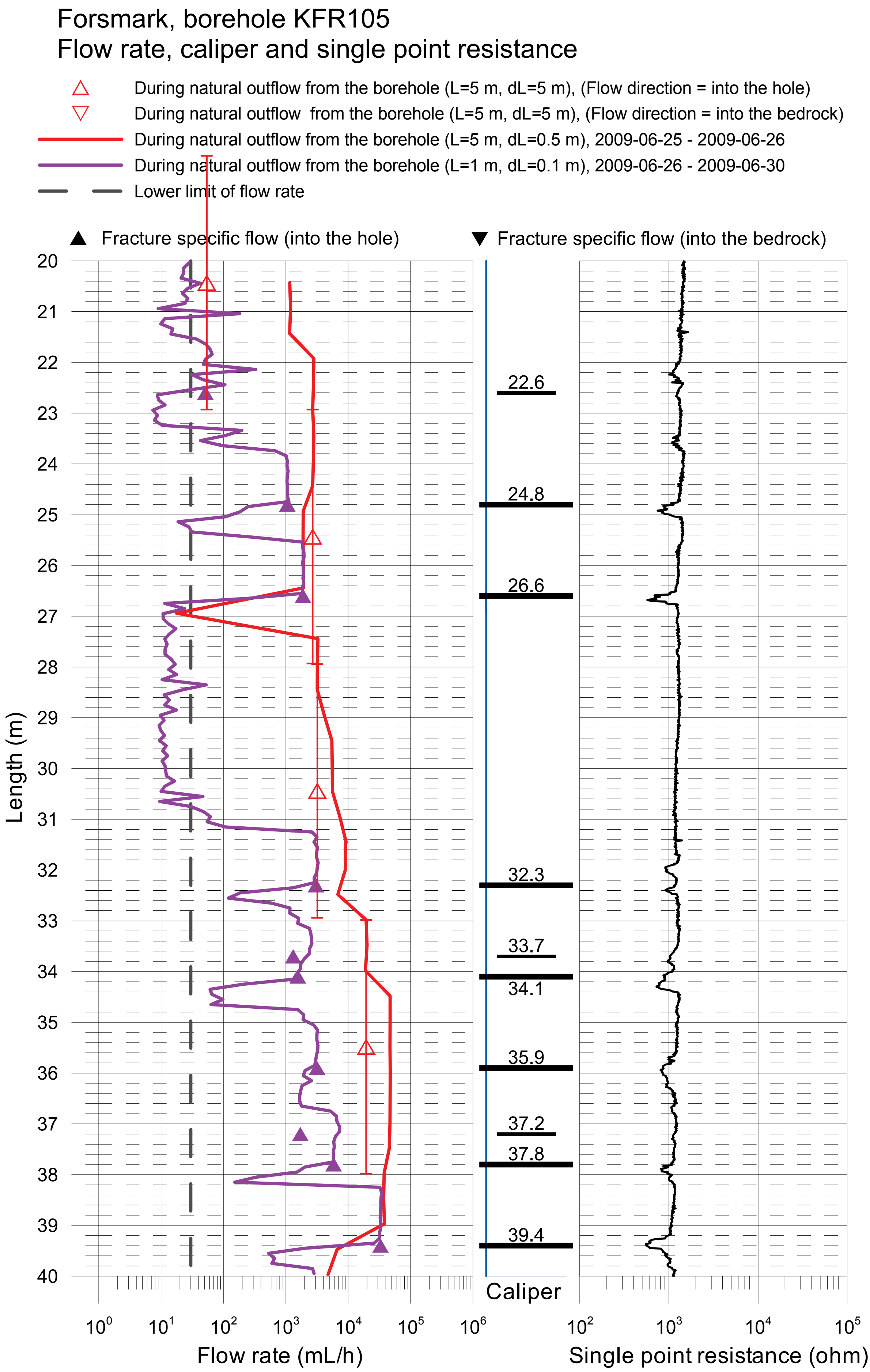
Forsmark, borehole KFR105
Flow rate, caliper and single point resistance
During natural outflow from the borehole (L=5 m, dL=5 m), (Flow direction = into the hole)
During natural outflow from the borehole (L=5 m, dL=5 m), (Flow direction = into the bedrock)
During natural outflow from the borehole (L=5 m, dL=0.5 m), 2009-06-25 - 2009-06-26
During natural outflow from the borehole (L=1 m, dL=0.1 m), 2009-06-26 - 2009-06-30
Lower limit of flow rate
Fracture specific flow (into the hole)
Fracture specific flow (into the bedrock)
Length (m)
22.6
24.8
26.6
32.3
33.7
34.1
35.9
37.2
37.8
39.4
Caliper
Flow rate (mL/h)
Single point resistance (ohm)

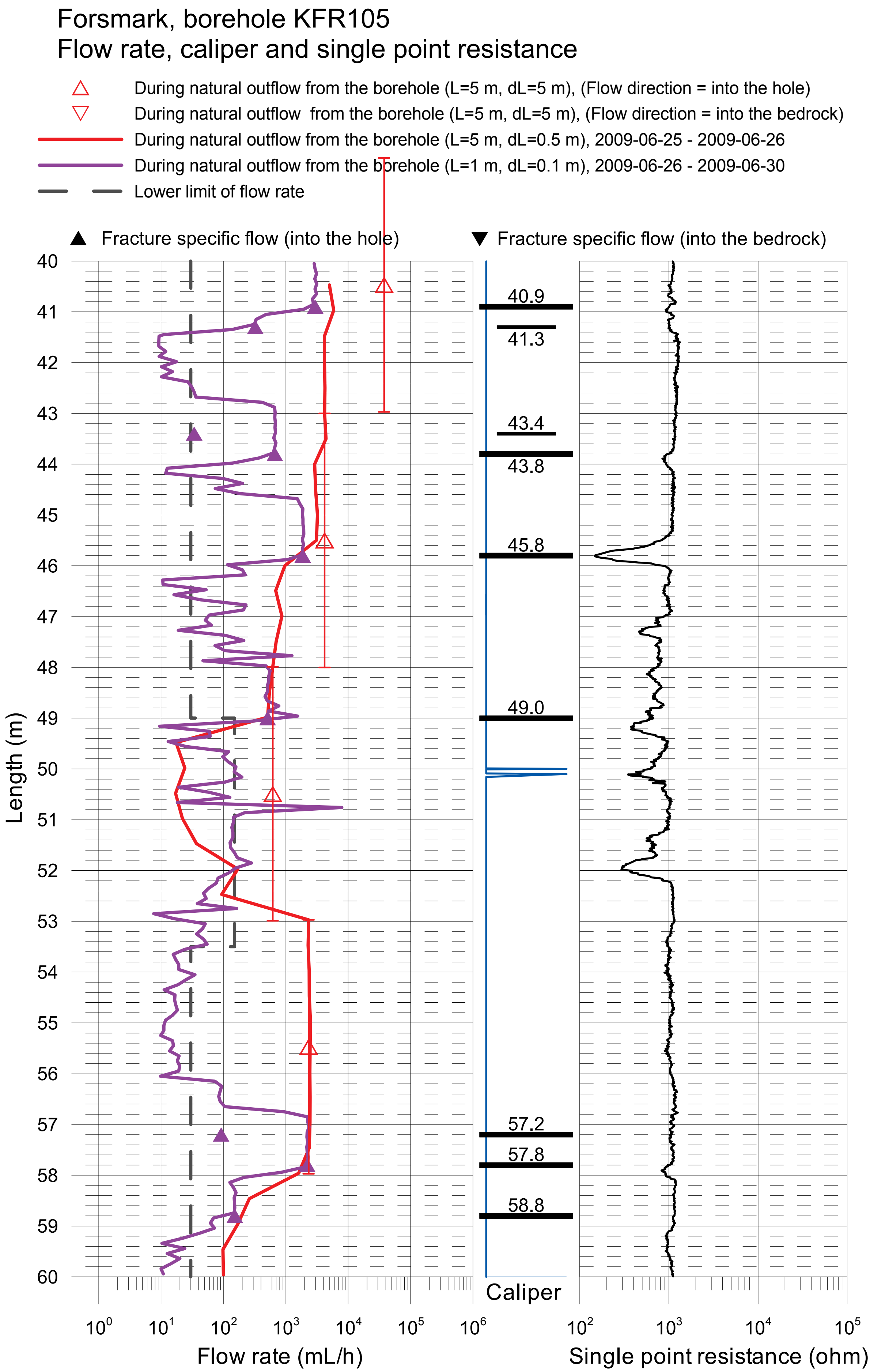
Forsmark, borehole KFR105
Flow rate, caliper and single point resistance
During natural outflow from the borehole (L=5 m, dL=5 m), (Flow direction = into the hole)
During natural outflow from the borehole (L=5 m, dL=5 m), (Flow direction = into the bedrock)
During natural outflow from the borehole (L=5 m, dL=0.5 m), 2009-06-25 - 2009-06-26
During natural outflow from the borehole (L=1 m, dL=0.1 m), 2009-06-26 - 2009-06-30
Lower limit of flow rate
Fracture specific flow (into the hole)
Fracture specific flow (into the bedrock)
Length (m)
40.9
41.3
43.4
43.8
45.8
49.0
57.2
57.8
58.8
Caliper
Flow rate (mL/h)
Single point resistance (ohm)

Forsmark, borehole KFR105
Flow rate, caliper and single point resistance

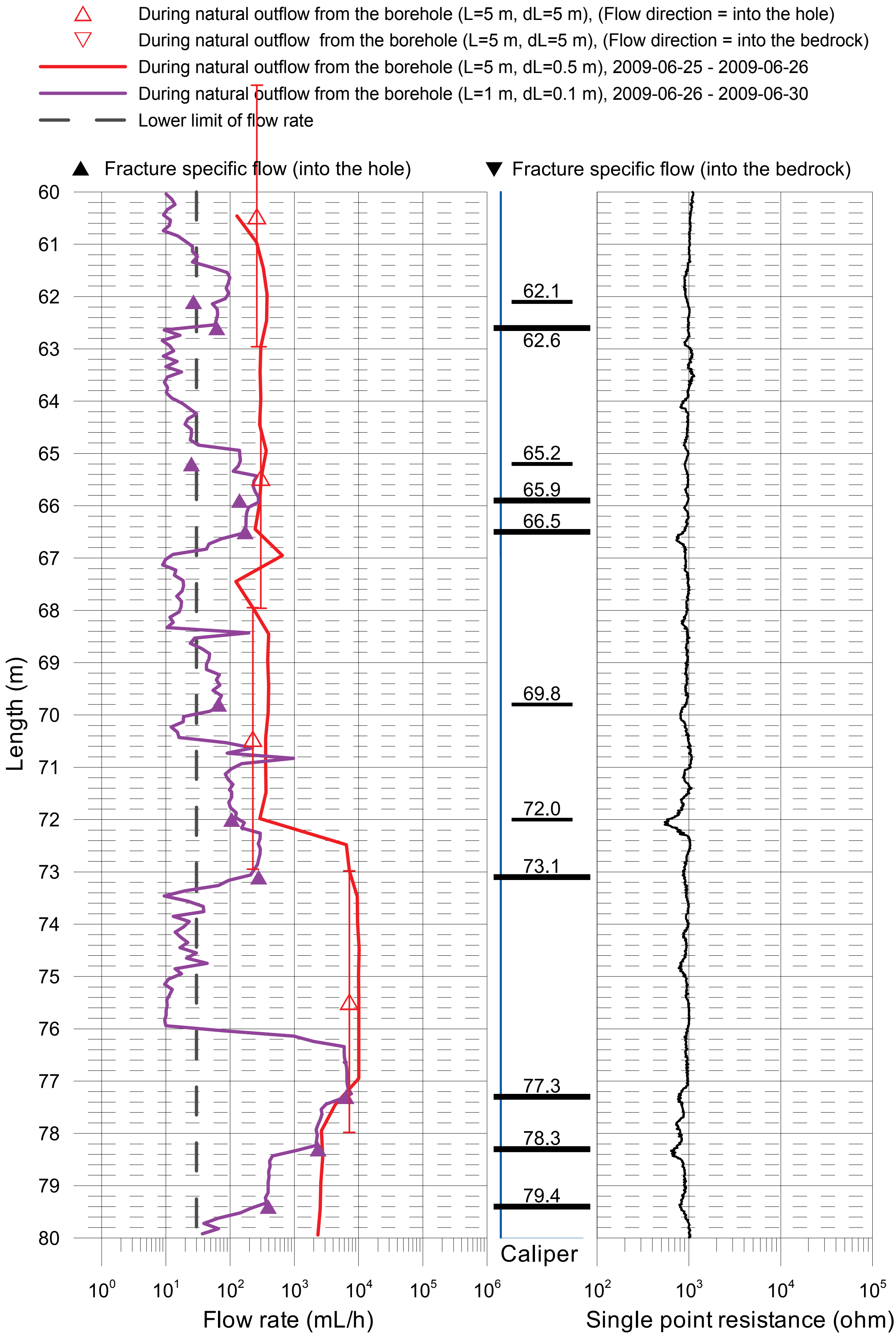

Forsmark, borehole KFR105
Flow rate, caliper and single point resistance

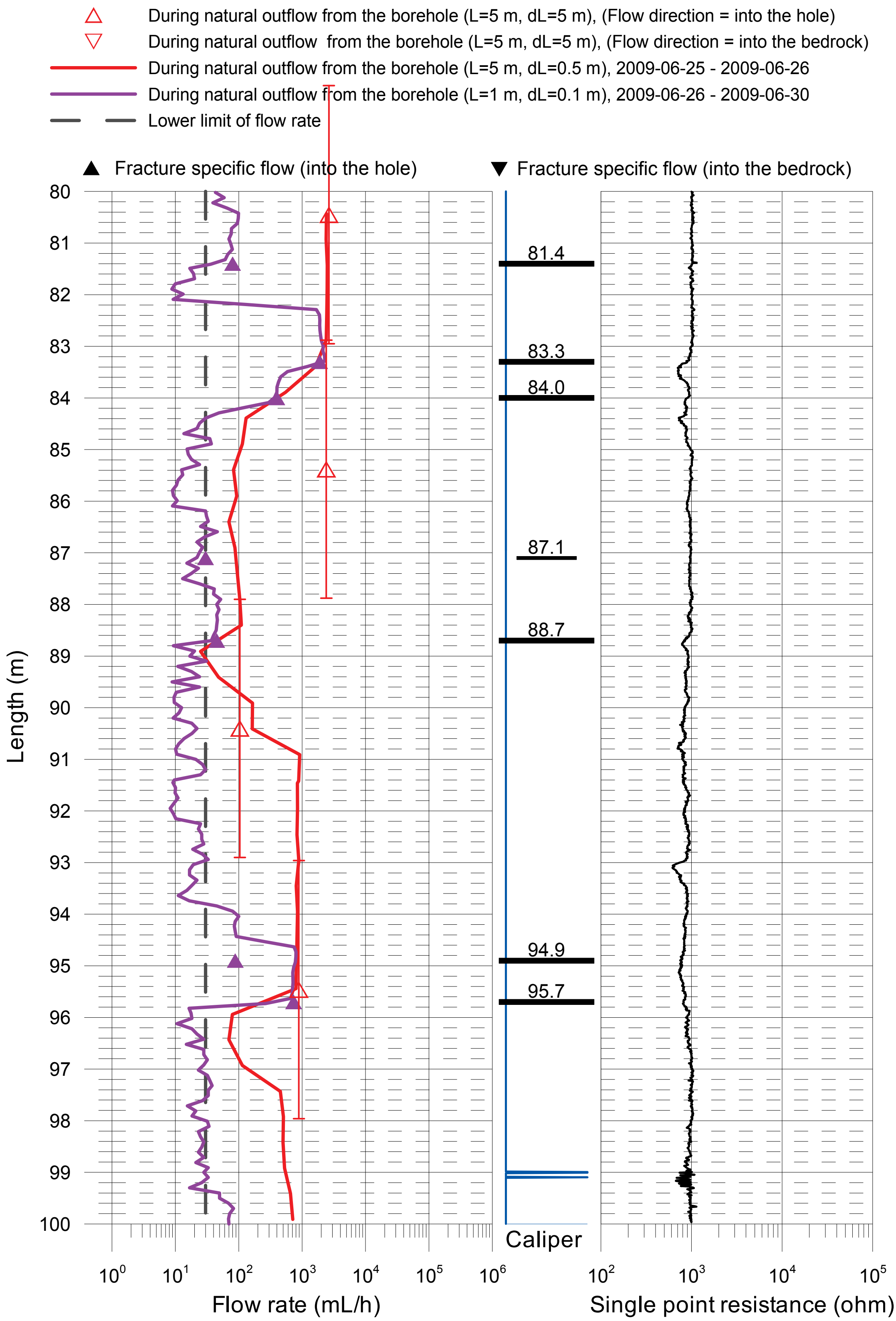

Forsmark, borehole KFR105
Flow rate, caliper and single point resistance

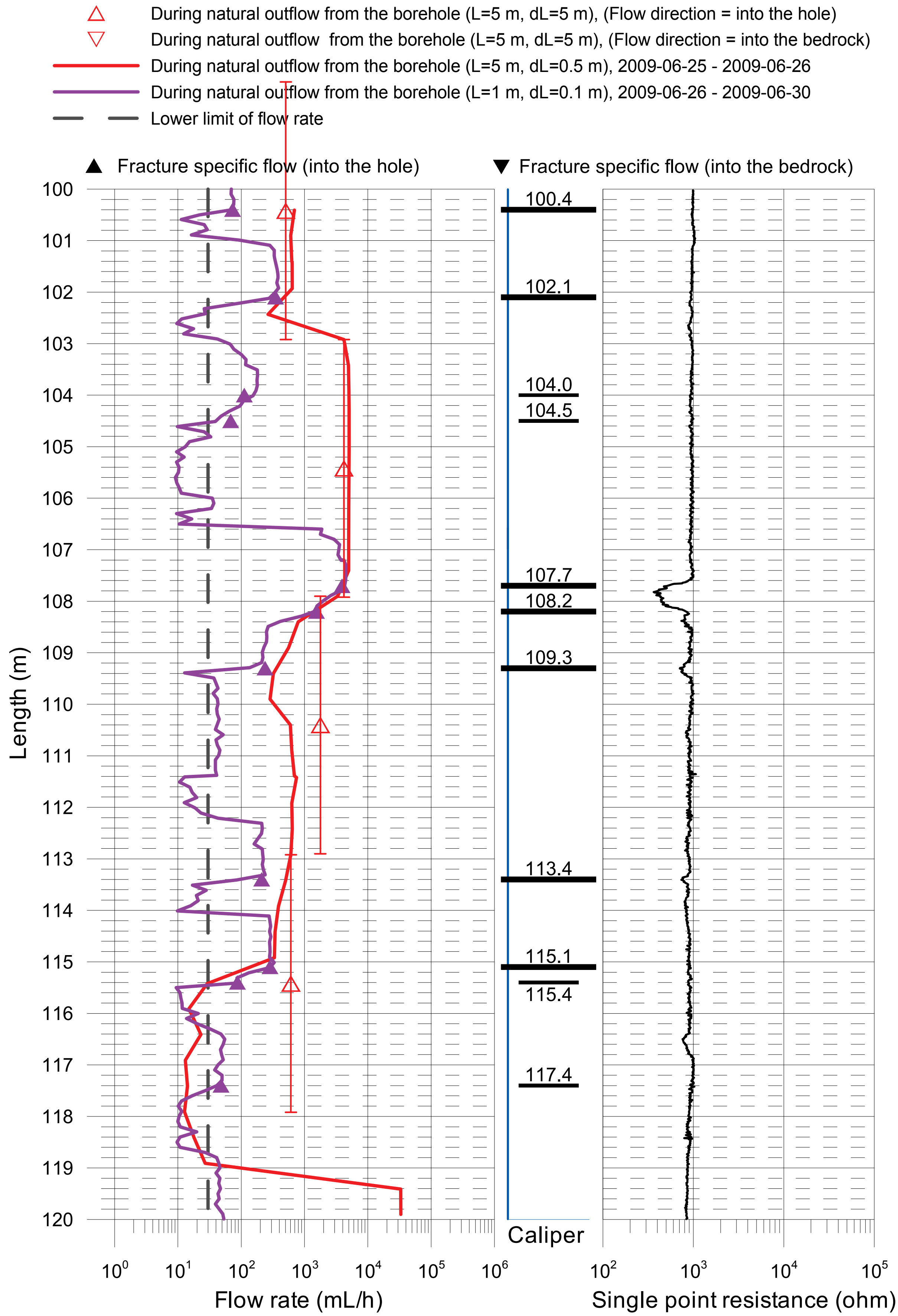

Forsmark, borehole KFR105
Flow rate, caliper and single point resistance

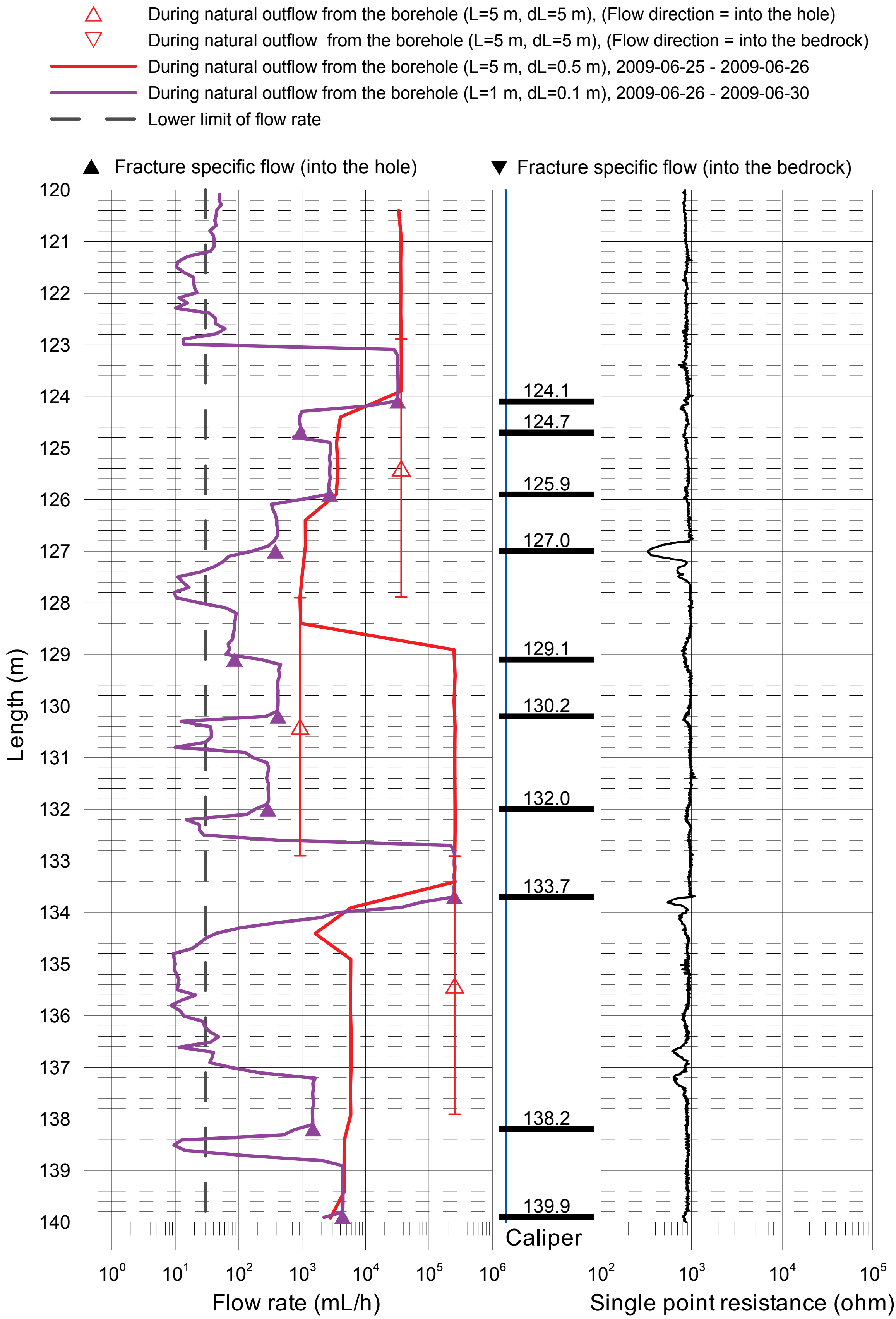

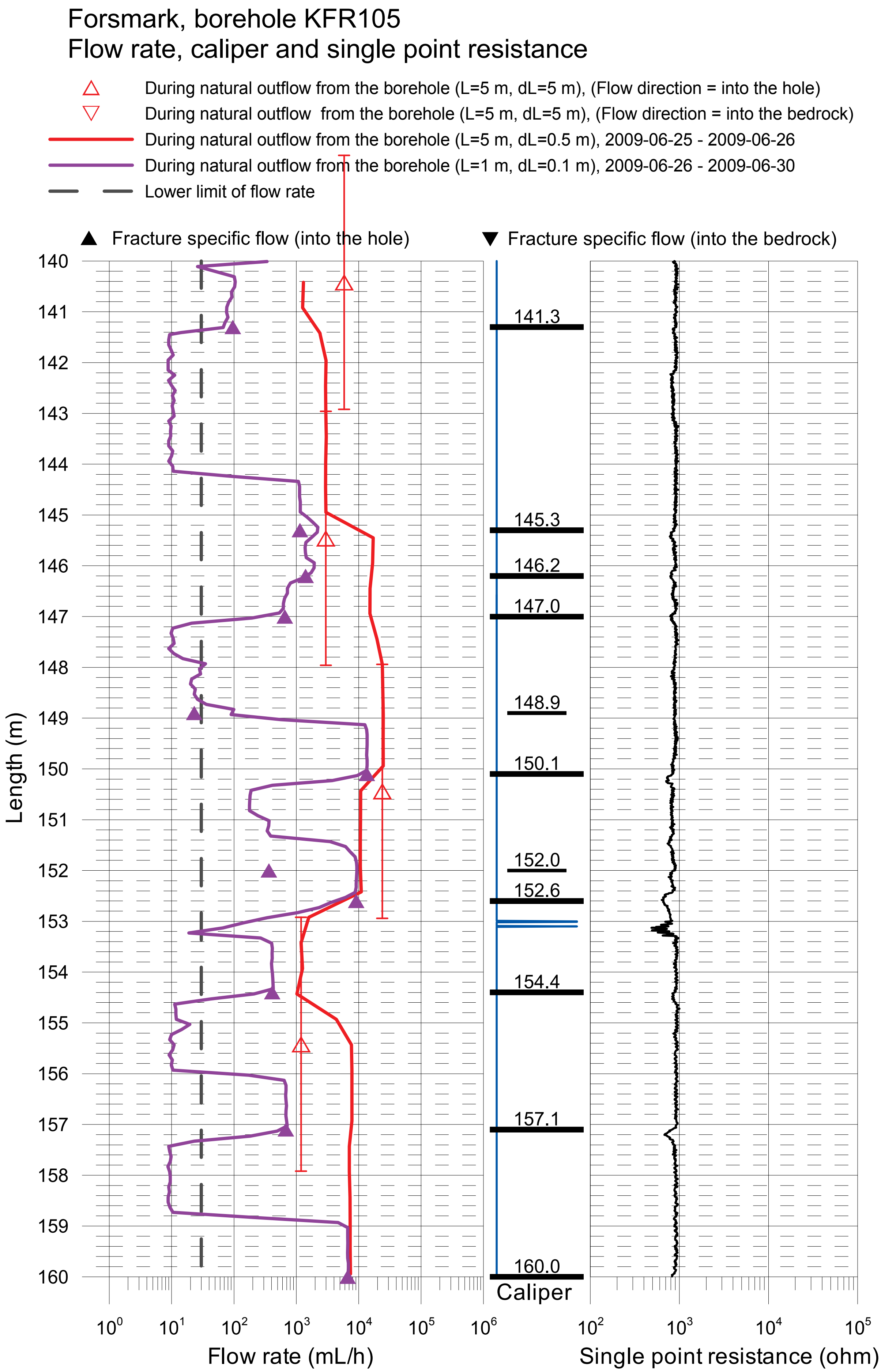
Forsmark, borehole KFR105
Flow rate, caliper and single point resistance
During natural outflow from the borehole (L=5 m, dL=5 m), (Flow direction = into the hole)
During natural outflow from the borehole (L=5 m, dL=5 m), (Flow direction = into the bedrock)
During natural outflow from the borehole (L=5 m, dL=0.5 m), 2009-06-25 - 2009-06-26
During natural outflow from the borehole (L=1 m, dL=0.1 m), 2009-06-26 - 2009-06-30
Lower limit of flow rate
Fracture specific flow (into the hole)
Fracture specific flow (into the bedrock)
Length (m)
140
141
142
143
144
145
146
147
148
149
150
151
152
153
154
155
156
157
158
159
160
141.3
145.3
146.2
147.0
148.9
150.1
152.0
152.6
154.4
157.1
160.0
Caliper
10^0
10^1
10^2
10^3
10^4
10^5
10^6
Flow rate (mL/h)
10^2
10^3
10^4
10^5
Single point resistance (ohm)

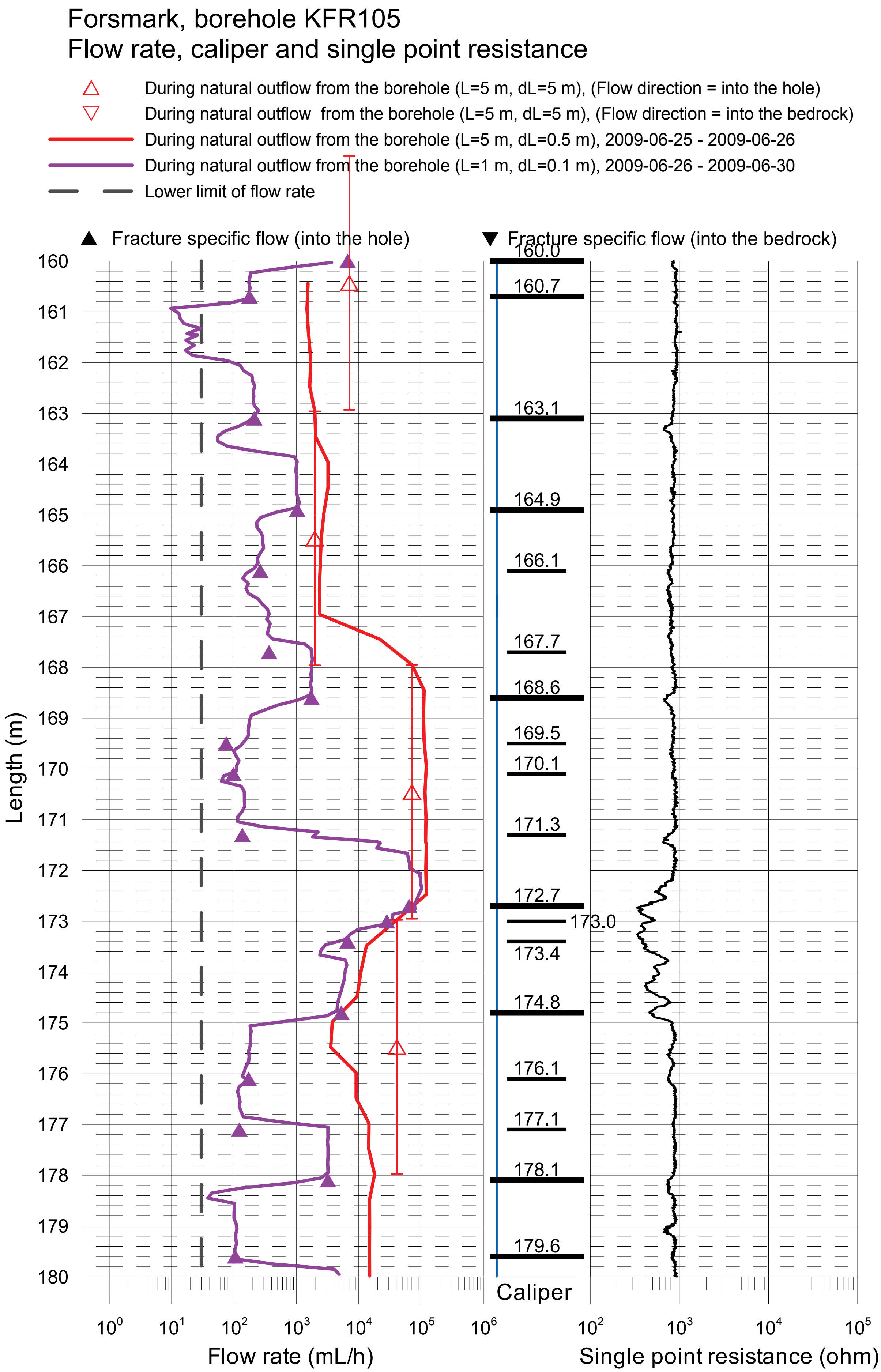
Forsmark, borehole KFR105
Flow rate, caliper and single point resistance
During natural outflow from the borehole (L=5 m, dL=5 m), (Flow direction = into the hole)
During natural outflow from the borehole (L=5 m, dL=5 m), (Flow direction = into the bedrock)
During natural outflow from the borehole (L=5 m, dL=0.5 m), 2009-06-25 - 2009-06-26
During natural outflow from the borehole (L=1 m, dL=0.1 m), 2009-06-26 - 2009-06-30
Lower limit of flow rate
Fracture specific flow (into the hole)
Fracture specific flow (into the bedrock)
Length (m)
Caliper
Flow rate (mL/h)
Single point resistance (ohm)
160.0
160.7
163.1
164.9
166.1
167.7
168.6
169.5
170.1
171.3
172.7
173.0
173.4
174.8
176.1
177.1
178.1
179.6

Forsmark, borehole KFR105
Flow rate, caliper and single point resistance

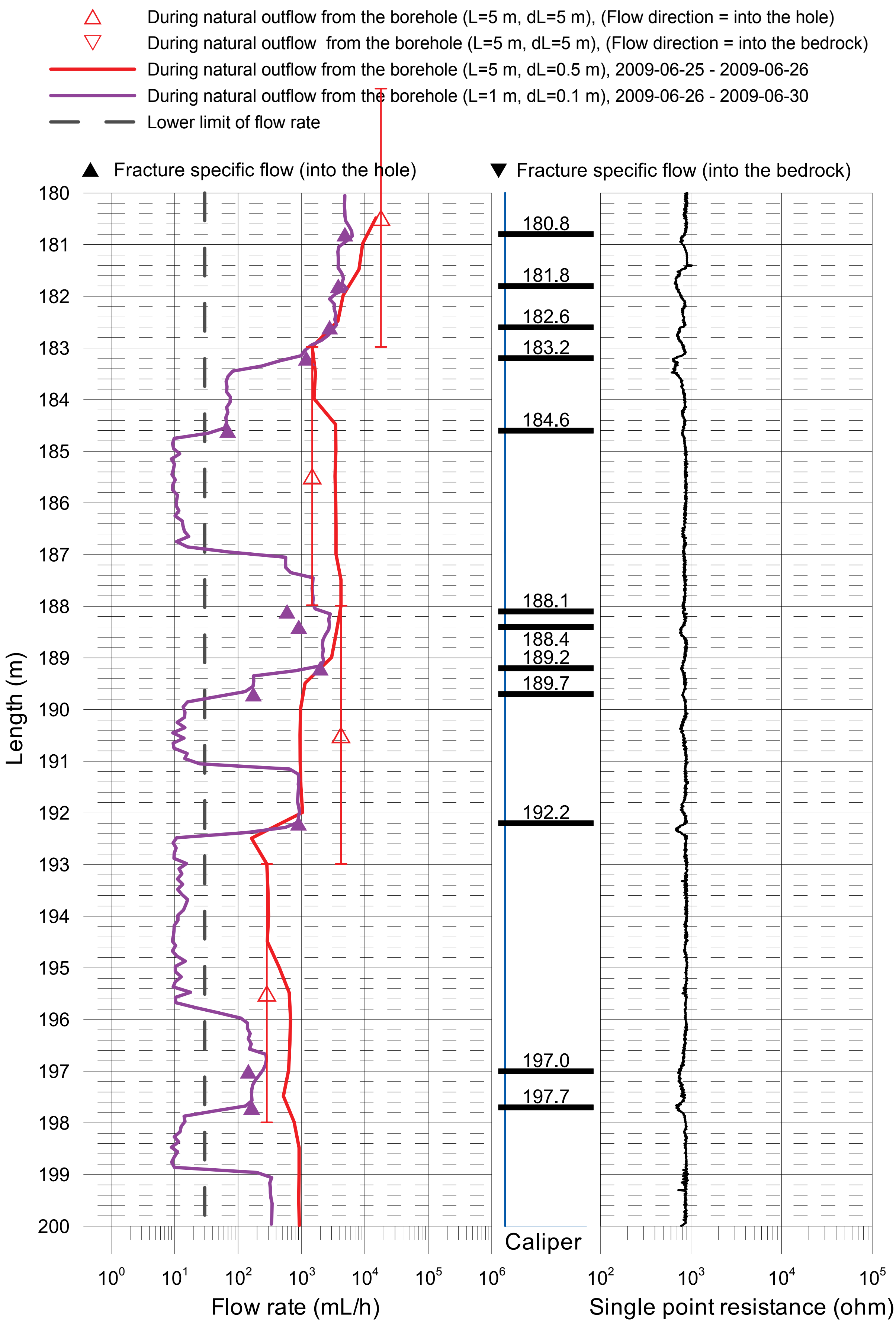

Forsmark, borehole KFR105
Flow rate, caliper and single point resistance

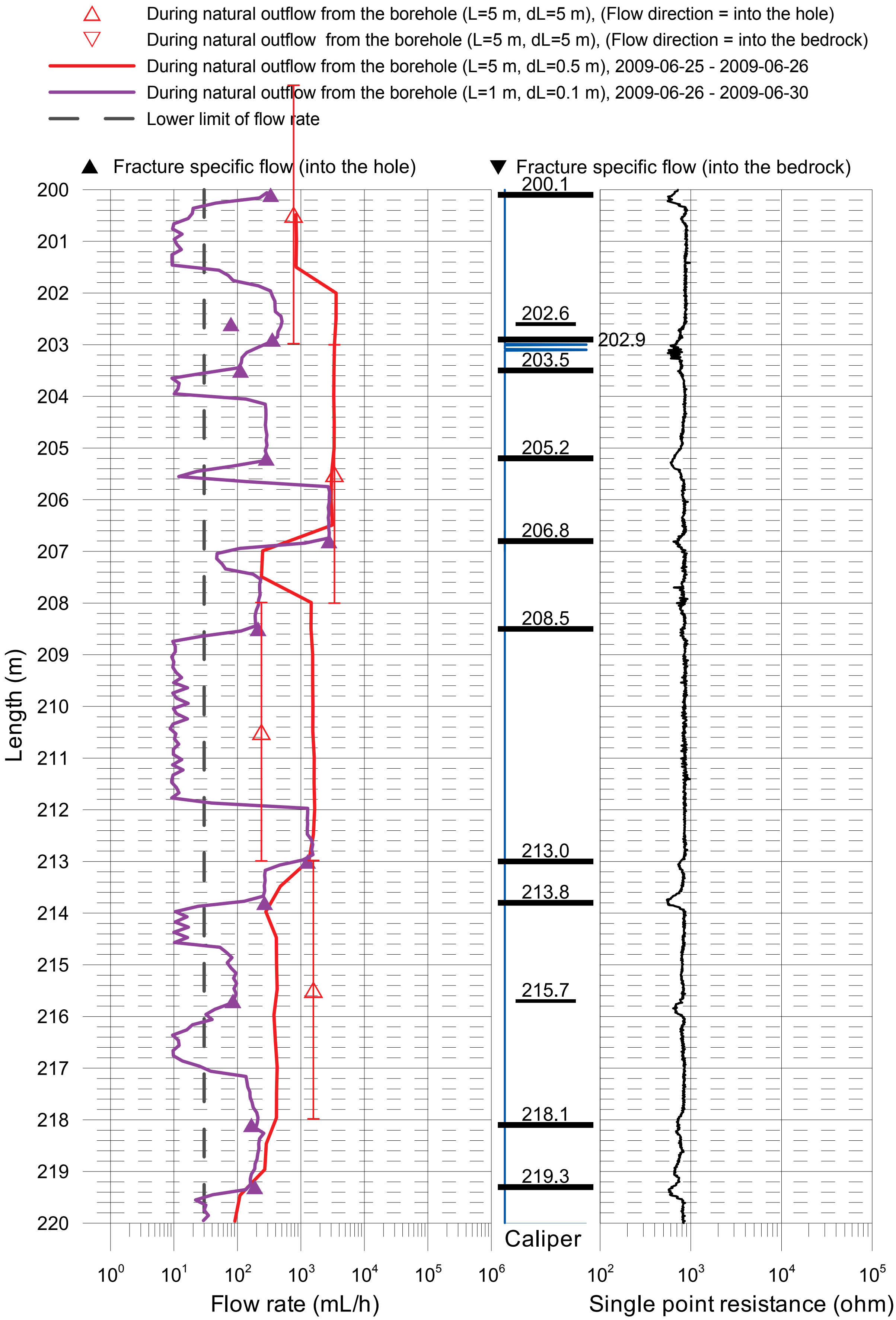

Forsmark, borehole KFR105
Flow rate, caliper and single point resistance

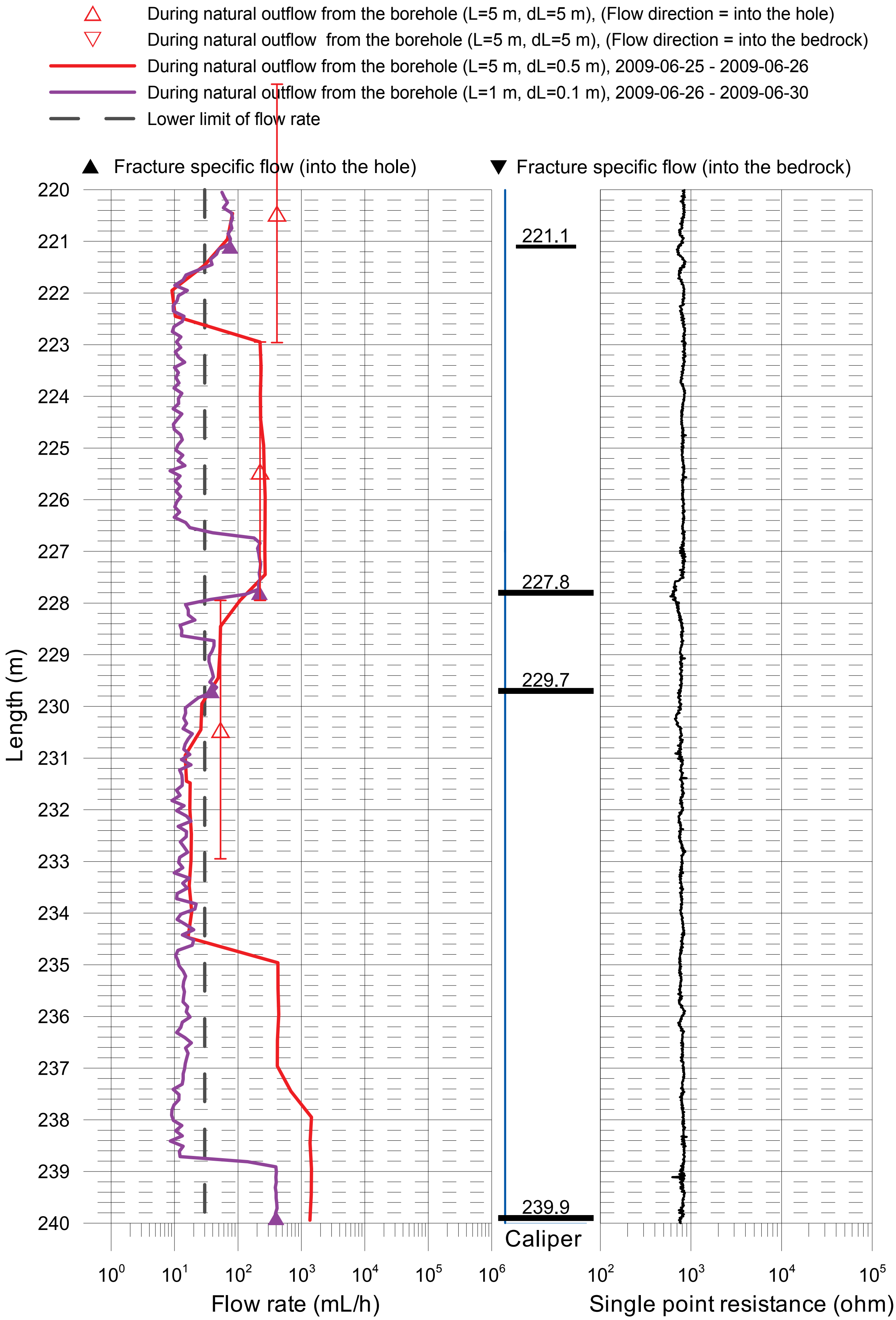

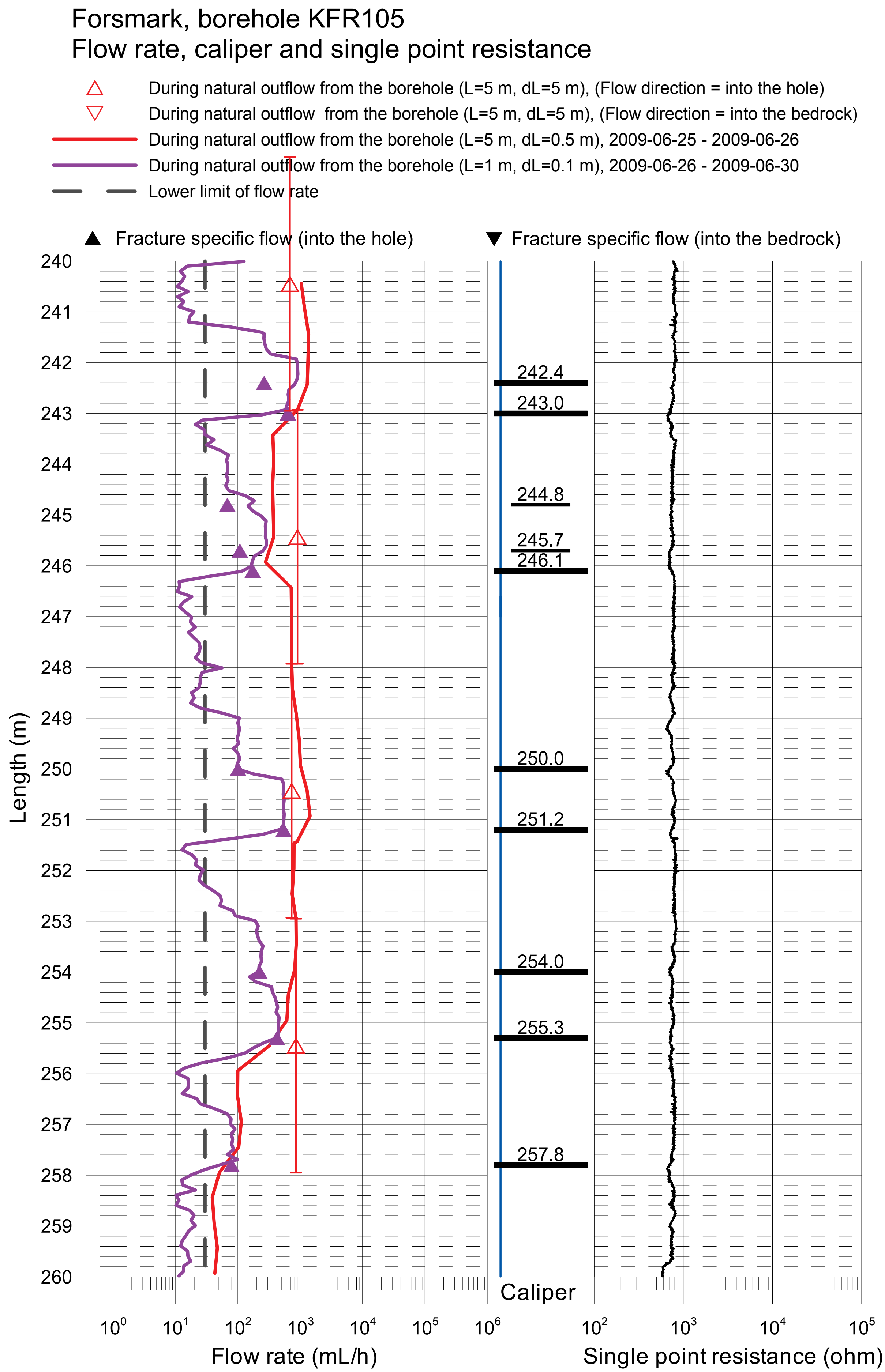

Forsmark, borehole KFR105
Flow rate, caliper and single point resistance
During natural outflow from the borehole (L=5 m, dL=5 m), (Flow direction = into the hole)
During natural outflow from the borehole (L=5 m, dL=5 m), (Flow direction = into the bedrock)
During natural outflow from the borehole (L=5 m, dL=0.5 m), 2009-06-25 - 2009-06-26
During natural outflow from the borehole (L=1 m, dL=0.1 m), 2009-06-26 - 2009-06-30
Lower limit of flow rate
Fracture specific flow (into the hole)
Fracture specific flow (into the bedrock)
Length (m)
240
241
242
243
244
245
246
247
248
249
250
251
252
253
254
255
256
257
258
259
260
242.4
243.0
244.8
245.7
246.1
250.0
251.2
254.0
255.3
257.8
Caliper
10^0
10^1
10^2
10^3
10^4
10^5
10^6
Flow rate (mL/h)
10^2
10^3
10^4
10^5
Single point resistance (ohm)

Forsmark, borehole KFR105
Flow rate, caliper and single point resistance

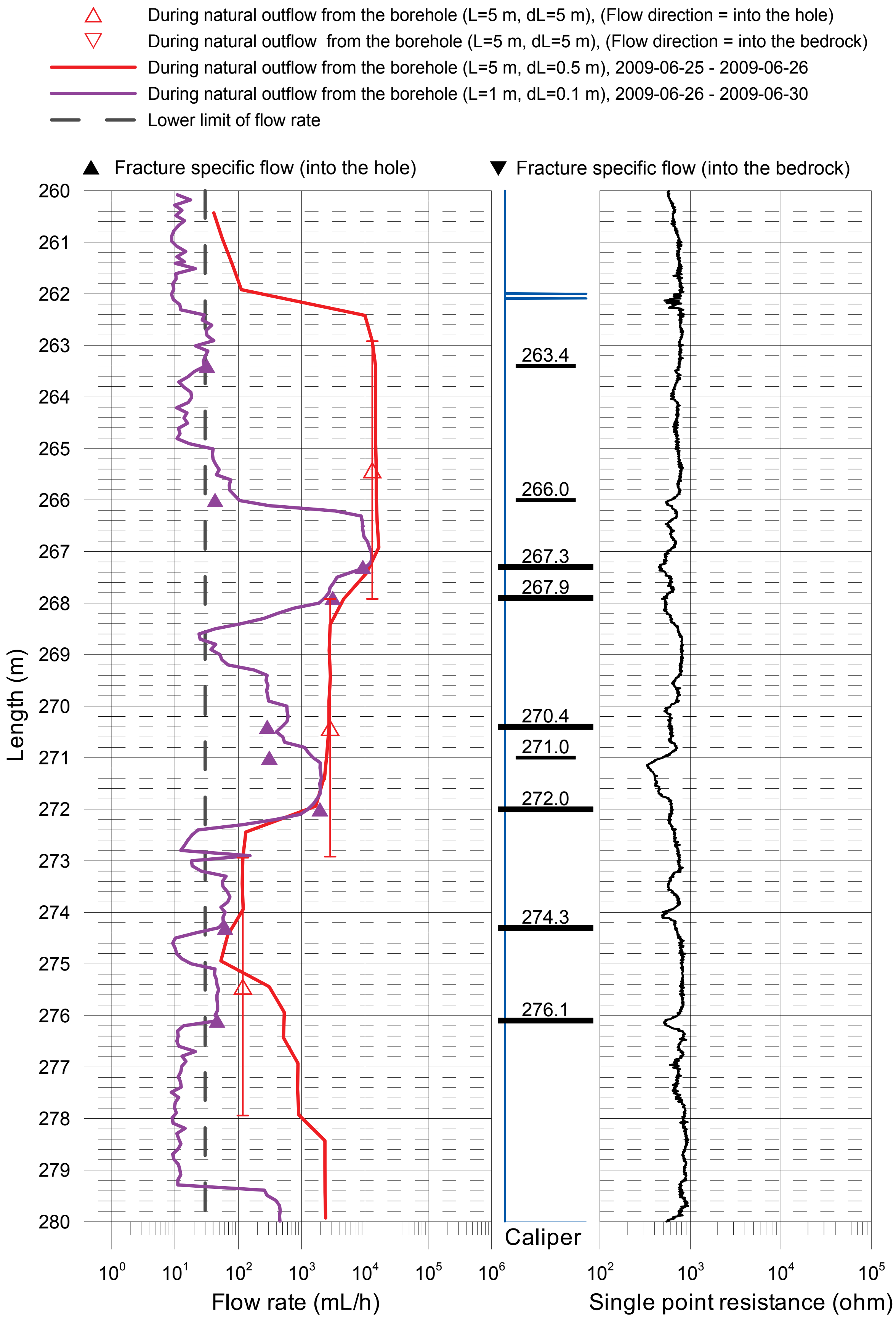

Forsmark, borehole KFR105
Flow rate, caliper and single point resistance

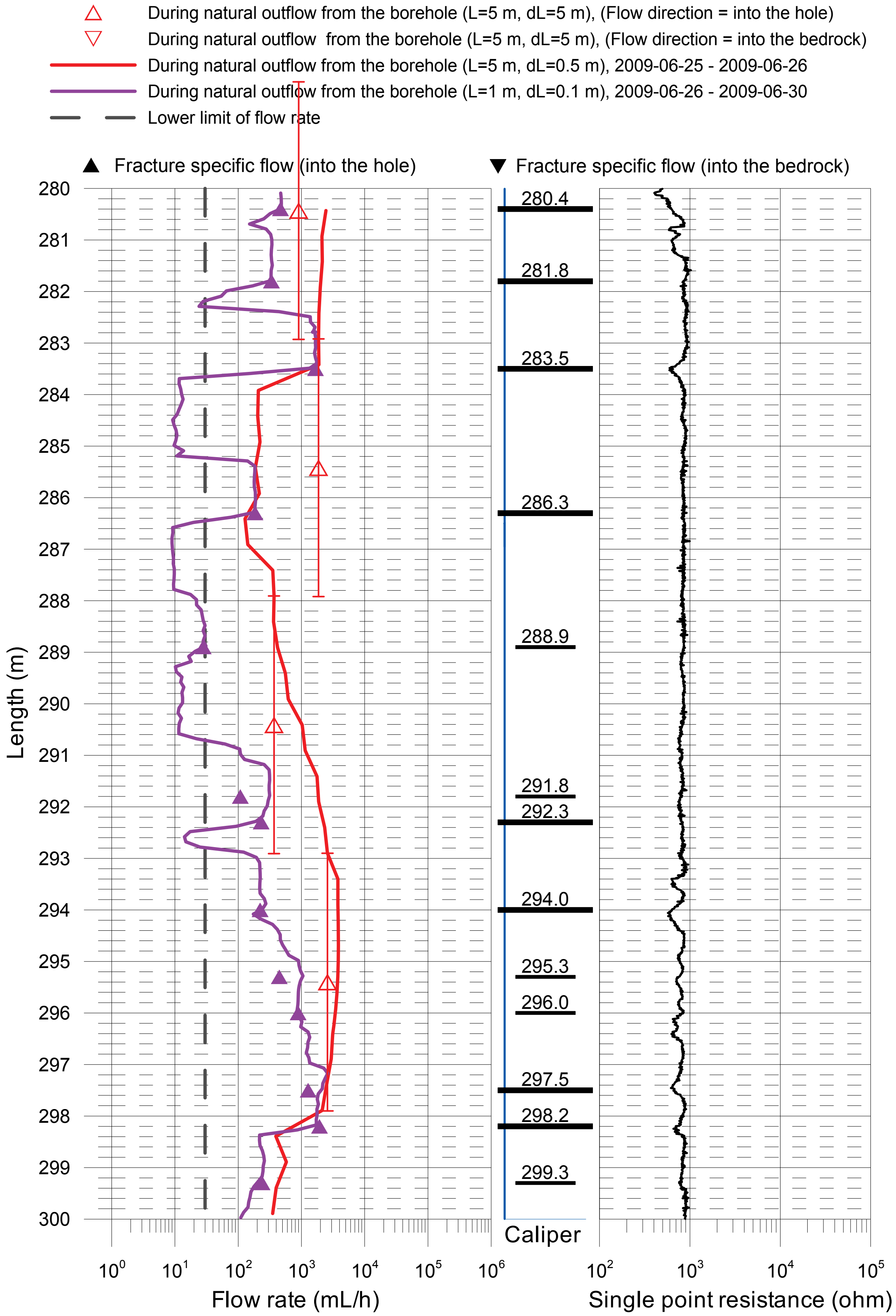

Forsmark, borehole KFR105
Flow rate, caliper and single point resistance

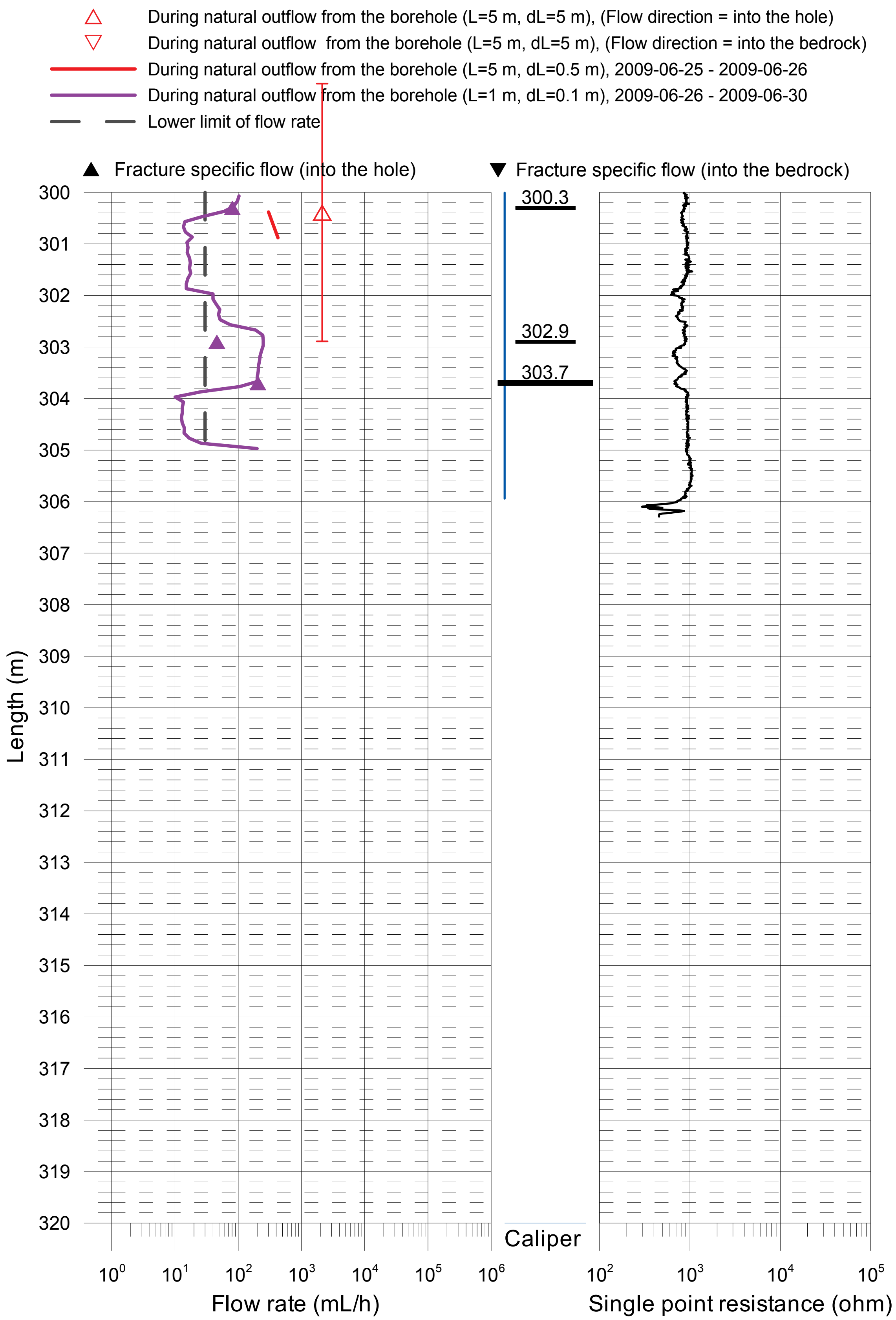

Explanations for the tables in Appendices 5 and 7.

Header	Unit	Explanations
Borehole		ID for borehole
Secup	m	Length along the borehole for the upper limit of the test section (based on corrected length L)
Seclow	m	Length along the borehole for the lower limit of the test section (based on corrected length L)
L	m	Corrected length along borehole based on SKB procedures for length correction.
Length to flow anom.	m	Length along the borehole to inferred flow anomaly during overlapping flow logging
Test type (1–6)	(–)	1A: Pumping test – wire-line eq. 1B:Pumping test-submersible pump, 1C: Pumping test-airlift pumping, 2: Interference test, 3: Injection test, 4: Slug test, 5A: Difference flow logging -PFL-DIFF-Sequential, 5B: Difference flow logging -PFL-DIFF-Overlapping, 6: Flow logging-Impeller
Date of test, start	YY-MM-DD	Date for start of pumping
Time of test, start	hh:mm	Time for start of pumping
Date of flowl. start .	YY-MM-DD	Date for start of the flow logging
Time of flowl. start	hh:mm	Time for start of the flow logging
Date of test, stop	YY-MM-DD	Date for stop of the test
Time of test, stop	hh:mm	Time for stop of the test
L_w	m	Section length used in the difference flow logging
dL	m	Step length (increment) used in the difference flow logging
Q_{p1}	m^3/s	Flow rate at surface by the end of the first pumping period of the flow logging
Q_{p2}	m^3/s	Flow rate at surface by the end of the second pumping period of the flow logging
t_{p1}	s	Duration of the first pumping period
t_{p2}	s	Duration of the second pumping period
t_{F1}	s	Duration of the first recovery period
t_{F2}	s	Duration of the second recovery period
h_0	m.a.s.l.	Initial hydraulic head before pumping. Elevation of water level in open borehole in the local co-ordinates system with z=0 m.
h_1	m.a.s.l.	Stabilized hydraulic head during the first pumping period. Elevation of water level in open borehole in the local co-ordinates system with z=0 m.
h_2	m.a.s.l.	Stabilized hydraulic head during the second pumping period. Elevation of water level in open borehole in the local co-ordinates system with z=0 m.
s_1	m	Drawdown of the water level in the borehole during first pumping period. Difference between the actual hydraulic head and the initial head (s1= h1-h0)
s_2	m	Drawdown of the water level in the borehole during second pumping period. Difference between the actual hydraulic head and the initial head (s2=h2-h0)
T	m^2/s	Transmissivity of the entire borehole
Q_0	m^3/s	Measured flow rate through the test section or flow anomaly under natural conditions (no pumping) with h=h0 in the open borehole
Q_1	m^3/s	Measured flow rate through the test section or flow anomaly during the first pumping period
Q_2	m^3/s	Measured flow rate through the test section or flow anomaly during the second pumping period
h_{0FW}	m.a.s.l.	Corrected initial hydraulic head along the hole due to e.g. varying salinity conditions of the borehole fluid before pumping
h_{1FW}	m.a.s.l.	Corrected hydraulic head along the hole due to e.g. varying salinity conditions of the borehole fluid during the first pumping period
h_{2FW}	m.a.s.l.	Corrected hydraulic head along the hole due to e.g. varying salinity conditions of the borehole fluid during the second pumping period
EC_w	S/m	Measured electrical conductivity of the borehole fluid in the test section during difference flow logging
Te_w	°C	Measured borehole fluid temperature in the test section during difference flow logging
EC_f	S/m	Measured fracture-specific electrical conductivity of the fluid in flow anomaly during difference flow logging
Te_f	°C	Measured fracture-specific fluid temperature in flow anomaly during difference flow logging
T_D	m^2/s	Transmissivity of section or flow anomaly based on 2D model for evaluation of formation properties of the test section based on PFL-DIFF.
$T\text{-measl}_{LT}$	m^2/s	Estimated theoretical lower measurement limit for evaluated TD. If the estimated TD equals TD-measlim, the actual TD is considered to be equal or less than TD-measlim.
$T\text{-measl}_{LP}$	m^2/s	Estimated practical lower measurement limit for evaluated TD. If the estimated TD equals TD-measlim, the actual TD is considered to be equal or less than TD-measlim.
$T\text{-meas}_{lU}$	m^2/s	Estimated upper measurement limit for evaluated TD. If the estimated TD equals TD-measlim, the actual TD is considered to be equal or less than TD-measlim.
h_i	m.a.s.l.	Calculated relative, natural freshwater head for test section or flow anomaly (undisturbed conditions)

Results of sequential flow logging.

Borehole ID	Secup L(m)	Seclow L(m)	L_w (m)	Q_0 (m^3/s)	h_{0FW} (m.a.s.l.)	Q_1 (m^3/s)	h_{1FW} (m.a.s.l.)	T_D (m^2/s)	h_i (m.a.s.l.)	Q-lower limit P (mL/h)	TD-$measl_{LT}$ (m^2/s)	TD- $measl_{LP}$ (m^2/s)	TD- $measl_U$ (m^2/s)	Comments
KFR105	2.90	7.90	5	–	0.00	–	–106.82	–	–	40	7.7E-11	1.0E-10	7.7E-07	
KFR105	7.91	12.91	5	–	0.00	3.03E-08	–106.82	2.8E-10	–	30	7.7E-11	7.7E-11	7.7E-07	
KFR105	12.92	17.92	5	–	0.00	–	–106.82	–	–	50	7.7E-11	1.3E-10	7.7E-07	
KFR105	17.93	22.93	5	–	0.00	1.50E-08	–106.82	1.4E-10	–	30	7.7E-11	7.7E-11	7.7E-07	
KFR105	22.93	27.93	5	–	0.00	7.50E-07	–106.82	6.9E-09	–	30	7.7E-11	7.7E-11	7.7E-07	
KFR105	27.94	32.94	5	–	0.00	8.86E-07	–106.82	8.2E-09	–	30	7.7E-11	7.7E-11	7.7E-07	
KFR105	32.98	37.98	5	–	0.00	5.39E-06	–106.82	5.0E-08	–	30	7.7E-11	7.7E-11	7.7E-07	
KFR105	37.97	42.97	5	–	0.00	1.05E-05	–106.82	9.7E-08	–	30	7.7E-11	7.7E-11	7.7E-07	
KFR105	43.00	48.00	5	–	0.00	1.16E-06	–106.82	1.1E-08	–	30	7.7E-11	7.7E-11	7.7E-07	
KFR105	47.99	52.99	5	–	0.00	1.71E-07	–106.82	1.6E-09	–	30	7.7E-11	7.7E-11	7.7E-07	
KFR105	52.97	57.97	5	–	0.00	6.44E-07	–106.82	6.0E-09	–	150	7.7E-11	3.9E-10	7.7E-07	
KFR105	57.96	62.96	5	–	0.00	7.25E-08	–106.82	6.7E-10	–	30	7.7E-11	7.7E-11	7.7E-07	
KFR105	62.96	67.96	5	–	0.00	8.33E-08	–106.82	7.7E-10	–	30	7.7E-11	7.7E-11	7.7E-07	
KFR105	67.95	72.95	5	–	0.00	6.28E-08	–106.82	5.8E-10	–	30	7.7E-11	7.7E-11	7.7E-07	
KFR105	72.98	77.98	5	–	0.00	1.99E-06	–106.82	1.8E-08	–	30	7.7E-11	7.7E-11	7.7E-07	
KFR105	77.95	82.95	5	–	0.00	7.33E-07	–106.82	6.8E-09	–	30	7.7E-11	7.7E-11	7.7E-07	
KFR105	82.88	87.88	5	–	0.00	6.69E-07	–106.82	6.2E-09	–	30	7.7E-11	7.7E-11	7.7E-07	
KFR105	87.90	92.90	5	–	0.00	2.89E-08	–106.82	2.7E-10	–	30	7.7E-11	7.7E-11	7.7E-07	
KFR105	92.96	97.96	5	–	0.00	2.46E-07	–106.82	2.3E-09	–	30	7.7E-11	7.7E-11	7.7E-07	
KFR105	97.92	102.92	5	–	0.00	1.41E-07	–106.82	1.3E-09	–	30	7.7E-11	7.7E-11	7.7E-07	
KFR105	102.92	107.92	5	–	0.00	1.17E-06	–106.82	1.1E-08	–	30	7.7E-11	7.7E-11	7.7E-07	
KFR105	107.90	112.90	5	–	0.00	4.94E-07	–106.82	4.6E-09	–	30	7.7E-11	7.7E-11	7.7E-07	
KFR105	112.92	117.92	5	–	0.00	1.69E-07	–106.82	1.6E-09	–	30	7.7E-11	7.7E-11	7.7E-07	
KFR105	117.91	122.91	5	–	0.00	–	–106.82	–	–	30	7.7E-11	7.7E-11	7.7E-07	
KFR105	122.89	127.89	5	–	0.00	1.02E-05	–106.82	9.4E-08	–	30	7.7E-11	7.7E-11	7.7E-07	

Borehole ID	Secup L(m)	Seclow L(m)	L_w (m)	Q_0 (m^3/s)	h_{0FW} (m.a.s.l.)	Q_1 (m^3/s)	h_{1FW} (m.a.s.l.)	T_D (m^2/s)	h_i (m.a.s.l.)	Q-lower limit P (mL/h)	TD-measl$_{LT}$ (m^2/s)	TD- measl$_{LP}$ (m^2/s)	TD- measl$_U$ (m^2/s)	Comments
KFR105	127.90	132.90	5	–	0.00	2.58E-07	–106.82	2.4E-09	–	30	7.7E-11	7.7E-11	7.7E-07	
KFR105	132.91	137.91	5	–	0.00	7.06E-05	–106.82	6.5E-07	–	30	7.7E-11	7.7E-11	7.7E-07	
KFR105	137.92	142.92	5	–	0.00	1.62E-06	–106.82	1.5E-08	–	30	7.7E-11	7.7E-11	7.7E-07	
KFR105	142.96	147.96	5	–	0.00	8.25E-07	–106.82	7.6E-09	–	30	7.7E-11	7.7E-11	7.7E-07	
KFR105	147.94	152.94	5	–	0.00	6.64E-06	–106.82	6.1E-08	–	30	7.7E-11	7.7E-11	7.7E-07	
KFR105	152.92	157.92	5	–	0.00	3.31E-07	–106.82	3.1E-09	–	30	7.7E-11	7.7E-11	7.7E-07	
KFR105	157.93	162.93	5	–	0.00	1.96E-06	–106.82	1.8E-08	–	30	7.7E-11	7.7E-11	7.7E-07	
KFR105	162.96	167.96	5	–	0.00	5.50E-07	–106.82	5.1E-09	–	30	7.7E-11	7.7E-11	7.7E-07	
KFR105	167.95	172.95	5	–	0.00	1.98E-05	–106.82	1.8E-07	–	30	7.7E-11	7.7E-11	7.7E-07	
KFR105	172.97	177.97	5	–	0.00	1.14E-05	–106.82	1.1E-07	–	30	7.7E-11	7.7E-11	7.7E-07	
KFR105	177.98	182.98	5	–	0.00	5.00E-06	–106.82	4.6E-08	–	30	7.7E-11	7.7E-11	7.7E-07	
KFR105	182.98	187.98	5	–	0.00	4.11E-07	–106.82	3.8E-09	–	30	7.7E-11	7.7E-11	7.7E-07	
KFR105	187.99	192.99	5	–	0.00	1.17E-06	–106.82	1.1E-08	–	30	7.7E-11	7.7E-11	7.7E-07	
KFR105	192.99	197.99	5	–	0.00	7.92E-08	–106.82	7.3E-10	–	30	7.7E-11	7.7E-11	7.7E-07	
KFR105	197.98	202.98	5	–	0.00	2.13E-07	–106.82	2.0E-09	–	30	7.7E-11	7.7E-11	7.7E-07	
KFR105	203.00	208.00	5	–	0.00	9.36E-07	–106.82	8.7E-09	–	30	7.7E-11	7.7E-11	7.7E-07	
KFR105	207.99	212.99	5	–	0.00	6.61E-08	–106.82	6.1E-10	–	30	7.7E-11	7.7E-11	7.7E-07	
KFR105	212.98	217.98	5	–	0.00	4.36E-07	–106.82	4.0E-09	–	30	7.7E-11	7.7E-11	7.7E-07	
KFR105	217.96	222.96	5	–	0.00	1.14E-07	–106.82	1.1E-09	–	30	7.7E-11	7.7E-11	7.7E-07	
KFR105	222.95	227.95	5	–	0.00	6.19E-08	–106.82	5.7E-10	–	30	7.7E-11	7.7E-11	7.7E-07	
KFR105	227.95	232.95	5	–	0.00	1.47E-08	–106.82	1.4E-10	–	30	7.7E-11	7.7E-11	7.7E-07	
KFR105	232.97	237.97	5	–	0.00	–	–106.82	–	–	30	7.7E-11	7.7E-11	7.7E-07	
KFR105	237.95	242.95	5	–	0.00	1.90E-07	–106.82	1.8E-09	–	30	7.7E-11	7.7E-11	7.7E-07	
KFR105	242.93	247.93	5	–	0.00	2.52E-07	–106.82	2.3E-09	–	30	7.7E-11	7.7E-11	7.7E-07	
KFR105	247.93	252.93	5	–	0.00	2.03E-07	–106.82	1.9E-09	–	30	7.7E-11	7.7E-11	7.7E-07	
KFR105	252.95	257.95	5	–	0.00	2.38E-07	–106.82	2.2E-09	–	30	7.7E-11	7.7E-11	7.7E-07	

Borehole ID	Secup L(m)	Seclow L(m)	L_w (m)	Q_0 (m^3/s)	h_{0FW} (m.a.s.l.)	Q_1 (m^3/s)	h_{1FW} (m.a.s.l.)	T_D (m^2/s)	h_i (m.a.s.l.)	Q-lower limit P (mL/h)	TD-measl$_{LT}$ (m^2/s)	TD- measl$_{LP}$ (m^2/s)	TD- measl$_U$ (m^2/s)	Comments
KFR105	257.94	262.94	5	–	0.00	–	–106.82	–	–	30	7.7E-11	7.7E-11	7.7E-07	
KFR105	262.92	267.92	5	–	0.00	3.64E-06	–106.82	3.4E-08	–	30	7.7E-11	7.7E-11	7.7E-07	
KFR105	267.92	272.92	5	–	0.00	7.83E-07	–106.82	7.3E-09	–	30	7.7E-11	7.7E-11	7.7E-07	
KFR105	272.94	277.94	5	–	0.00	3.28E-08	–106.82	3.0E-10	–	30	7.7E-11	7.7E-11	7.7E-07	
KFR105	277.93	282.93	5	–	0.00	2.51E-07	–106.82	2.3E-09	–	30	7.7E-11	7.7E-11	7.7E-07	
KFR105	282.92	287.92	5	–	0.00	5.17E-07	–106.82	4.8E-09	–	30	7.7E-11	7.7E-11	7.7E-07	
KFR105	287.91	292.91	5	–	0.00	1.02E-07	–106.82	9.5E-10	–	30	7.7E-11	7.7E-11	7.7E-07	
KFR105	292.90	297.90	5	–	0.00	7.17E-07	–106.82	6.6E-09	–	30	7.7E-11	7.7E-11	7.7E-07	
KFR105	297.89	302.89	5	–	0.00	5.92E-07	–106.82	5.5E-09	–	30	7.7E-11	7.7E-11	7.7E-07	

Q_0 was not measured. It was assumed to be zero.

h_{0FW} was assumed to be zero (sea level).

h_{1FW} was same as the elevation of top of the casing tube.

Because of these assumptions the value of T is a rough estimate.

Forsmark, borehole KFR105
Flow rates of 5 m sections

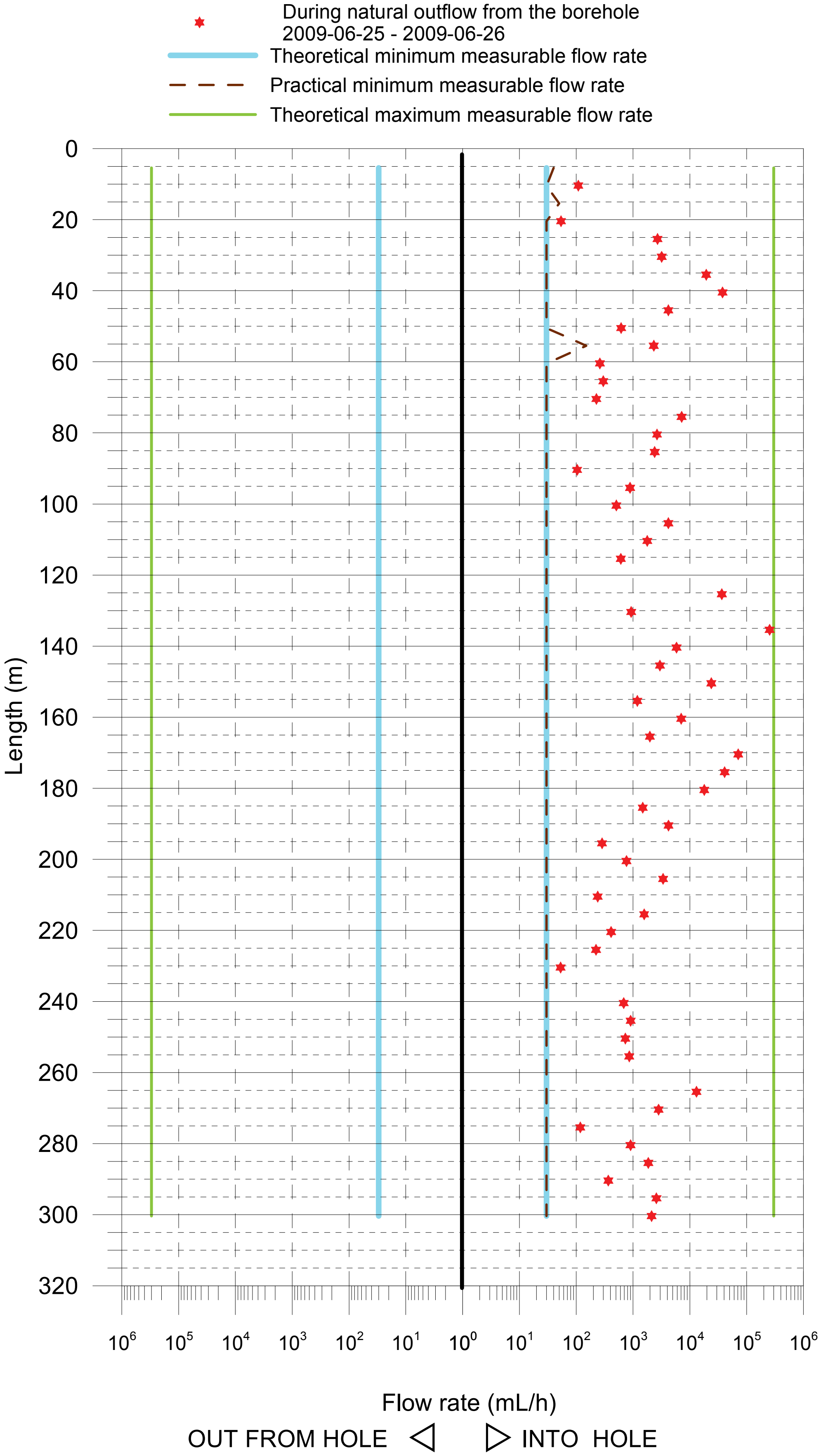

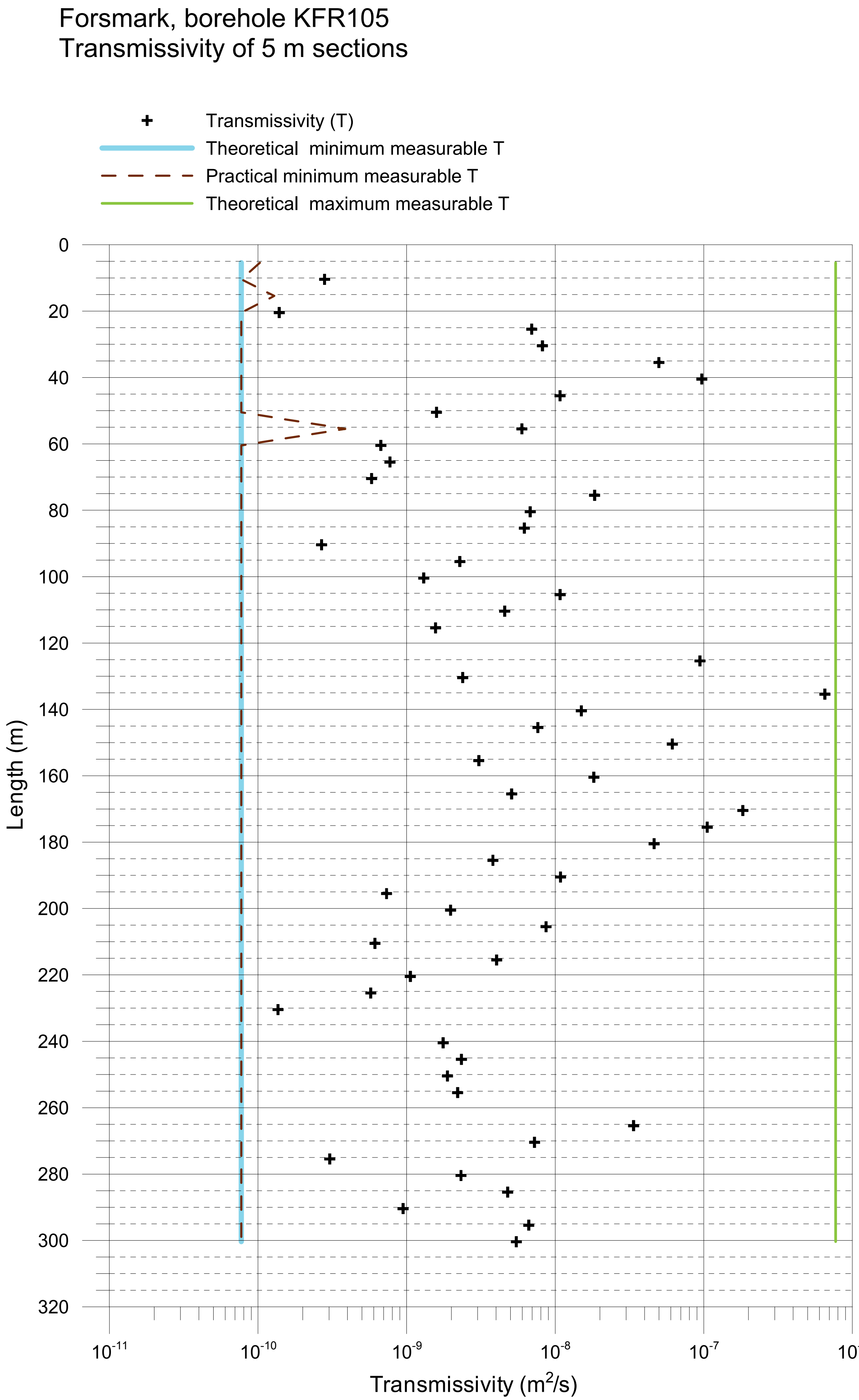
Forsmark, borehole KFR105
Transmissivity of 5 m sections
Transmissivity (T)
Theoretical minimum measurable T
Practical minimum measurable T
Theoretical maximum measurable T
Length (m)
0
20
40
60
80
100
120
140
160
180
200
220
240
260
280
300
320
10-11
10-10
10-9
10-8
10-7
10-6
Transmissivity (m2/s)

Borehole ID	Length to flow anom. L (m)	Lw (m)	d_L (m)	Q_0 (m^3/s)	h_{0FW} (m.a.s.l.)	Q1 (m^3/s)	h1FW (m.a.s.l.)	T_D (m^2/s)	h_i (m.a.s.l.)	Comments
KFR105	9.3	1	0.1	–	0.00	1.97E-08	–106.82	1.8E-10	–	*
KFR105	22.6	1	0.1	–	0.00	1.42E-08	–106.82	1.3E-10	–	*
KFR105	24.8	1	0.1	–	0.00	2.94E-07	–106.82	2.7E-09	–	
KFR105	26.6	1	0.1	–	0.00	5.25E-07	–106.82	4.9E-09	–	
KFR105	32.3	1	0.1	–	0.00	8.44E-07	–106.82	7.8E-09	–	
KFR105	33.7	1	0.1	–	0.00	3.64E-07	–106.82	3.4E-09	–	*
KFR105	34.1	1	0.1	–	0.00	4.33E-07	–106.82	4.0E-09	–	
KFR105	35.9	1	0.1	–	0.00	8.81E-07	–106.82	8.2E-09	–	
KFR105	37.2	1	0.1	–	0.00	4.75E-07	–106.82	4.4E-09	–	*
KFR105	37.8	1	0.1	–	0.00	1.62E-06	–106.82	1.5E-08	–	
KFR105	39.4	1	0.1	–	0.00	9.14E-06	–106.82	8.5E-08	–	
KFR105	40.9	1	0.1	–	0.00	8.19E-07	–106.82	7.6E-09	–	
KFR105	41.3	1	0.1	–	0.00	9.00E-08	–106.82	8.3E-10	–	*
KFR105	43.4	1	0.1	–	0.00	9.44E-09	–106.82	8.7E-11	–	*
KFR105	43.8	1	0.1	–	0.00	1.85E-07	–106.82	1.7E-09	–	
KFR105	45.8	1	0.1	–	0.00	5.17E-07	–106.82	4.8E-09	–	
KFR105	49.0	1	0.1	–	0.00	1.42E-07	–106.82	1.3E-09	–	
KFR105	57.2	1	0.1	–	0.00	2.56E-08	–106.82	2.4E-10	–	
KFR105	57.8	1	0.1	–	0.00	6.14E-07	–106.82	5.7E-09	–	
KFR105	58.8	1	0.1	–	0.00	4.22E-08	–106.82	3.9E-10	–	
KFR105	62.1	1	0.1	–	0.00	7.50E-09	–106.82	6.9E-11	–	*
KFR105	62.6	1	0.1	–	0.00	1.72E-08	–106.82	1.6E-10	–	
KFR105	65.2	1	0.1	–	0.00	6.94E-09	–106.82	6.4E-11	–	*
KFR105	65.9	1	0.1	–	0.00	3.89E-08	–106.82	3.6E-10	–	
KFR105	66.5	1	0.1	–	0.00	4.75E-08	–106.82	4.4E-10	–	
KFR105	69.8	1	0.1	–	0.00	1.83E-08	–106.82	1.7E-10	–	*
KFR105	72.0	1	0.1	–	0.00	2.94E-08	–106.82	2.7E-10	–	*
KFR105	73.1	1	0.1	–	0.00	7.72E-08	–106.82	7.2E-10	–	
KFR105	77.3	1	0.1	–	0.00	1.77E-06	–106.82	1.6E-08	–	
KFR105	78.3	1	0.1	–	0.00	6.53E-07	–106.82	6.0E-09	–	
KFR105	79.4	1	0.1	–	0.00	1.09E-07	–106.82	1.0E-09	–	
KFR105	81.4	1	0.1	–	0.00	2.22E-08	–106.82	2.1E-10	–	
KFR105	83.3	1	0.1	–	0.00	5.25E-07	–106.82	4.9E-09	–	
KFR105	84.0	1	0.1	–	0.00	1.11E-07	–106.82	1.0E-09	–	
KFR105	87.1	1	0.1	–	0.00	8.33E-09	–106.82	7.7E-11	–	*
KFR105	88.7	1	0.1	–	0.00	1.25E-08	–106.82	1.2E-10	–	
KFR105	94.9	1	0.1	–	0.00	2.44E-08	–106.82	2.3E-10	–	
KFR105	95.7	1	0.1	–	0.00	2.03E-07	–106.82	1.9E-09	–	
KFR105	100.4	1	0.1	–	0.00	2.03E-08	–106.82	1.9E-10	–	
KFR105	102.1	1	0.1	–	0.00	9.69E-08	–106.82	9.0E-10	–	
KFR105	104.0	1	0.1	–	0.00	3.11E-08	–106.82	2.9E-10	–	*
KFR105	104.5	1	0.1	–	0.00	1.89E-08	–106.82	1.8E-10	–	*

Borehole ID	Length to flow anom. L (m)	Lw (m)	d_L (m)	Q_0 (m^3/s)	h_{0FW} (m.a.s.l.)	Q1 (m^3/s)	h1FW (m.a.s.l.)	T_D (m^2/s)	h_i (m.a.s.l.)	Comments
KFR105	107.7	1	0.1	–	0.00	1.09E-06	–106.82	1.0E-08	–	
KFR105	108.2	1	0.1	–	0.00	4.28E-07	–106.82	4.0E-09	–	
KFR105	109.3	1	0.1	–	0.00	6.58E-08	–106.82	6.1E-10	–	
KFR105	113.4	1	0.1	–	0.00	5.83E-08	–106.82	5.4E-10	–	
KFR105	115.1	1	0.1	–	0.00	7.89E-08	–106.82	7.3E-10	–	
KFR105	115.4	1	0.1	–	0.00	2.42E-08	–106.82	2.2E-10	–	*
KFR105	117.4	1	0.1	–	0.00	1.33E-08	–106.82	1.2E-10	–	*
KFR105	124.1	1	0.1	–	0.00	8.92E-06	–106.82	8.3E-08	–	
KFR105	124.7	1	0.1	–	0.00	2.61E-07	–106.82	2.4E-09	–	
KFR105	125.9	1	0.1	–	0.00	7.58E-07	–106.82	7.0E-09	–	
KFR105	127.0	1	0.1	–	0.00	1.05E-07	–106.82	9.8E-10	–	
KFR105	129.1	1	0.1	–	0.00	2.39E-08	–106.82	2.2E-10	–	
KFR105	130.2	1	0.1	–	0.00	1.16E-07	–106.82	1.1E-09	–	
KFR105	132.0	1	0.1	–	0.00	8.03E-08	–106.82	7.4E-10	–	
KFR105	133.7	1	0.1	–	0.00	7.00E-05	–106.82	6.5E-07	–	
KFR105	138.2	1	0.1	–	0.00	4.14E-07	–106.82	3.8E-09	–	
KFR105	139.9	1	0.1	–	0.00	1.22E-06	–106.82	1.1E-08	–	
KFR105	141.3	1	0.1	–	0.00	2.67E-08	–106.82	2.5E-10	–	
KFR105	145.3	1	0.1	–	0.00	3.17E-07	–106.82	2.9E-09	–	
KFR105	146.2	1	0.1	–	0.00	3.92E-07	–106.82	3.6E-09	–	
KFR105	147.0	1	0.1	–	0.00	1.81E-07	–106.82	1.7E-09	–	
KFR105	148.9	1	0.1	–	0.00	6.39E-09	–106.82	5.9E-11	–	*
KFR105	150.1	1	0.1	–	0.00	3.75E-06	–106.82	3.5E-08	–	
KFR105	152.0	1	0.1	–	0.00	1.01E-07	–106.82	9.3E-10	–	*
KFR105	152.6	1	0.1	–	0.00	2.54E-06	–106.82	2.4E-08	–	
KFR105	154.4	1	0.1	–	0.00	1.14E-07	–106.82	1.1E-09	–	
KFR105	157.1	1	0.1	–	0.00	1.89E-07	–106.82	1.8E-09	–	
KFR105	160.0	1	0.1	–	0.00	1.85E-06	–106.82	1.7E-08	–	
KFR105	160.7	1	0.1	–	0.00	4.94E-08	–106.82	4.6E-10	–	
KFR105	163.1	1	0.1	–	0.00	5.89E-08	–106.82	5.5E-10	–	
KFR105	164.9	1	0.1	–	0.00	2.86E-07	–106.82	2.7E-09	–	
KFR105	166.1	1	0.1	–	0.00	7.31E-08	–106.82	6.8E-10	–	*
KFR105	167.7	1	0.1	–	0.00	1.02E-07	–106.82	9.4E-10	–	*
KFR105	168.6	1	0.1	–	0.00	4.83E-07	–106.82	4.5E-09	–	
KFR105	169.5	1	0.1	–	0.00	2.08E-08	–106.82	1.9E-10	–	*
KFR105	170.1	1	0.1	–	0.00	2.72E-08	–106.82	2.5E-10	–	*
KFR105	171.3	1	0.1	–	0.00	3.78E-08	–106.82	3.5E-10	–	*
KFR105	172.7	1	0.1	–	0.00	1.79E-05	–106.82	1.7E-07	–	
KFR105	173.0	1	0.1	–	0.00	7.89E-06	–106.82	7.3E-08	–	*
KFR105	173.4	1	0.1	–	0.00	1.84E-06	–106.82	1.7E-08	–	*
KFR105	174.8	1	0.1	–	0.00	1.46E-06	–106.82	1.4E-08	–	
KFR105	176.1	1	0.1	–	0.00	4.75E-08	–106.82	4.4E-10	–	*
KFR105	177.1	1	0.1	–	0.00	3.39E-08	–106.82	3.1E-10	–	*

Borehole ID	Length to flow anom. L (m)	Lw (m)	d_L (m)	Q_0 (m^3/s)	h_{0FW} (m.a.s.l.)	Q1 (m^3/s)	h1FW (m.a.s.l.)	T_D (m^2/s)	h_i (m.a.s.l.)	Comments
KFR105	178.1	1	0.1	–	0.00	8.89E-07	–106.82	8.2E-09	–	
KFR105	179.6	1	0.1	–	0.00	2.92E-08	–106.82	2.7E-10	–	
KFR105	180.8	1	0.1	–	0.00	1.34E-06	–106.82	1.2E-08	–	
KFR105	181.8	1	0.1	–	0.00	1.06E-06	–106.82	9.8E-09	–	
KFR105	182.6	1	0.1	–	0.00	7.72E-07	–106.82	7.2E-09	–	
KFR105	183.2	1	0.1	–	0.00	3.33E-07	–106.82	3.1E-09	–	
KFR105	184.6	1	0.1	–	0.00	1.92E-08	–106.82	1.8E-10	–	
KFR105	188.1	1	0.1	–	0.00	1.65E-07	–106.82	1.5E-09	–	
KFR105	188.4	1	0.1	–	0.00	2.52E-07	–106.82	2.3E-09	–	
KFR105	189.2	1	0.1	–	0.00	5.50E-07	–106.82	5.1E-09	–	
KFR105	189.7	1	0.1	–	0.00	4.86E-08	–106.82	4.5E-10	–	
KFR105	192.2	1	0.1	–	0.00	2.50E-07	–106.82	2.3E-09	–	
KFR105	197.0	1	0.1	–	0.00	4.06E-08	–106.82	3.8E-10	–	
KFR105	197.7	1	0.1	–	0.00	4.58E-08	–106.82	4.2E-10	–	
KFR105	200.1	1	0.1	–	0.00	9.28E-08	–106.82	8.6E-10	–	
KFR105	202.6	1	0.1	–	0.00	2.19E-08	–106.82	2.0E-10	–	*
KFR105	202.9	1	0.1	–	0.00	9.86E-08	–106.82	9.1E-10	–	
KFR105	203.5	1	0.1	–	0.00	3.11E-08	–106.82	2.9E-10	–	
KFR105	205.2	1	0.1	–	0.00	7.89E-08	–106.82	7.3E-10	–	
KFR105	206.8	1	0.1	–	0.00	7.67E-07	–106.82	7.1E-09	–	
KFR105	208.5	1	0.1	–	0.00	5.89E-08	–106.82	5.5E-10	–	
KFR105	213.0	1	0.1	–	0.00	3.53E-07	–106.82	3.3E-09	–	
KFR105	213.8	1	0.1	–	0.00	7.44E-08	–106.82	6.9E-10	–	
KFR105	215.7	1	0.1	–	0.00	2.36E-08	–106.82	2.2E-10	–	*
KFR105	218.1	1	0.1	–	0.00	4.61E-08	–106.82	4.3E-10	–	
KFR105	219.3	1	0.1	–	0.00	5.19E-08	–106.82	4.8E-10	–	
KFR105	221.1	1	0.1	–	0.00	2.08E-08	–106.82	1.9E-10	–	*
KFR105	227.8	1	0.1	–	0.00	6.06E-08	–106.82	5.6E-10	–	
KFR105	229.7	1	0.1	–	0.00	1.06E-08	–106.82	9.8E-11	–	
KFR105	239.9	1	0.1	–	0.00	1.11E-07	–106.82	1.0E-09	–	
KFR105	242.4	1	0.1	–	0.00	7.36E-08	–106.82	6.8E-10	–	
KFR105	243.0	1	0.1	–	0.00	1.76E-07	–106.82	1.6E-09	–	
KFR105	244.8	1	0.1	–	0.00	1.89E-08	–106.82	1.8E-10	–	*
KFR105	245.7	1	0.1	–	0.00	3.00E-08	–106.82	2.8E-10	–	*
KFR105	246.1	1	0.1	–	0.00	4.83E-08	–106.82	4.5E-10	–	
KFR105	250.0	1	0.1	–	0.00	2.81E-08	–106.82	2.6E-10	–	
KFR105	251.2	1	0.1	–	0.00	1.51E-07	–106.82	1.4E-09	–	
KFR105	254.0	1	0.1	–	0.00	6.25E-08	–106.82	5.8E-10	–	
KFR105	255.3	1	0.1	–	0.00	1.18E-07	–106.82	1.1E-09	–	
KFR105	257.8	1	0.1	–	0.00	2.19E-08	–106.82	2.0E-10	–	
KFR105	263.4	1	0.1	–	0.00	8.89E-09	–106.82	8.2E-11	–	*
KFR105	266.0	1	0.1	–	0.00	1.19E-08	–106.82	1.1E-10	–	*
KFR105	267.3	1	0.1	–	0.00	2.57E-06	–106.82	2.4E-08	–	

Borehole ID	Length to flow anom. L (m)	Lw (m)	d_L (m)	Q_0 (m^3/s)	h_{0FW} (m.a.s.l.)	Q1 (m^3/s)	h1FW (m.a.s.l.)	T_D (m^2/s)	h_i (m.a.s.l.)	Comments
KFR105	267.9	1	0.1	–	0.00	8.61E-07	–106.82	8.0E-09	–	
KFR105	270.4	1	0.1	–	0.00	7.97E-08	–106.82	7.4E-10	–	
KFR105	271.0	1	0.1	–	0.00	8.58E-08	–106.82	8.0E-10	–	*
KFR105	272.0	1	0.1	–	0.00	5.42E-07	–106.82	5.0E-09	–	
KFR105	274.3	1	0.1	–	0.00	1.72E-08	–106.82	1.6E-10	–	
KFR105	276.1	1	0.1	–	0.00	1.28E-08	–106.82	1.2E-10	–	
KFR105	280.4	1	0.1	–	0.00	1.30E-07	–106.82	1.2E-09	–	
KFR105	281.8	1	0.1	–	0.00	9.31E-08	–106.82	8.6E-10	–	
KFR105	283.5	1	0.1	–	0.00	4.64E-07	–106.82	4.3E-09	–	
KFR105	286.3	1	0.1	–	0.00	5.14E-08	–106.82	4.8E-10	–	
KFR105	288.9	1	0.1	–	0.00	7.78E-09	–106.82	7.2E-11	–	*
KFR105	291.8	1	0.1	–	0.00	3.00E-08	–106.82	2.8E-10	–	*
KFR105	292.3	1	0.1	–	0.00	6.44E-08	–106.82	6.0E-10	–	
KFR105	294.0	1	0.1	–	0.00	6.17E-08	–106.82	5.7E-10	–	
KFR105	295.3	1	0.1	–	0.00	1.24E-07	–106.82	1.2E-09	–	*
KFR105	296.0	1	0.1	–	0.00	2.46E-07	–106.82	2.3E-09	–	*
KFR105	297.5	1	0.1	–	0.00	3.56E-07	–106.82	3.3E-09	–	
KFR105	298.2	1	0.1	–	0.00	5.36E-07	–106.82	5.0E-09	–	
KFR105	299.3	1	0.1	–	0.00	6.61E-08	–106.82	6.1E-10	–	*
KFR105	300.3	1	0.1	–	0.00	2.25E-08	–106.82	2.1E-10	–	*
KFR105	302.9	1	0.1	–	0.00	1.28E-08	–106.82	1.2E-10	–	*
KFR105	303.7	1	0.1	–	0.00	5.69E-08	–106.82	5.3E-10	–	

* Uncertain = The flow rate is less than 30 mL/h or the flow anomalies are overlapping or they are unclear because of noise.
Q_0 was not measured. It was assumed to be zero.
h_{0FW} was assumed to be zero (sea level).
h_{1FW} was same as the elevation of top of the casing tube.
Because of these assumptions the value of T is a rough estimate.

Forsmark, borehole KFR105
Transmissivity of detected fractures

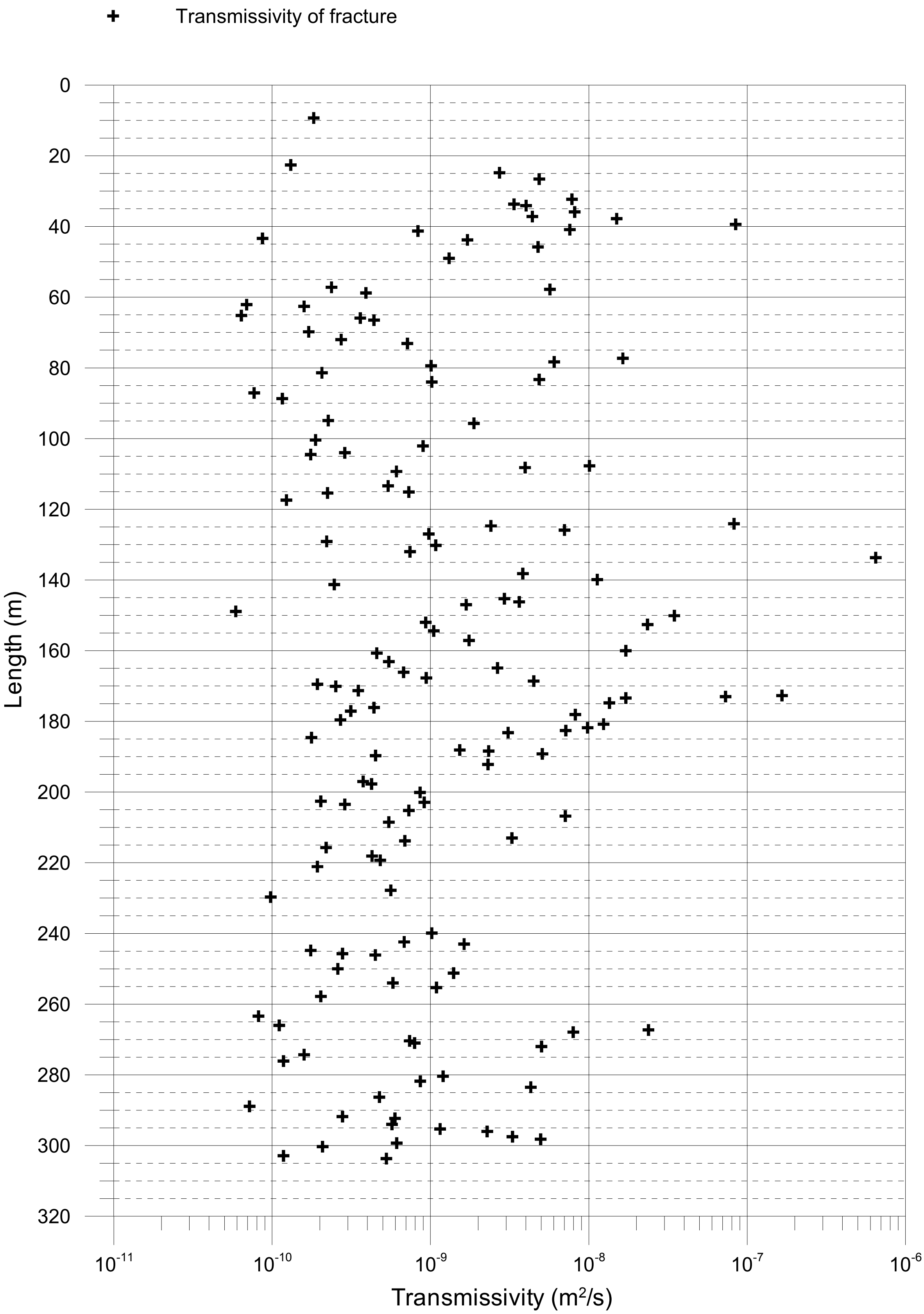

Forsmark, borehole KFR105
Comparison between section transmissivity and fracture transmissivity

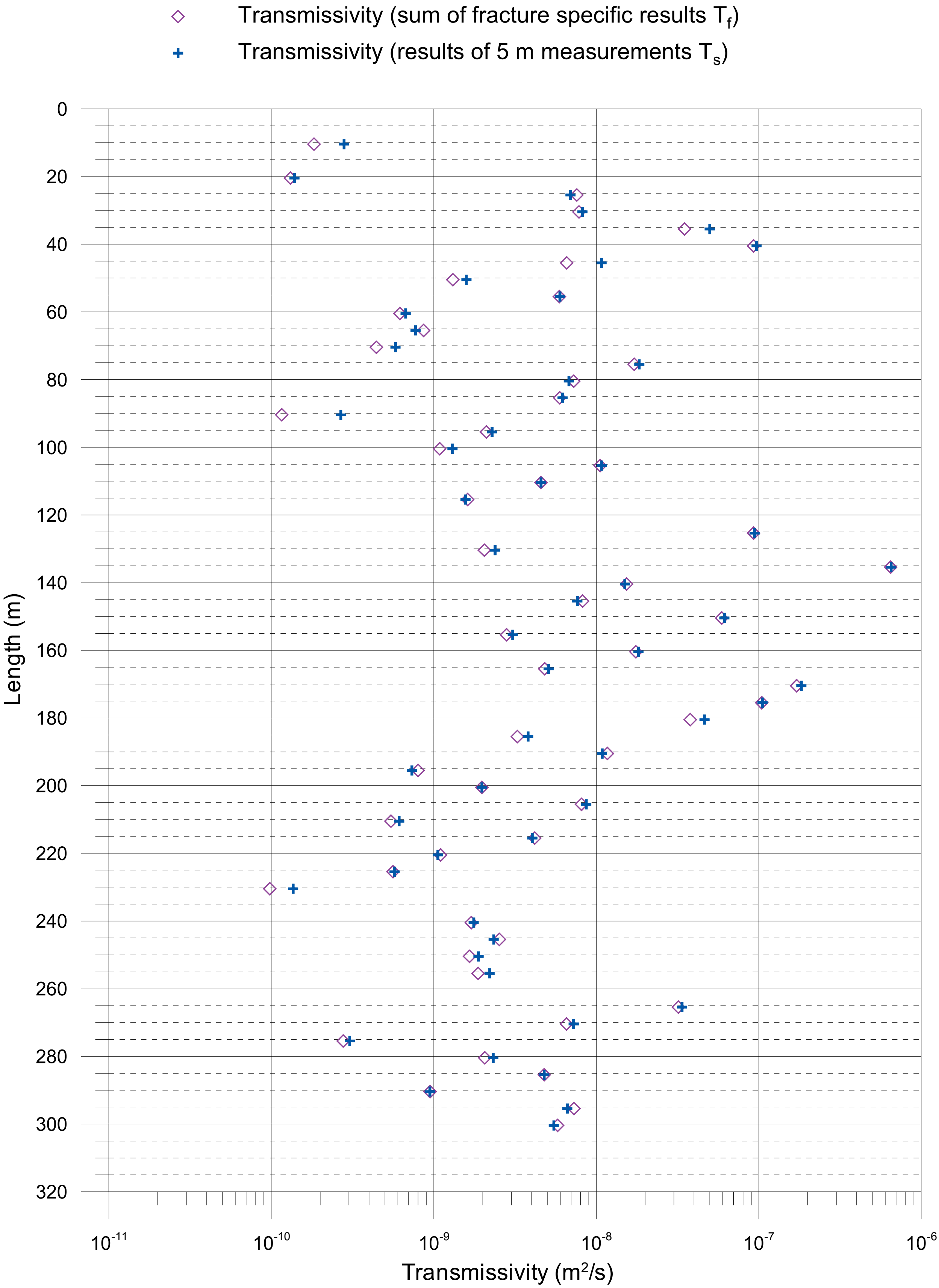

Forsmark, borehole KFR105
Borehole pressure and natural outflow from the borehole

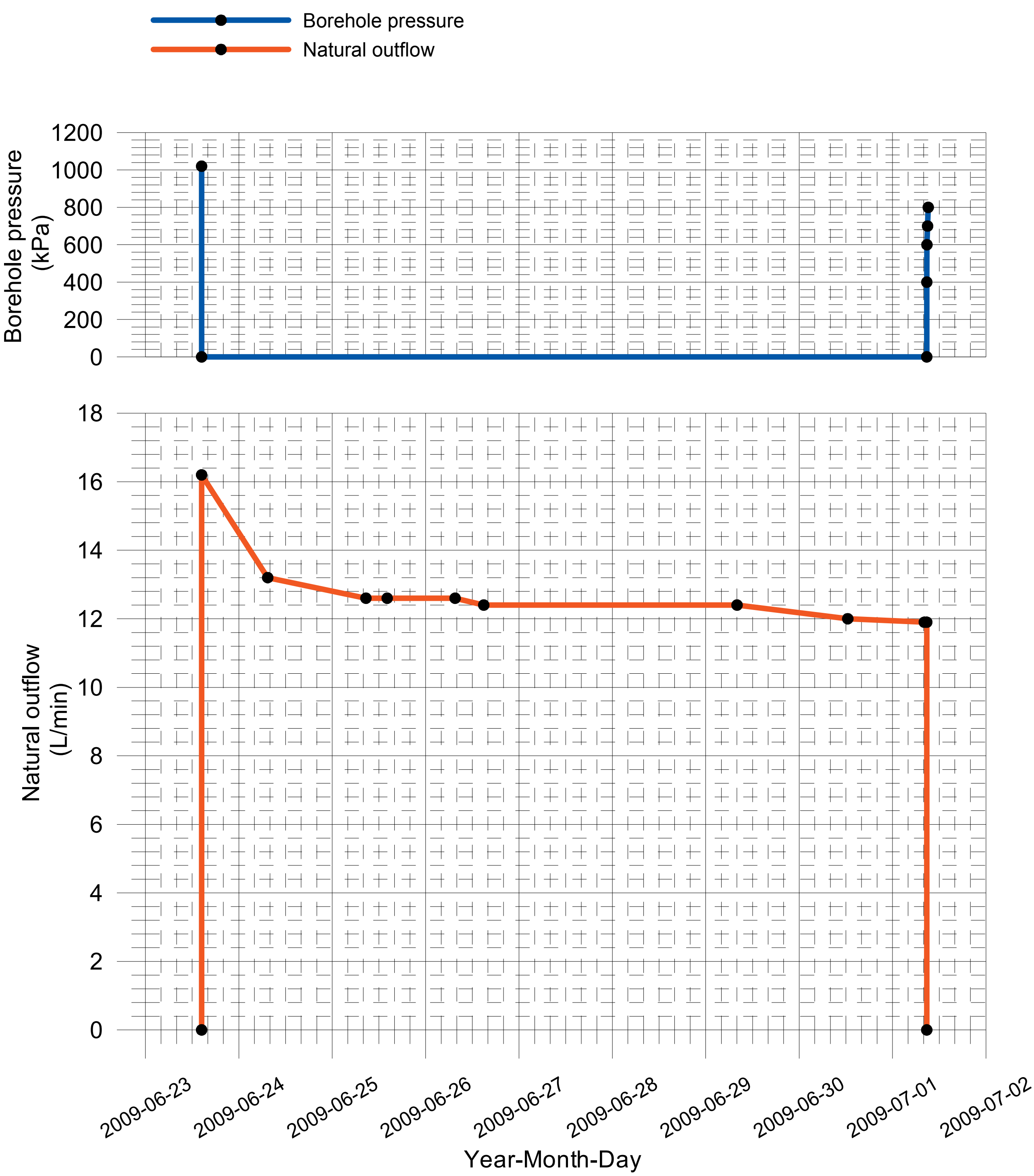

Forsmark, borehole KFR105
Pressure build-up test
Measured by Geosigma Ab

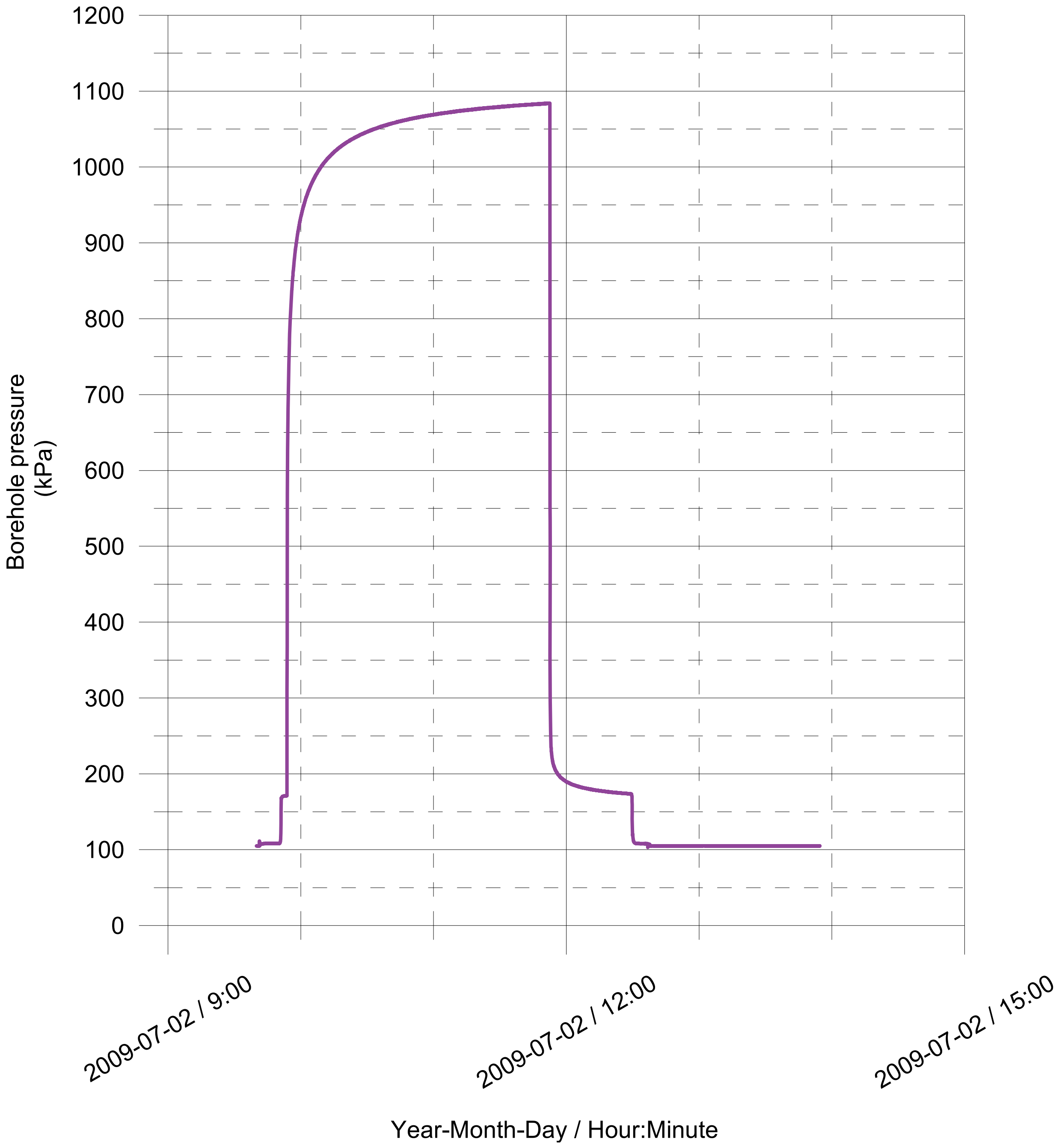

Forsmark, borehole KFR105
Fracture-specific EC results by date

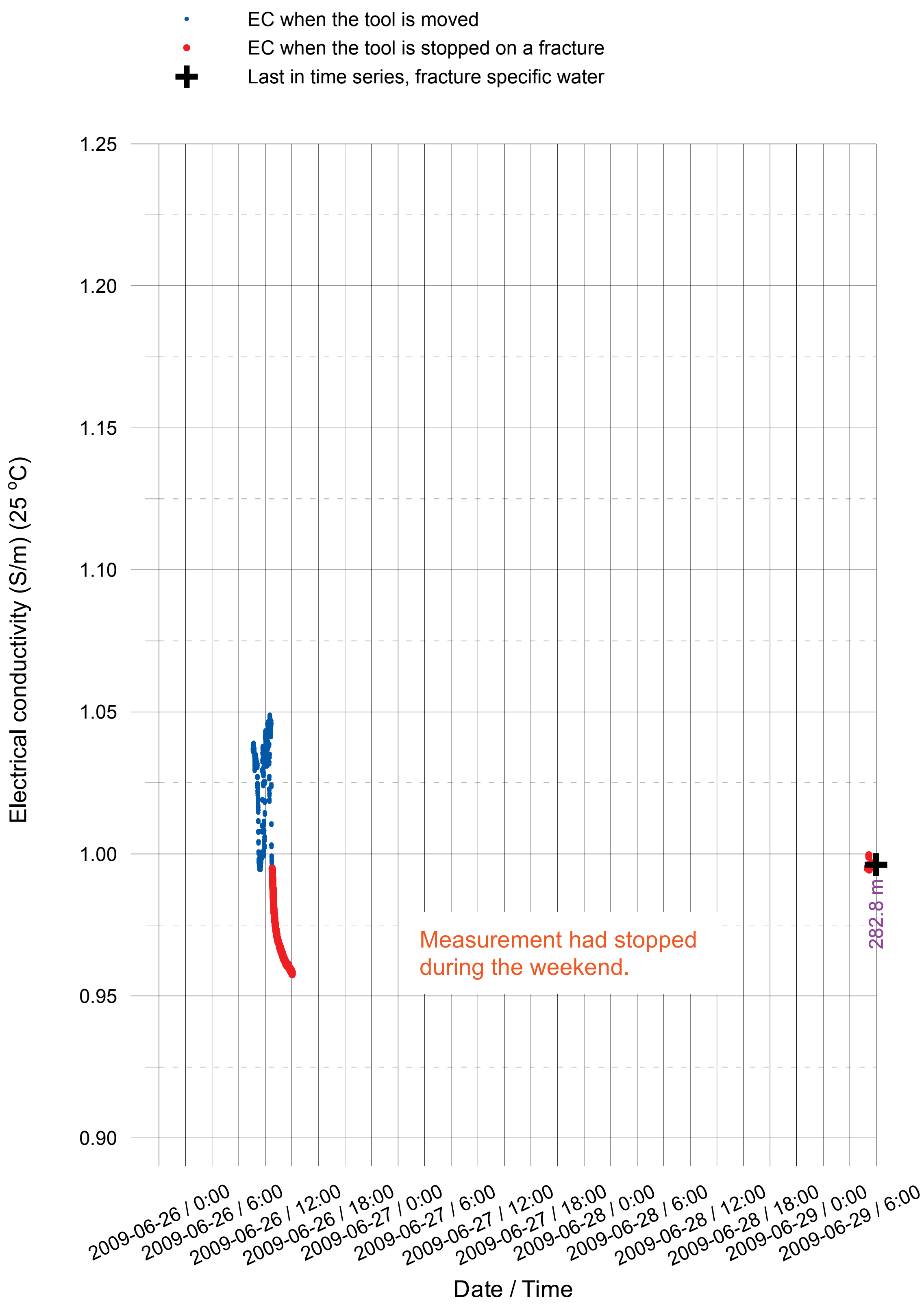

Forsmark, borehole KFR105
Fracture-specific EC results by date

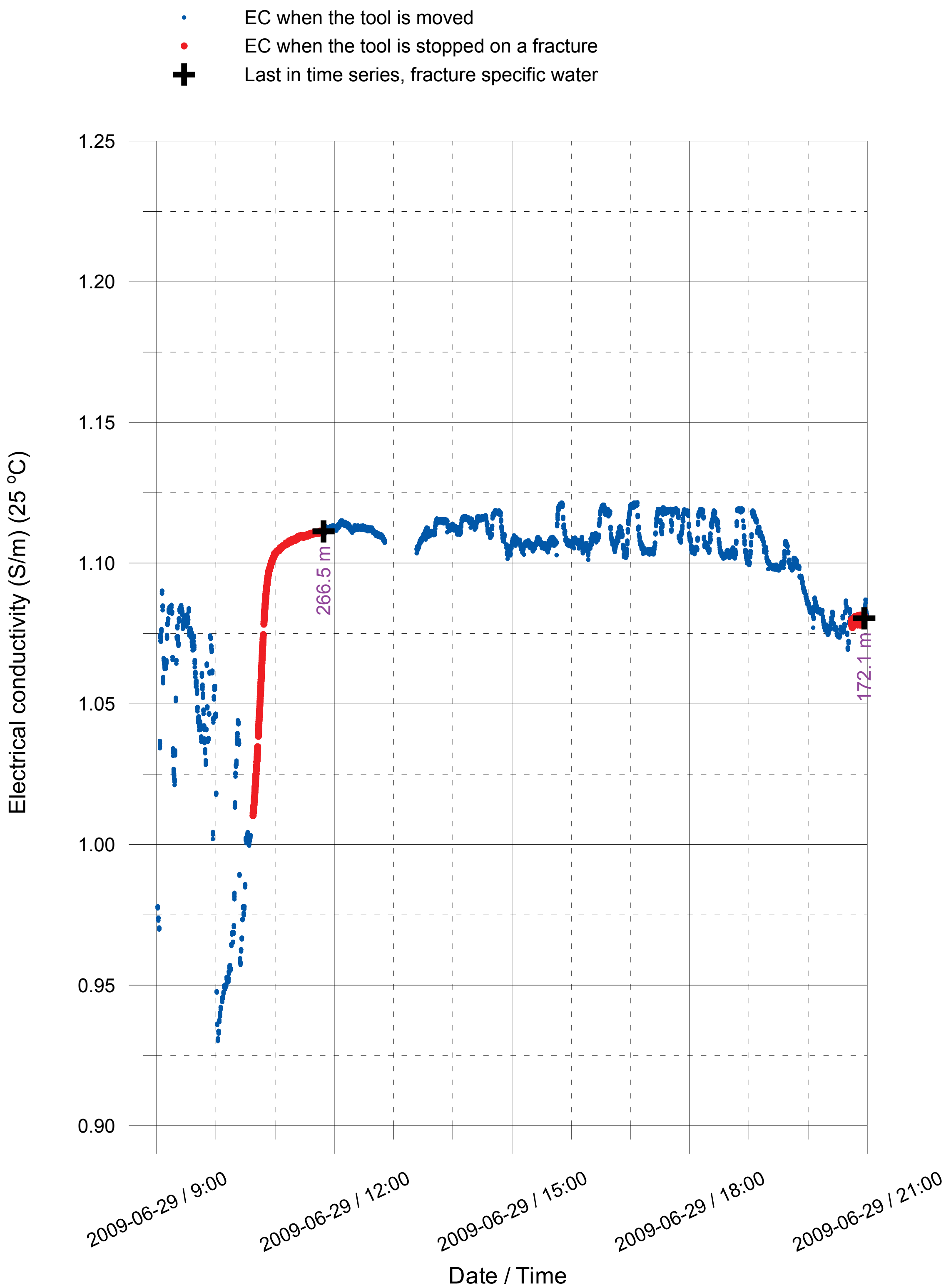

Forsmark, borehole KFR105
Fracture-specific EC results by date